THE UNIVERSITY OF QUEENSLAND

AUSTRALIA

Interactions between iron and fat in non-alcoholic fatty liver disease

Laurence James Britton

MBChB FRACP

A thesis submitted for the degree of Doctor of Philosophy at

The University of Queensland in 2018

Faculty of Medicine

Thesis Abstract

Non-alcoholic fatty disease (NAFLD) is estimated to affect approximately one billion people worldwide. However, the pathogenesis of this common disease is not well understood. This has hampered the development of effective treatments that might prevent complications such as liver failure, liver cancer and cardiac disease. Iron and mutations of the haemochromatosis gene (*HFE*) have long been considered to have pathogenic roles in the development of NAFLD although their significance and mechanisms of effect remain controversial. Recent data indicate a role for modest increases in iron in the generation of insulin resistance and adipose tissue dysfunction, both hallmark features of NAFLD.

Modest increases in iron have been shown to occur with heterozygous *HFE* gene mutations. Due to their high prevalence, heterozygous *HFE* gene mutations are frequently observed in individuals with co-existent NAFLD and such mutations have been hypothesised to have a co-toxic role in NAFLD pathogenesis. Homozygous deletion of *Hfe* has been shown to lead to dysregulated lipid metabolism and liver injury in a mouse model of NAFLD. Chapter 3 describes a model of heterozygous deletion of the *Hfe* gene in mice fed a high calorie diet. This led to impaired homeostasis of both iron and glucose, although there were no alterations in hepatic lipid metabolism or liver injury.

Chapter 4 seeks to further examine the links between iron and insulin resistance. Hepatic iron concentration (HIC) was measured using MR Ferriscan and serum concentrations of six adipokines were determined using a multiplex ELISA array from a cohort of 60 adults with NAFLD. After patients were randomised to six months of venesection and dietary advice (n=23) versus dietary advice alone (n=28), no differences were seen between groups in change in serum concentrations of adiponectin, leptin, resistin, retinol binding protein-4 (RBP-4), tumour necrosis factor alpha (TNFα) and interleukin-6 (IL-6). However, unexpectedly, a significant positive correlation between baseline HIC and serum adiponectin was found. This strengthened further after correction for age, gender and body mass index (rho=0.36, p=0.007). Furthermore, significant inverse correlations were identified between HIC and six surrogate measures of insulin resistance; Adipo-IR, serum insulin, serum glucose, HOMA-IR, HbA1C and hepatic steatosis. A positive correlation was noted between HIC and insulin sensitivity index. These data indicate that HIC positively correlates with serum adiponectin concentration and insulin sensitivity in patients with NAFLD, although at present, causality cannot be established.

Adipose tissue dysfunction secondary to iron has been increasingly implicated in NAFLD pathogenesis. The remainder of the thesis focuses on adipose tissue iron homeostasis and its effects on adipose tissue biology. A model of adipocyte-specific ferroportin (*Fpn1*) knockout (FKO) was developed in order to selectively load in into adipocytes. This involved an *Adipoq*-Cre recombinase driven floxed deletion of *Fpn1* in adipocytes (Chapter 5). This model demonstrated successful selective deletion of *Fpn1*, however this did not result in increased adipocyte iron stores. Similarly, FKO mice did not demonstrate evidence of adipokine dysregulation, or altered insulin sensitivity in hyperinsulinaemic-euglycaemic clamp studies. Likewise, there was no effect of adipocyte-specific ferroportin deletion on liver injury. This study has demonstrated that ferroportin is not a key determinant of adipocyte iron homeostasis in this model. Further studies are required in order to establish the key factors that regulate adipocyte iron homeostasis in animal models and humans.

Finally, to test the hypothesis that iron modulates adipokine release, an *in vitro* model of adipocyte iron loading using differentiated Simpson-Golabi-Behmel Syndrome (SGBS) pre-adipocytes was developed (Chapter 6). Using a proteomic approach of stable isotope labelled amino acids in cell culture (SILAC), the effects of iron on the human adipocyte secretome were examined. This identified 60 proteins with a greater than two-fold change in secretome concentration and $p<0.05$ with iron treatment. Of these, it was found that secreted apolipoprotein E (ApoE) was reduced by 58% ($p=0.001$) and 76% ($p=0.007$) by SILAC and western blot respectively. Intracellular ApoE levels were increased more than 11-fold ($p=0.0005$) with iron treatment. These findings suggest that secretion of ApoE from adipocytes is inhibited by iron. This may be highly relevant with regard to NAFLD pathogenesis given the observation that ApoE knockout leads to steatohepatitis in mice fed a Western diet. Moreover, the broad range of proteins with differential secretion secondary to iron provides a platform for multiple future studies.

In conclusion, this thesis describes a number of novel links between iron, insulin sensitivity and adipokine regulation relevant to NAFLD pathogenesis. In particular, impaired glucose homeostasis in a mouse model of heterozygous *Hfe* deletion was observed. Notably consistent links between HIC and multiple measures of insulin sensitivity were seen in a human cohort of patients with NAFLD. Finally the effect of iron on the human adipocyte secretome was examined, identifying profound inhibition of ApoE secretion by iron. These findings may offer opportunities for the development of effective new therapies for the treatment of NAFLD.

Declaration by author

This thesis is composed of my original work, and contains no material previously published or written by another person except where due reference has been made in the text. I have clearly stated the contribution by others to jointly-authored works that I have included in my thesis.

I have clearly stated the contribution of others to my thesis as a whole, including statistical assistance, survey design, data analysis, significant technical procedures, professional editorial advice, financial support and any other original research work used or reported in my thesis. The content of my thesis is the result of work I have carried out since the commencement of my higher degree by research candidature and does not include a substantial part of work that has been submitted to qualify for the award of any other degree or diploma in any university or other tertiary institution. I have clearly stated which parts of my thesis, if any, have been submitted to qualify for another award.

I acknowledge that an electronic copy of my thesis must be lodged with the University Library and, subject to the policy and procedures of The University of Queensland, the thesis be made available for research and study in accordance with the Copyright Act 1968 unless a period of embargo has been approved by the Dean of the Graduate School.

I acknowledge that copyright of all material contained in my thesis resides with the copyright holder(s) of that material. Where appropriate I have obtained copyright permission from the copyright holder to reproduce material in this thesis and have sought permission from co-authors for any jointly authored works included in the thesis.

Publications during candidature

Thesis related publications

1. Britton LJ, Subramaniam VN, Crawford DHG
   Iron and non-alcoholic fatty liver disease
   World J Gastroeneterol. 22(36): 8112-22, Sep 2016

2. Britton LJ, Jaskowski L, Bridle KR, Santrampurwala N, Reiling J, Musgrave N, Subramaniam VN, Crawford DHG
   Heterozygous Hfe gene deletion leads to impaired glucose homeostasis but not liver injury in mice fed a high calorie diet.
   Physiological Reports. 4 (12), e12837, 2016

3. Britton LJ, Bridle KR, Reiling J, Santrampurwala N, Wockner L, Ching H, Stuart KA, Subramaniam VN, Jeffrey G, St Pierre T, House M, Gummer J, Trengove R, Olynyk J, Crawford DHG, Adams LA
   Hepatic iron concentration correlates with insulin sensitivity in non-alcoholic fatty liver disease
   Hepatology Communications 2018 Apr 27;2(6):644-653

4. Britton LJ, Jaskowski L, Bridle KR, Secondes E, Wallace D, Santrampurwala N, Reiling J, Miller G, Mangiafico S, Andrikopoulos S, Subramaniam VN, Crawford DHG
   Adipocyte-specific Ferroportin knockout in mice: no effect on iron accumulation or metabolic responses to fast food diet
   Cellular and Molecular Gastroenterology and Hepatology 5 (3) 319-331 Mar 2018

5. Britton LJ, Bridle KR, Jaskowski L, He J, Ng C, Ruelcke J, Mohamed A, Reiling J, Santrampurwala N, Hill MM, Whitehead JP, Subramaniam VN, Crawford DHG
   Iron inhibits the secretion of apolipoprotein E in cultured human adipocytes
   Cellular and Molecular Gastroenterology and Hepatology 2018 Apr 16;6(2):215-217

Non-thesis related publications

1. Heritage M, Jaskowski L, Bridle K, Campbell C, Briskey D, Britton L, Fletcher L, Vitetta L, Subramaniam VN, Crawford D.
   Combination curcumin and vitamin E treatment attenuates diet-induced steatosis in Hfe-/- mice.
   World J Gastrointest Pathophysiol. 2017 May 15;8(2):67-76

2. Urea production during normothermic machine perfusion: Price of success?
   Reiling J, Lockwood DS, Simpson AH, Campbell CM, Bridle KR, Santrampurwala N, Britton LJ, Crawford DH, Dejong CH, Fawcett J.
   Liver Transpl. 2015 May;21(5):700-3

3. Low-Dose Lipopolysaccharide Causes Biliary Injury by Blood Biliary Barrier Impairment in a Rat Hepatic Ischemia/Reperfusion Model.
   Reiling J, Bridle KR, Gijbels M, Schaap FG, Jaskowski L, Santrampurwala N, Britton LJ, Campbell CM, Olde Damink SW, Crawford DH, Dejong CH, Fawcett J.
   Liver Transpl. 2017 Feb;23(2):194-206.

4. Heritage M, Jaskowski L, Bridle K, Campbell C, Briskey D, Britton L, Fletcher L, Vitetta L, Subramaniam VN, Crawford D.
   Combination curcumin and vitamin E treatment attenuates diet-induced steatosis in Hfe-/- mice.
   World J Gastrointest Pathophysiol. 2017 May 15;8(2):67-76

5. Reiling J, Bridle KR, Schaap FG, Jaskowski L, Santrampurwala N, Britton LJ, Campbell CM, Jansen PLM, Damink S, Crawford DHG, Dejong CHC, Fawcett J.
   The role of macrophages in the development of biliary injury in a lipopolysaccharide-aggravated hepatic ischaemia-reperfusion model.
   Biochim Biophys Acta. 2017 Jul 12. pii: S0925-4439(17)30226-0. doi: 10.1016/j.bbadis.2017.06.028. [Epub ahead of print]

Thesis related conference abstracts

1. Britton LJ, Jaskowski L, Wilkinson A, Bridle K, Subramaniam N, Crawford D
   Heterozygous deletion of the *Hfe* gene contributes to hepatic iron loading but not steatosis in mice fed a high fat diet.
   Bioiron 2013, London
   American Journal of Hematology: 88(5) E204, May 2013

2. Britton LJ, Jaskowski L, Wilkinson A, Bridle K, Subramaniam N, Crawford D
   Heterozygous deletion of the *Hfe* gene contributes to hepatic iron loading but not steatosis in mice fed a high fat diet.
   Asian Pacific association for the study of the liver, APASL 2013, Singapore
   Liver International 7 Supplement, June 2013

3. Britton LJ, Jaskowski L, Wilkinson A, Bridle K, Subramaniam N, Crawford D
   Heterozygous deletion of the *Hfe* gene contributes to hepatic iron loading but not steatosis in mice fed a high fat diet.
   Australian Gastroenterology Week Oct 2013, Melbourne
   Journal of Gastroenterology and Hepatology: 28 (Suppl S2), Oct 2013

4. Britton LJ, Bridle KR, Reiling J, Santrampurwala N, Wockner L, Ching H, Subramaniam VN, Crawford DHG, Adams LA
   Serum adipokines in response to venesection in patients with non-alcoholic fatty liver disease
   Gastro 2015 (Conference of the World Gastroenterology Organisation), Brisbane
   Journal of Gastroenterology and Hepatology: 30 (Suppl S1), Sept 2015

5. Britton LJ, Bridle K, Jaskowski LA, He J, Ng C, Ruelcke JE, Reiling J, Santrampurwala N, Hill MM, Whitehead JP, Subramaniam VN, Crawford DHG
   Australian Gastroenterology Week 2017, Gold Coast
   Journal of Gastroenterology and Hepatology: 32(Suppl S2), Aug 2017AGW 2017
   Iron blocks the secretion of apolipoprotein E in cultured human adipocytes

Non-thesis related conference abstracts

1. Wilkinson AS, Heritage ML, Jaskowski LA, Britton LJ, Tan TC, Clouston A, Bridle K, Macdonald GA, Anderson G, Fletcher LM, Subramaniam N, Crawford DH
   Curcumin and vitamin E combination treatment reduces the severity of disease in a diet-induced mouse model of NAFLD
   Australian Gastroenterology Week 2012, Adelaide
   Journal of Gastroenterology and Hepatology: 27(Suppl S4), Oct 2012

2. Wilkinson AS, Heritage ML, Jaskowski LA, Britton LJ, Tan TC, Clouston A, Bridle K, Macdonald GA, Anderson G, Fletcher LM, Subramaniam N, Crawford DH
   The progression of NAFLD to NASH in a mouse model of *Hfe*-/- -associated steatohepatitis is attenuated by co-administration of curcumin and vitamin E
   Australian Gastroenterology Week 2012, Adelaide
   Journal of Gastroenterology and Hepatology: 27(Suppl S4), Oct 2012

3. Heritage M, Jaskowski L, Wilkinson AS, Britton LJ, Tan TC, Clouston AD, Bridle K, Anderson GJ, Macdonald GA, Fletcher LM, Subramaniam VN, Crawford DH
   The progression of NAFLD to NASH in a mouse model of *Hfe*-/- associated steatohepatitis is attenuated by coadministration of curcumin and vitamin E. (AASLD 2012, Boston)
   Hepatology: 56 (Suppl S1), Oct 2012

4. Wilkinson AS, Bridle KR, Britton LJ, Jaskowski LA, Fletcher LM, Subramaniam N, Crawford DH
   An iron-deficient diet attenuates diet-induced hepatic steatosis in *HFE*-associated non-alcoholic fatty liver disease using *Hfe*-/- mice
   American association for the study of the Liver – AASLD 2013, Washington D.C.
   Hepatology: 58 (Suppl S1), Oct 2013

5. Wilkinson AS, Bridle KR, Britton LJ, Jaskowski LA, Fletcher LM, Subramaniam N, Crawford DH
   An iron-deficient diet attenuates diet-induced hepatic steatosis in HFE-associated non-alcoholic fatty liver disease using *Hfe*-/- mice
   Australian Gastroenterology Week Oct 2013, Melbourne
   Journal of Gastroenterology and Hepatology: 28 (Suppl S2), Oct 2013

6. Reiling J, Bridle KR, Santrampurwala N, Britton LJ, Crawford DHG, Dejong CHC, Fawcett J
   The potential role of lipopolysaccharides in the development of biliary injury in an animal partial liver ischaemia model.
   Australian Gastroenterology Week 2014, Gold Coast
   Journal of Gastroenterology and Hepatology: 29 (Suppl S2), Oct 2014

7. Reiling J, Lockwood DSR, Simpson AH, Campbell CM, Bridle KR, Santrampurwala N, Britton LJ, Crawford DHG, Dejong CHC, Fawcett J
   Successful ex-vivo normothermic oxygenated machine perfusion of human donor livers.
   Australian Gastroenterology Week 2014, Gold Coast
   Journal of Gastroenterology and Hepatology 29 (Suppl S2), Oct 2014

8. Reiling J, Lockwood DSR, Simpson AH, Campbell CM, Bridle KR, Santrampurwala N, Britton LJ, Crawford DHG, Dejong CHC, Fawcett J
   Successful ex-vivo normothermic oxygenated perfusion of human donor livers
   American association for the study of the liver – AASLD 2014, Boston, U.S.A
   Hepatology: 60 (Suppl S1), Oct 2014

9. Reiling J, Bridle KR, Campbell C, Santrampurwala N, Britton LJ, Dejong CHC, Cohen A, Crawford DHG, Fawcett J
   Pre-treatment with TIMP-3 prevents the development of biliary injury in an LPS-enhanced ischaemia-reperfusion
   GESA Hepatology and Gastrointestinal Research Workshop 2015, Bowral

10. Santrampurwala N, Bridle KR, Reiling J, Britton LJ, Jaskowski LA, Subramaniam VN, Crawford DHG
    Free fatty acid treatment reduces BMP6 signalling in AML12 hepatocytes
    GESA Hepatology and Gastrointestinal Research Workshop 2015, Bowral

11. Santrampurwala N, Bridle KR, Reiling J, Britton LJ, Jaskowski LA, Subramaniam VN, Crawford DHG
    Free fatty acid treatment reduces BMP6 signalling in AML12 hepatocytes
    Gastro 2015 (Conference of the World Gastroenterology Organisation), Brisbane
    Journal of Gastroenterology and Hepatology: 30 (Suppl S1), Sept 2015

12. Reiling J, Bridle K, Thevenot P, Frank A, Campbell C, Santrampurwala N, Britton LJ, Crawford D, Dejong C, Cohen A, Fawcett J
    Pre-treatment with TIMP-3 prevents the development of biliary injury in an LPS enhanced ischaemia-reperfusion animal model
    World Congress of Gastroenterology 2015, Brisbane
    Journal of Gastroenterology and Hepatology: 30 (Suppl S1), Sept 2015

13. Reiling J, Bridle K, Thevenot P, Frank A, Campbell C, Santrampurwala N, Britton LJ, Crawford D, Dejong C, Cohen A, Fawcett J
    Pre-treatment with TIMP-3 prevents the development of biliary injury in an LPS enhanced ischaemia-reperfusion animal model
    American association for the study of the liver – AASLD 2015, San Francisco, U.S.A
    Hepatology: 62 (Suppl S1), Oct 2015

14. Reiling J, Lockwood DSR, Simpson AH, Campbell CM, Bridle KR, Santrampurwala N, Britton LJ, Crawford DHG, Dejong CHC, Fawcett J
    The application of normothermic machine perfusion to bench-test human donor livers
    Australian Gastroenterology Week 2016, Adelaide
    Journal of Gastroenterology and Hepatology: 31 (Suppl S2), Oct 2015

15. Owen NE, Pugh P, Belham M, See TC, Snowdon V, Britton LJ, Alexander GJM, Sen S

    Determining prevalence of cardiopulmonary complications in patients with end stage liver disease

    British Association for the Study of the Liver – BASL 2016, Manchester, U.K.

16. Owen NE, Pugh P, Belham M, See TC, Snowdon V, Britton LJ, Halsall DJ, Alexander GJM, Sen S

    NT-proBNP as a marker for pulmonary hypertension in advanced chronic liver disease

    British Association for the Study of the Liver – BASL 2016, Manchester, U.K.

Publications included in this thesis

1. Britton LJ, Subramaniam VN, Crawford DHG
   Iron and non-alcoholic fatty liver disease
   World J Gastroeneterol. 22(36): 8112-22, Sep 2016
   Incorporated as Chapter 2

Contributor	Statement of contribution
Author Britton LJ (Candidate)	Conception and design (100%) Analysis and interpretation (60%) Drafting and production (60%)
Author Subramaniam VN	Conception and design (0%) Analysis and interpretation (20%) Drafting and production (20%)
Author Crawford DHG	Conception and design (0%) Analysis and interpretation (20%) Drafting and production (20%)

2. Britton LJ, Jaskowski L, Bridle KR, Santrampurwala N, Reiling J, Musgrave N, Subramaniam VN, Crawford DHG
   Heterozygous Hfe gene deletion leads to impaired glucose homeostasis but not liver injury in mice fed a high calorie diet.
   Physiological Reports. 4 (12), e12837, 2016
   Incorporated as Chapter 3

Contributor	**Statement of contribution**
Author Britton LJ (Candidate)	Conception and design (25%) Analysis and interpretation (50%) Drafting and production (60%)
Author Jaskowski L	Conception and design (0%) Analysis and interpretation (20%) Drafting and production (5%)
Author Bridle K	Conception and design (25%) Analysis and interpretation (5%) Drafting and production (10%)
Author Santrampurwala N	Conception and design (0%) Analysis and interpretation (5%) Drafting and production (5%)
Author Reiling J	Conception and design (0%) Analysis and interpretation (5%) Drafting and production (5%)
Author Musgrave N	Conception and design (0%) Analysis and interpretation (5%) Drafting and production (0%)
Author Subramaniam VN	Conception and design (25%) Analysis and interpretation (5%) Drafting and production (5%)
Author Crawford DHG	Conception and design (25%) Analysis and interpretation (5%) Drafting and production (10%)

3. Britton LJ, Bridle KR, Reiling J, Santrampurwala N, Wockner L, Ching H, Stuart KA, Subramaniam VN, Jeffrey G, St Pierre T, House M, Gummer J, Trengove R, Olynyk J, Crawford DHG, Adams LA

   Hepatic iron concentration correlates with insulin sensitivity in non-alcoholic fatty liver disease

   Hepatology Communications, in press, 2018

   Incorporated as Chapter 4

Contributor	**Statement of contribution**
Author Britton LJ (Candidate)	Conception and design (30%) Analysis and interpretation (40%) Drafting and production (45%)
Author Bridle KR	Conception and design (15%) Analysis and interpretation (0%) Drafting and production (5%)
Author Reiling J	Conception and design (0%) Analysis and interpretation (0%) Drafting and production (5%)
Author Santrampurwala N	Conception and design (0%) Analysis and interpretation (0%) Drafting and production (5%)
Author Wockner L	Conception and design (0%) Analysis and interpretation (20%) Drafting and production (0%)
Author Ching H	Conception and design (0%) Analysis and interpretation (5%) Drafting and production (0%)
Author Stuart KA	Conception and design (0%) Analysis and interpretation (0%) Drafting and production (5%)
Author Subramaniam VN	Conception and design (0%) Analysis and interpretation (0%) Drafting and production (5%)
Author Jeffery G	Conception and design (0%) Analysis and interpretation (0%)

	Drafting and production (5%)
Author St Pierre T	Conception and design (0%) Analysis and interpretation (5%) Drafting and production (0%)
Author House M	Conception and design (0%) Analysis and interpretation (5%) Drafting and production (0%)
Author Gummer J	Conception and design (0%) Analysis and interpretation (5%) Drafting and production (0%)
Author Trengrove R	Conception and design (0%) Analysis and interpretation (5%) Drafting and production (0%)
Author Olynyk J	Conception and design (10%) Analysis and interpretation (0%) Drafting and production (5%)
Author Crawford DHG	Conception and design (15%) Analysis and interpretation (0%) Drafting and production (10%)
Author Adams LA	Conception and design (30%) Analysis and interpretation (15%) Drafting and production (10%)

4. Britton LJ, Jaskowski L, Bridle KR, Secondes E, Wallace D, Santrampurwala N, Reiling J, Miller G, Mangiafico S, Andrikopoulos S, Subramaniam VN, Crawford DHG

   Adipocyte-specific Ferroportin knockout in mice: no effect on iron accumulation or metabolic response to fast food diet

   Cellular and Molecular Gastroenterology and Hepatology 5 (3) 319-331 Mar 2018

   Incorporated as Chapter 5

Contributor	**Statement of contribution**
Author Britton LJ (Candidate)	Conception and design (60%) Analysis and interpretation (30%) Drafting and production (60%)
Author Jaskowski L	Conception and design (5%) Analysis and interpretation (30%) Drafting and production (0%)
Author Bridle KR	Conception and design (10%) Analysis and interpretation (5%) Drafting and production (20%)
Author Secondes E	Conception and design (0%) Analysis and interpretation (5%) Drafting and production (0%)
Author Wallace D	Conception and design (5%) Analysis and interpretation (0%) Drafting and production (0%)
Author Santrampurwala N	Conception and design (0%) Analysis and interpretation (5%) Drafting and production (0%)
Author Reiling J	Conception and design (0%) Analysis and interpretation (5%) Drafting and production (0%)
Author Miller G	Conception and design (0%) Analysis and interpretation (5%) Drafting and production (0%)
Author Mangiafico S	Conception and design (0%) Analysis and interpretation (5%)

	Drafting and production (0%)
Author Andrikopoulos S	Conception and design (0%) Analysis and interpretation (5%) Drafting and production (0%)
Author Subramaniam VN	Conception and design (10%) Analysis and interpretation (0%) Drafting and production (0%)
Author Crawford DHG	Conception and design (10%) Analysis and interpretation (5%) Drafting and production (20%)

5. Britton LJ, Bridle KR, Jaskowski L, He J, Ng C, Ruelcke J, Mohamed A, Reiling J, Santrampurwala N, Hill MM, Whitehead JP, Subramaniam VN, Crawford DHG
Iron inhibits the secretion of apolipoprotein E in cultured human adipocytes
Cellular and Molecular Gastroenterology and Hepatology, in press, 2018
Incorporated in published (abridged) form in Appendix A
Incorporated as original full manuscript in Chapter 6

Contributor	**Statement of contribution**
Author Britton LJ (Candidate)	Conception and design (25%) Analysis and interpretation (40%) Drafting and production (50%)
Author Bridle K	Conception and design (10%) Analysis and interpretation (5%) Drafting and production (10%)
Author Jaskowski L	Conception and design (0%) Analysis and interpretation (20%) Drafting and production (0%)
Author He J	Conception and design (5%) Analysis and interpretation (5%) Drafting and production (0%)
Author Ng C	Conception and design (0%) Analysis and interpretation (5%) Drafting and production (0%)
Author Ruelcke J	Conception and design (0%) Analysis and interpretation (5%) Drafting and production (0%)
Author Mohamed A	Conception and design (0%) Analysis and interpretation (5%) Drafting and production (0%)
Author Reiling J	Conception and design (0%) Analysis and interpretation (0%) Drafting and production (5%)
Author Santrampurwala N	Conception and design (0%) Analysis and interpretation (0%) Drafting and production (5%)

Author Hill MM	Conception and design (25%) Analysis and interpretation (5%) Drafting and production (5%)
Author Whitehead JP	Conception and design (25%) Analysis and interpretation (10%) Drafting and production (10%)
Author Subramaniam VN	Conception and design (0%) Analysis and interpretation (0%) Drafting and production (5%)
Author Crawford DHG	Conception and design (10%) Analysis and interpretation (0%) Drafting and production (10%)

Contributions by others to the thesis

Chapter 2

Prof Darrell Crawford provided assistance with critical review of the manuscript.

Prof Nathan Subramaniam provided assistance with critical review of the manuscript.

Chapter 3

Ms Lesley-Anne Jaskowski provided assistance with non-routine technical work, analysis and interpretation of the research data and critical review of the manuscript.

Dr Kim Bridle provided assistance with conception and design of the project, analysis and interpretation of the research data and critical review of the manuscript.

Dr Nishreen Santrampurwala provided assistance with analysis and interpretation of the research data and critical review of the manuscript.

Dr Janske Reiling provided assistance with analysis and interpretation of the research data and critical review of the manuscript.

Dr Nicholas Musgrave provided assistance with analysis and interpretation of the research data (histopathology interpretation).

Prof Nathan Subramaniam provided assistance with conception and design of the project, analysis and interpretation of the research data and critical review of the manuscript.

Prof Darrell Crawford provided assistance with conception and design of the project, analysis and interpretation of the research data and critical review of the manuscript.

Chapter 4

Dr Kim Bridle provided assistance with conception and design of the project, analysis and interpretation of the research data and critical review of the manuscript.

Dr Janske Reiling provided assistance with conception and design of the project, analysis and interpretation of the research data and critical review of the manuscript.

Dr Nishreen Santrampurwala provided assistance with conception and design of the project, analysis and interpretation of the research data and critical review of the manuscript.

Dr Leesa Wockner provided assistance with analysis and interpretation of the research data (statistical support) and critical review of the manuscript.

Ms Helena Ching provided assistance with non-routine technical support (study coordinator), analysis and interpretation of the research data and critical review of the manuscript.

Dr Katherine Stuart provided assistance with analysis and interpretation of the research data and critical review of the manuscript.

Prof Nathan Subramaniam provided assistance with analysis and interpretation of the research data and critical review of the manuscript.

Prof Gary Jeffery provided assistance with analysis and interpretation of the research data and critical review of the manuscript.

Prof Timothy St Pierre provided assistance with analysis and interpretation of the research data (Magnetic Resonance Imaging data) and critical review of the manuscript.

A/Prof Michael House provided assistance with analysis and interpretation of the research data (Magnetic Resonance Imaging data) and critical review of the manuscript.

Dr Joel Gummer provided assistance with non-routine technical support (development and use of hepcidin assays), analysis and interpretation of the research data and critical review of the manuscript.

A/Prof Robert Trengrove provided assistance with non-routine technical support (development and use of hepcidin assays), analysis and interpretation of the research data and critical review of the manuscript.

Prof John Olynyk provided assistance with analysis and interpretation of the research data and critical review of the manuscript.

Prof Darrell Crawford provided assistance with conception and design of the project, analysis and interpretation of the research data and critical review of the manuscript.

Prof Leon Adams provided assistance with conception and design of the project, analysis and interpretation of the research data and critical review of the manuscript.

Chapter 5

Ms Lesley-Anne Jaskowski provided assistance with non-routine technical work, analysis and interpretation of the research data and critical review of the manuscript.

Dr Kim Bridle provided assistance with conception and design of the project, analysis and interpretation of the research data and critical review of the manuscript.

Ms Eriza Secondes provided assistance with non-routine technical work (animal breeding), analysis and interpretation of the research data and critical review of the manuscript.

Dr Daniel Wallace provided assistance analysis and interpretation of the research data and critical review of the manuscript.

Dr Nishreen Santrampurwala provided assistance analysis and interpretation of the research data and critical review of the manuscript.

Dr Janske Reiling provided assistance analysis and interpretation of the research data and critical review of the manuscript.

Dr Gregory Miller provided assistance with analysis and interpretation of the research data (histopathology interpretation) and critical review of the manuscript.

Dr Salvatore Mangiafico provided assistance with non-routine technical work and analysis and interpretation of the research data (hyperinsulinaemic clamp studies).

Prof Sof Andrikopoulis provided assistance with analysis and interpretation of the research data (hyperinsulinaemic clamp studies).

Prof Nathan Subramaniam provided assistance with conception and design of the project, analysis and interpretation of the research data and critical review of the manuscript.

Prof Darrell Crawford provided assistance with conception and design of the project, analysis and interpretation of the research data and critical review of the manuscript.

Chapter 6

Dr Kim Bridle provided assistance with conception and design of the project, analysis and interpretation of the research data and critical review of the manuscript.

Ms Lesley-Anne Jaskowski provided assistance with non-routine technical work, analysis and interpretation of the research data and critical review of the manuscript.

Dr Jingjing He provided assistance with non-routine technical work (tissue culture), analysis and interpretation of the research data and critical review of the manuscript.

Dr Choaping Ng provided assistance with non-routine technical work (tissue culture), analysis and interpretation of the research data and critical review of the manuscript.

Ms Jayde Ruelke provided assistance with non-routine technical work (mass spectrometry), analysis and interpretation of the research data and critical review of the manuscript.

Dr Ahmed Mohamed provided assistance with non-routine technical work (bioinformatics), analysis and interpretation of the research data and critical review of the manuscript.

Dr Janske Reiling provided assistance with analysis and interpretation of the research data and critical review of the manuscript.

Dr Nishreen Santrampurwala provided assistance with analysis and interpretation of the research data and critical review of the manuscript.

A/Prof Michelle Hill provided assistance with conception and design of the project, analysis and interpretation of the research data (mass spectrometry and statistics) and critical review of the manuscript.

Prof Jonathan Whitehead provided assistance with conception and design of the project, non-routine technical work (tissue culture), analysis and interpretation of the research data and critical review of the manuscript.

Prof Nathan Subramaniam provided assistance with analysis and interpretation of the research data and critical review of the manuscript.

Prof Darrell Crawford provided assistance with conception and design of the project, analysis and interpretation of the research data and critical review of the manuscript.

Statement of parts of the thesis submitted to qualify for the award of another degree

None

Research Involving Human or Animal Subjects

Research in Chapters 3 and 5 was approved by the QIMR Berghofer Medical Research Institute's Animal Ethics Committee, under projects P1446, P1462, P1489 with animal ethics approval numbers A1203-602, A1210-611M and A1210-610 respectively.

Research in Chapter 4 was approved by the Greenslopes Private Hospital Human Research Ethics Committee, protocol 11/56, approval date: 9th September 2014.

Approval letters from these committees are included in Appendix B: Ethics committee approvals.

Acknowledgements

Firstly, I wish to thank my exceptional supervisors, Darrell Crawford and Kim Bridle. Darrell, you have provided such expert and calm mentorship. You have always been able to see the big picture and have provided me with boundless enthusiasm, career advice and opportunity. Kim, what can I say? You have dealt with it all, from big picture stuff to the nitty-gritty and everything in between. You have always been enormously supportive. Thank you so much to both of you.

Next I would like to thank Lesley Jaskowski for teaching me nearly everything I know in the lab from PCR to western blots. A huge thanks to you for your patience and for performing lab work so efficiently when deadlines loomed.

Next I would like to thank my buddies who have helped me in the lab, but mostly just kept me entertained over the years. Nishreen and Janske, you have been there for most of it and have given me many laughs. Bijay and Justin, thank you for the late night and weekend debriefs when nothing seemed to be working and we all just decided to keep pushing on. More recently thank you to the new band of PhD students, Ritu, Raji and Sean for all your support.

I have been lucky enough to foster fruitful collaborations with genuine experts in their fields. Jon Whitehead, thank you for teaching me all about adipose tissue and for all your positive energy and encouragement. Also thank you for enlightening me that fat is actually an acronym for “fabulous adipose tissue”. I never knew that. To Michelle Hill, thank you for introducing me to the world of proteomics and for your attention to detail and encouragement always. Thank you to Jacob George for planting the seed of SILAC proteomics in my mind. A major thank you is due to Leon Adams who has collaborated with us on the human study and has always been very open with his time, data and serum samples. Thank you Leon for your encouragement, expertise and fine example of scientific writing.

Graeme Macdonald and Greg Anderson served with Jon Whitehead on my milestone review panel. Thank you to all three of you for your wise counsel and encouragement. I feel that you all contributed to that panel in such a meaningful and constructive way. I suspect many students are not so lucky as to have this experience with their panels.

I wish to thank those that have gone before and have laid such strong foundations in this field for us in Brisbane. We are truly standing on the shoulders of giants. Other than those already mentioned above, I wish to thank in particular, Lawrie Powell, June Halliday and Graham Cooksley who have provided a lasting legacy for hepatology research in Brisbane. Also, thank you to Terrence Tan. Your paper on homozygous *Hfe* knockout was the catalyst for my entire thesis and was the high standard of research and writing that I always aspired in vain to match.

There are countless others that have helped me along the way and not all can be mentioned here. These include Lisa, Jingjing and Chaoping who had the patience to teach me cell culture from scratch. Jayde and Ahmed who made it all possible for me to do a mass spectrometry analysis, which is well beyond what I could ever have imagined doing. Thank you Barbara Matthews for going above and beyond to work out how to measure iron concentration in adipose tissue and adipocytes, when so many others have failed. Thank you Erika and Eriza for your kind heartedness and patience with me.

Thank you Dan for all your expertise and time and helping me to understand nuances in genetics. Thank you Sof and Sal who made the hyperinsulinaemic-euglycaemic clamp studies possible in such a short space of time. Thank you Leesa for helping with the statistics on all chapters, in particular on the human study. Your grasp of biological research statistics, pragmatism and communication skills made it a joy to work with you.

Thank you to Greg Miller and Nick Musgrave. Despite your very busy schedules, you found time to go through endless histology slides with me and the thesis greatly benefits from your expertise.

I am very grateful for the financial support that I have received from the Gastroenterological Society of Australia (GESA) and the Gallipoli Medical Research Foundation (GMRF). In particular I wish to thank Miriam Dwyer, her entire team at the Gallipoli Medical Research Institute and all our wonderful donors who have provided me with world-class facilities and expertise to help get this work done.

I wish to thank all my clinical colleagues and support staff who have kept me going through the years, even those who thought it was mightily amusing to keep asking, “have you still not submitted that PhD?” Particular thanks to all the staff at Queensland Gastroenterology and especially Irene, who always understood the demands on my time.

This PhD has presented me with many unique challenges. To Brad and Jono, enormous thanks to both of you for helping me navigate through it all. It is a privilege to know you. To all my friends and wider family, thank you for all your support.

To my sister, thank you for always encouraging me along the way. To my mother and father, thank you for sacrificing so much for so long to give me opportunity. Thank you for teaching me to always have fun along the way.

To my wife, you have been such an enormous rock of support throughout. I can never ever thank you enough. To my two wonderful daughters, born during the course of these studies, you make it all so special.

Financial support

This research was supported by the Gallipoli Medical Research Foundation, the Gastroenterological Society of Australia and the National Health and Medical Research Council.

Keywords

iron, haemochromatosis, non-alcoholic fatty liver disease, non-alcoholic steatohepatitis, adipokines, insulin resistance, adipocytes

Australian and New Zealand Standard Research Classifications (ANZSRC)

ANZSRC code: 110307 Gastroenterology and Hepatology (100%)

Fields of Research (FoR) Classification

FoR code: 1103 Clinical Sciences (100%)

Dedication

To my hero, my father, Peter Laurence Britton (1942-2008).

Table of Contents

List of Figures

List of Tables

List of abbreviations

AAS: atomic absorption spectroscopy

Adipoq: adiponectin gene

Adipo-R2: adiponectin receptor-2 gene

ALT: alanine aminotransferase

ANCOVA: analysis of covariance

ANOVA: analysis of variance

ApoB100: apolipoprotein B100

ApoE: apolipoprotein E

AST: aspartate aminotransferase

ATF4: Activating transcription factor 4

AUC: area under the curve

β2-mg: beta-2-microglobulin gene

BiP: immunoglobulin binding protein

BMI: body mass index

bp: base pairs

Btf3: basic transcription factor-3 gene

CD: control diet

ChIP: chromatin immunoprecipitation

CHOP: CCAAT/enhancer-binding protein homologous protein

CK-18: cytokeratin-18

Cpt1: carnitine palmitoyl transferase-1 gene

CRN: clinical research network

CRP: C-reactive protein

DAB: 3,3’-diaminobenzidine

DIOS: dysmetabolic iron overload syndrome

DMEM: Dulbecco's Modified Eagle Medium

DMT-1: divalent metal transporter

EDEM: ER-degradation-enhancing-α-mannidose-like protein

EDTA: ethylenediaminetetraacetic acid

EFP: epididymal fat pad

ELISA: enzyme-linked immunosorbent assay

EPIC: European Prospective Investigation in Cancer and Nutrition

ER: endoplasmic reticulum

FAC: ferric ammonium citrate

Fas: fatty acid synthase

FFA: free fatty acids

FFD: fast food diet

FGF-1: fibroblast growth factor-1

FKO: ferroportin knockout

Fpn1: ferroportin gene

Gapdh: glyceraldehyde-3-phosphate dehydrogenase gene

GPX-1: glutathione peroxidase

H&E: haematoxylin and eosin

Hamp1: hepcidin gene

HCD: high calorie diet

HDL: high density lipoprotein

HbA1C: glycosylated haemoglobin

HH: Hereditary hemochromatosis

HIC: hepatic iron concentration

Hmox1: heme oxygenase 1

HMW: high molecular weight

HOMA-IR: homeostatic model assessment of insulin resistance

HRP: horseradish peroxidase

hsCRP: high sensitivity C-reactive protein

Hprt: hypoxanthine guanine phosphoribosyl transferase gene

IL-6: interleukin-6

ISI: insulin sensitivity index

LC-MS/MS: liquid chromatography tandem mass spectrometry

LDL: low density lipoprotein

LMW: low molecular weight

MRI: magnetic resonance imaging

MS: mass spectrometry

NAFLD: non-alcoholic fatty liver disease

NAS: NAFLD activity score

NASH: non-alcoholic steatohepatitis

NHANES: National Health and Nutritional Education Survey

NS: non-significant

NTBI: non-transferrin bound iron

pAKT: phospho-protein kinase B

PBS: phosphate buffered saline

Polr2a: RNA Polymerase II Subunit A gene

Pparα: Peroxisome proliferator activated receptor alpha gene

PVDF: polyvinyldene fluoride

QPPC: Quantitative Proteomics P-value Calculator

RBP-4: retinol binding protein-4

RR: relative risk

RT-qPCR: real-time quantitative polymerase chain reaction

Scd1: stearoyl caA desaturase-1 gene

SFRP5: secreted frizzled related protein 5

SGBS: Simpson-Golabi-Behmel Syndrome

SILAC: stable isotope labelled amino acids in cell culture

SOCS-3: suppressor of cytokine signalling-3

SREBP-1: sterol regulatory element binding protein-1

TMPRSS6: trans-membrane protease serine-6

TNFα: tumour necrosis factor alpha

TFA: trifluoroacetic acid

Tfr1: transferrin receptor-1

VLDL: very low density lipoprotein

WT: wild type

XBP-1: X-box binding protein

8-oxodG: 7,8-dihydro-8-oxo’ deoxyguanosine

Chapter 1 : Introduction

Non-alcoholic fatty liver disease (NAFLD) has emerged as a major 21st century public health problem, affecting around one billion people globally.[1] NAFLD increases the risk of death from liver failure, liver cancer and cardiac disease.[2] The epidemic of obesity and unhealthy lifestyles are undoubtedly major contributors to disease pathogenesis. However, a detailed understanding of the mechanisms leading to liver injury is lacking.[3, 4] A greater understanding of the pathogenesis of NAFLD will be hugely important in order to identify effective treatments for this disease.

Although iron is an essential micronutrient, it is toxic in excess, such as seen in iron overload conditions such as hereditary haemochromatosis (HH).[5] It has been shown that the added insult of NAFLD in HH leads to a greater degree of liver injury.[6] However, the extent of adverse effects of lesser degrees of iron loading on NAFLD pathogenesis and disease progression are less certain. Iron has long been proposed as a co-factor in NAFLD pathogenesis, although a detailed understanding of the interactions between iron and NAFLD have remained elusive.[7, 8] Two particularly relevant aspects of the role of iron in NAFLD pathogenesis relate to the contribution of heterozygous *HFE* gene mutations and the emerging role of iron in the regulation of adipose tissue function.[7, 9]

In this thesis, the effects on NAFLD pathogenesis of dysregulated iron homeostasis in several tissues is examined. This includes the role of dysregulated gut absorption of iron due to HFE and hepcidin deficiency. In addition, the relationships between hepatic iron and insulin resistance are studied. Finally, the effects of adipocyte iron on adipose tissue function are addressed in detail and form the major focus of the latter part of this thesis.

Generally throughout this thesis, the term NAFLD is used rather than non-alcoholic steatohepatitis (NASH), despite steatohepatitis being the more significant lesion on liver histology. There are two reasons for this choice of term. Firstly, it is increasingly recognised that many of the insults previously referred to as “second hits” in Day and James’ two-hit hypothesis [10] have since been shown to drive steatosis itself, leading us to consider NAFLD as a disease of multiple concurrent and additive “hits”. [11] Secondly, much of the proposed effect of iron on NAFLD and NASH pathogenesis relates to insulin resistance, a near universal observation across the spectrum of NAFLD. [12]

Chapter 2 reports on a review of the literature regarding links between iron and NAFLD in humans as well as the proposed mechanisms of co-toxicity of iron and fat determined from animal and tissue culture models.

One such mechanism of iron's involvement in NAFLD pathogenesis relates to mutations in the *HFE* gene. Heterozygous p.C282Y mutations of the *HFE* gene are found in approximately 11% of Caucasian populations and are associated with increased iron stores.[13] Such mutations are very commonly seen in individuals with NAFLD and a role for these mutations in NAFLD pathogenesis has been postulated.[14] Previously it has been shown that homozygous deletion of *Hfe* in mice fed a high calorie diet leads to dysregulated hepatic lipid metabolism, steatohepatitis and early fibrosis, compared to simple steatosis alone in wild-type controls fed the same diet.[15] Chapter 3 examines a mouse model of *Hfe* heterozygous knockout fed a high calorie diet. Effects on iron, glucose and lipid metabolism as well as liver injury are assessed.

Continuing on the theme regarding the impact of modest alterations of iron homeostasis, Chapter 4 explores the relationships between iron and NAFLD in a cohort of human participants with NAFLD. This study focuses on the relationship between iron and multiple measures of insulin resistance, a hallmark feature of NAFLD.[2] In addition the relationships between hepatic iron concentration and polypeptides that undergo regulated secretion from adipose tissue, termed adipokines, are explored. Many adipokines have been shown to have significant roles in promoting insulin resistance and liver injury in NAFLD. [16] Serum concentrations of six such adipokines with established roles in NAFLD pathogenesis, namely adiponectin, leptin, resistin, retinol binding protein-4 (RBP-4), tumour necrosis factor-alpha (TNFα) and interleukin-6 (IL-6) are studied.[16] Adiponectin, leptin, resistin and RBP-4 have all been proposed to be regulated by iron, although substantial human data is lacking.[17-20]

Chapters 5 and 6 continue to focus on adipose tissue as a site of iron-related dysregulation in NAFLD pathogenesis. It is increasingly recognised that adipose tissue function has an important role in metabolic health and also the pathogenesis of insulin resistance and NAFLD.[21] Recently it has been shown that adipocytes utilise much of the same iron handling apparatus as other cells such as hepcidin and transferrin receptor.[22, 23] It has become increasingly recognised that adipose tissue rather than the liver itself, may be the key site at which iron mediates liver injury in NAFLD.[7] Indeed it has recently

been shown that mice fed a high fat diet undergo a repartitioning of iron from the liver to adipocytes, with a four-fold increase in adipocyte iron concentration.[24]

In order to scrutinise the relationships between iron and adipose tissue function, *in vivo* (Chapter 5) and *in vitro* (Chapter 6) models of adipocyte iron overload were developed. Chapter 5 examines the effects of adipocyte specific deletion of the iron-exporter, ferroportin, using a Cre-lox mouse model (*Adipoq-Cre:Fpn1*$^{fl/fl}$) in the setting of a dietary model of NASH (the fast food diet model[25]). Adipocyte specific deletion of ferroportin has been proposed as a method of generating adipocyte specific iron loading in mouse models.[17, 18] However the iron loading phenotype has not been well described and the hepatic effects are unknown. Also, models previously used have relied on an adipocyte protein-2 (AP2) Cre. AP2 has been shown to be expressed in other cell types, in particular macrophages and as such, the AP2-Cre: *Fpn1*$^{fl/fl}$ model may be regarded as insufficiently specific for its purpose.[26] Therefore, the more adipocyte specific Adipoq-Cre,[27] in which a bacterial artificial chromosome with a Cre recombinase in the promoter region of the adiponectin gene (Adipoq) is employed.

In Chapter 6, differentiated human pre-adipocytes, Simpson-Golabi-Behmel Syndrome (SGBS) cells, are exposed to increased concentrations of iron. A proteomic approach is employed to describe the differential secretion of adipokines in response to iron. The technique of stable isotope labelled amino acids in cell culture (SILAC) has enabled a detailed characterisation of the human adipocyte secretome and the effects of iron upon it. This serves as broad platform for multiple funding studies investigating iron-related adipocyte dysfunction.

In Chapter 7, a summary of the major findings from the thesis is made. The potential implications of these findings and future directions for research in this field are discussed in detail.

Chapter 2 : Iron and non-alcoholic fatty liver disease (Literature Review)

In this literature review, the relationships between iron and NAFLD, based on data from tissue culture, animal models and human studies are explored.

This review is published in the World Journal of Gastroenterology.

Britton LJ, Subramaniam VN, Crawford DHG
Iron and non-alcoholic fatty liver disease
World J Gastroeneterol. 22(36): 8112-22, Sep 2016

Iron and non-alcoholic fatty liver disease

Laurence J Britton[1,2,3], V. Nathan Subramaniam[3], Darrell HG Crawford[1,]

1. Gallipoli Medical Research Institute, The University of Queensland, Brisbane, Australia
2. The Princess Alexandra Hospital, Brisbane, Australia
3. QIMR Berghofer Medical Research Institute, Brisbane, Australia

Abstract

The mechanisms that promote liver injury in non-alcoholic fatty liver disease (NAFLD) are yet to be thoroughly elucidated. As such, effective treatment strategies are lacking and novel therapeutic targets are required. Iron has been widely implicated in the pathogenesis of NAFLD and represents a potential target for treatment. Relationships between serum ferritin concentration and NAFLD are noted in a majority of studies, although serum ferritin is an imprecise measure of iron loading. Numerous mechanisms for a pathogenic role of hepatic iron in NAFLD have been demonstrated in animal and cell culture models. However, the human data linking hepatic iron to liver injury in NAFLD is less clear, with seemingly conflicting evidence, supporting either an effect of iron in hepatocytes or within reticulo-endothelial cells. Adipose tissue has emerged as a key site at which iron may have a pathogenic role in NAFLD. Evidence for this comes indirectly from studies that have evaluated the role of adipose tissue iron with respect to insulin resistance. Adding further complexity, multiple strands of evidence support an effect of NAFLD itself on iron metabolism. In this review, we summarize the human and basic science data that has evaluated the role of iron in NAFLD pathogenesis.

Introduction

The worldwide epidemic of obesity has led to a disturbing rise in the incidence of non-alcoholic fatty liver disease (NAFLD) and its complications.[1, 28] NAFLD, regarded as the “hepatic manifestation of the metabolic syndrome”, is now estimated to affect one billion individuals worldwide.[1] Non-alcoholic steatohepatitis (NASH), the aggressive form of the disease, can lead to cirrhosis and liver failure.[2, 29] Indeed, NASH is predicted to soon become the predominant cause of advanced liver disease in the developed world [30] and the leading indication for liver transplantation.[29] NAFLD has also been increasingly recognized as an independent risk factor for the development of type II diabetes mellitus, cardiovascular disease and hepatocellular carcinoma, the latter of which may occur even

in non-cirrhotic individuals.[2, 31, 32] The factors that predispose patients to the development of steatohepatitis and fibrosis in NAFLD are not well understood and effective treatment strategies are lacking.[4]

There is evidence that a modest degree of iron overload is associated with more advanced liver injury in NAFLD, although the mechanisms by which this might occur remain unclear.[7, 8] A syndrome of increased hepatic iron in conjunction with the metabolic syndrome is commonly observed and has been termed dysmetabolic iron overload syndrome (DIOS).[7, 33]

To date, the majority of studies have focused mainly on the role of hepatic iron and mutations in the *HFE* gene, the gene mutated in type 1 hereditary hemochromatosis. Recently, however, it has become increasingly evident, that adipose tissue iron plays an important role in the pathogenesis of insulin resistance and therefore possibly NAFLD.[3, 34]

In this review, the potential involvement of iron in NAFLD pathogenesis is explored using the available data from human studies, as well as animal and cell culture models. In addition, the counterview that implicates NAFLD itself in the dysregulation of iron metabolism is outlined.

Human iron homeostasis

Iron is an essential nutrient required for erythropoiesis and multiple cellular metabolic functions.[35, 36] An excess of iron is also, however, a potent cause of cellular injury from oxidative stress due to the generation of reactive oxygen species by the Fenton reaction.[5] Under usual conditions, intracellular protection from iron-induced oxidative stress is facilitated by sequestration of iron within ferritin.[35]

Total body iron homeostasis is achieved predominantly by regulation of iron release from duodenal enterocytes and macrophages by the hormone hepcidin.[36-38] Predominantly produced by hepatocytes, hepcidin binds the enterocyte basal membrane iron transporter, ferroportin, causing its internalization and eventual degradation, thus reducing iron release from duodenal enterocytes and other cells.[36, 38] Ferroportin has been shown to be highly expressed in enterocytes, reticuloendothelial cells, and more recently, in adipocytes.[17, 36] Thus, hepcidin regulates systemic iron balance by reducing intestinal iron absorption.[36]

An understanding of the regulation of hepcidin (*HAMP*) gene expression has come about from studying human subjects with various forms of hereditary hemochromatosis, and by analysis of gene knockout rodent models. Hepcidin is regulated by many factors, including erythropoiesis, iron status, intracellular oxygen tension and inflammation.[38]

Pathologic states of iron overload often lead to saturation of serum iron transporter, transferrin. As a result, serum levels of toxic non-transferrin bound iron (NTBI) rise. NTBI is readily absorbed by tissues such as the liver and cardiac muscle.[38] Tissue iron overload with NTBI results in increased oxidative stress and lipid peroxidation, leading to organ dysfunction. The common causes of iron overload include hereditary hemochromatosis, iron loading anemias (such as thalassemia) and parenteral iron overload from multiple blood transfusions.[38]

Insulin resistance and the pathogenesis of NAFLD

It has become evident that insulin resistance is associated with a more subtle degree of iron overload than is seen in hereditary hemochromatosis and thalassemia.[7, 8, 34] This is important as insulin resistance is central to the pathogenesis of NAFLD.[2, 39] The presence of abdominal obesity and accompanying insulin resistance provide fertile conditions for the development of NAFLD. Indeed, NAFLD is often considered as the hepatic manifestation of insulin resistance and the metabolic syndrome.[2] Central obesity is associated with adipose tissue dysfunction, characterized by infiltration of adipose tissue with macrophages.[40] Dysfunctional adipose tissue produces adipokines that promote the development of insulin resistance.[34] The key sites of insulin action and resistance are the liver, skeletal muscle and adipose tissue.[41] In adipose tissue itself, insulin resistance potentiates lipolysis of triglycerides by hormone sensitive lipase.[42] This generates the majority of free fatty acid flux to the liver in NAFLD.[43] Insulin resistance in skeletal muscle leads to reduced uptake of glucose, whereas in the liver, insulin resistance enhances gluconeogenesis.[44] The resultant compensatory hyperinsulinemia and relative hyperglycemia promote hepatic *de novo* lipogenesis and cholesterol synthesis and reduced catabolism of free fatty acid by oxidation.[2]

Increased hepatic free fatty acid flux resulting from this dysregulation of hepatic lipid metabolism and more importantly by adipose tissue lipolysis, appears to be central to the pathogenesis of steatohepatitis via direct lipotoxicity.[2, 45, 46] A number of other mechanisms have been well demonstrated to be responsible for not only the development

of steatohepatitis, but also steatosis itself. These mechanisms include dysregulated adipokine production,[16, 21] abnormal bile acid signaling,[47] cytokine mediated effects[48], in particular as a result of increased gut cell permeability and TLR-4 receptor activation,[49] endoplasmic reticulum stress[50, 51] and oxidative stress[48, 52]. Hepatocellular injury promotes cell death and steatohepatitis through a combination of apoptosis and cell necrosis.[2] These mechanisms also contribute to hepatic stellate cell activation and resultant development of hepatic fibrosis.[53]

Iron and insulin resistance

The association between hyperferritinemia, insulin resistance and type II diabetes is compelling. There is an increased prevalence of type II diabetes associated with two common iron overload conditions, HFE-hereditary hemochromatosis (HH) and β-thalassemia major.[34] HH can lead to β-cell pancreatic loss and type I diabetes, but whether HH causes type II diabetes by unmasking insulin resistance through pancreatic β-cell loss or by causing insulin resistance itself remains controversial.[34] Animal data suggest that insulin sensitivity is enhanced in HH, but it has been difficult to tease out the relative contributions of β-cell loss and insulin resistance in human studies.[34, 54] The case of β-thalassemia major is more clear, with evidence suggesting that both β-cell loss and insulin resistance are at play.[34]

In those who have neither hereditary hemochromatosis nor another cause of overt iron overload such as thalassemia, the evidence for a pathogenic role of iron is also strong. In the National Health and Nutritional Education Survey (NHANES), 9486 US adults were studied.[55] The odds ratios for developing diabetes in those with elevated serum ferritin levels were high at 3.61 for women and 4.94 for men.[55] A further analysis of the NHANES cohort revealed that even after accounting for other factors such as age, race, alcohol consumption and C-reactive protein (CRP) levels, elevated serum ferritin concentration still accounted for a two-fold increase in the risk of the metabolic syndrome.[55] The risk of diabetes itself, has been shown to be strongly linked to serum ferritin concentration in healthy women, even within the normal range of ferritin.[56] In 2012, the European Prospective Investigation in Cancer and Nutrition (EPIC)-Potsdam study followed 27,548 European adults for 7 years.[57] In this time, 849 subjects developed type II diabetes. Serum ferritin concentration in the highest vs lowest quintile had a relative risk (RR) of 1.73 for the development of diabetes. This observation was made after adjusting for multiple variables including age, sex, body mass index, waist

circumference, sports activity, education, occupational activity, alcohol, liver function test parameters, high sensitivity CRP (hsCRP), adiponectin, high density lipoprotein (HDL) and serum triglyceride concentration.[57]

A recent review of 43 studies further supported these findings.[58] In this meta-analysis, the cohorts with the highest and lowest quartile of serum ferritin concentration were compared. The multivariable adjusted RR for the presence of diabetes was 1.91. This finding was consistent after including only studies that adjusted for inflammation (mostly hsCRP), RR 1.67. This related to a serum ferritin that was 43.54ng/ml higher in type II diabetics compared to controls. Studies assessing the relationship between type II diabetes and transferrin saturation have yielded conflicting results.[58-60]

The persistence of association between serum ferritin concentration and type II diabetes after correction for hsCRP implies that inflammation alone does not entirely explain the association between hyperferritinemia and diabetes. However, it might be argued that even hsCRP may not reflect subtle degrees of inflammation as strongly as serum ferritin concentration.

Serum ferritin concentration and NAFLD

The association between hyperferritinemia and histologic markers of liver injury in NAFLD is reasonably strong. In 2004, Bugienesi *et al*. found that serum ferritin concentration is not associated with hepatic iron concentration in NAFLD, but is a marker of severe histologic damage.[61] Kowdley *et al*. demonstrated in the large NASH Clinical Research Network (CRN) cohort of 628 patients that a serum ferritin concentration greater than 1.5 times the upper limit of normal was independently associated with advanced fibrosis and increased NAFLD activity score.[62] Sumida *et al*., have demonstrated the utility of incorporating serum ferritin into a clinical scoring system to predict steatohepatitis in Japanese patients with NAFLD.[63]

However, other studies have not found such a clear association.[64, 65] Notably, Valenti *et al*. showed in an Italian cohort of 587 patients with NAFLD that serum ferritin concentration did not predict fibrosis stage >1, although the proportion of patients with fibrosis stage >1 in this cohort was relatively small.[64] As would be expected, serum ferritin concentration was higher in the patients who had hepatic iron staining than those who did not, but those with non-parenchymal iron had much higher ferritin values (606µg/L) than those with hepatocellular iron (serum ferritin 354µg/L) $p<0.0001$. This might suggest that macrophage

iron can cause hyperferritinemia either by direct release of ferritin or cytokine-mediated stimulation of ferritin release by other cells. An earlier study by Chitturi *et al*. of 93 patients with NASH, 33% of whom had advanced fibrosis, found that serum ferritin concentration was not an independent predictor of advanced fibrosis.[66]

In a large prospective population-based study from South Korea, 2410 healthy men aged 30 to 59 without sonographic evidence of steatosis were followed for 7545.9 person years.[67] Of these, 586 (24.3%) patients developed ultrasongraphically detectable fatty liver. Baseline serum ferritin concentration was found to be a strong predictor of steatosis. This evidence is notable as it demonstrates an association early in the disease suggesting that the process that elevates serum ferritin concentration is contributing to NAFLD pathogenesis very early in the disease and pre-dates the development of steatosis. This implies that the ferritin association with NAFLD is not simply a result of NAFLD itself causing hyperferritinemia. Moreover, the results might tend to suggest that the link between hyperferritinemia and NAFLD could be explained by insulin resistance.

The strengths of these studies lie in the large numbers of individuals studied. However, serum ferritin concentration is an imprecise surrogate for body iron stores and its associations with both NAFLD and, type II diabetes are clearly not enough to attribute causality with respect to iron in either of these conditions.

Hepatic iron and NAFLD

The role of hepatic iron in NAFLD pathogenesis has largely focused on the generation of oxidative stress by iron. Given that oxidative stress is an established key component of NASH pathogenesis, [48] a role for iron mediating liver injury in NAFLD via this mechanism has been well studied. In NASH, oxidative stress leads to cell death via depletion of ATP, NAD and glutathione, and by direct damage to DNA, lipids and proteins within hepatocytes.[48] Furthermore, oxidative stress leads to an increase in the production of pro-inflammatory cytokines and a fibrogenic response.[48] Not only does oxidative stress potentiate steatohepatitis, characterized by inflammation and cell death, it can also increase steatosis by preventing the secretion of very low density lipoprotein (VLDL) by causing increased degradation of apolipoprotein B100 (ApoB100).[68] In cultured primary rodent hepatocytes, the iron chelator desferrioxamine was able to restore ApoB100 and enhance VLDL export.[68]

Reduced oxidative stress has been observed in the livers of rats fed an iron-deficient diet and after phlebotomy.[69] In a series of liver biopsies from patients with NAFLD, increased hepatic iron stores were found to be associated with increased lipid peroxidation.[70] In humans, iron overload has been shown to correlate with hepatic immunohistochemical staining for 7,8-dihydro-8-oxo-2' deoxyguanosine (8-oxodG), a product of oxidative damage to DNA.[71] In this study, staining for 8-oxodG was significantly reduced with venesection.[71] Patients with NASH have been shown to have elevated levels of serum thioredoxin, a marker of oxidative stress, which declined following venesection.[72] In cultured AML-12 hepatocytes iron generated oxidative stress and led to impaired insulin signaling.[73]

Iron also appears to have a direct role in the activation of hepatic macrophages and hepatic stellate cells. In humans with NAFLD, reticulo-endothelial iron has been shown to be associated with apoptosis, indicated by increased serum cytokeratin-18 (CK-18) fragments and increased hepatic TUNEL staining of liver sections.[74] *In vitro*, iron activates inflammatory signaling via hepatic macrophages.[75] Recently, dietary iron loading in leptin-receptor deficient mice was found to lead to inflammasome and immune cell activation with hepatocellular ballooning.[76] Furthermore, ferritin treatment of rat hepatic stellate cells has been shown to lead to a pro-inflammatory cascade by nuclear factor kappaB signaling.[77]

Iron may also contribute to liver injury in NAFLD by generating endoplasmic reticulum stress.[50, 51] In a mouse model of dietary iron overload and NAFLD, iron induced an unfolded protein response and endoplasmic reticulum stress.[78] Additionally, hepatic iron loading in mice up-regulates cholesterol biosynthesis pathways and this has been proposed as an additional mechanism of iron-induced liver injury in NASH.[79] The proposed mechanisms relating to hepatic iron in NAFLD pathogenesis are summarized in Table 2.1.

Table 2.1 Proposed mechanisms for the involvement of iron in NAFLD pathogenesis

Site	Mechanism
Hepatic iron	Oxidative Stress[32, 53-57]
	Reduced VLDL export[52]
	Macrophage activation[58-60]
	Stellate cell activation[61]
	Endoplasmic reticulum stress[62]
	Increased cholesterol synthesis[63]
Adipose tissue iron	Reduced adiponectin[19,75]
	Reduced leptin[77]
	Increased resistin[76]
	Increased lipolysis[78,79]

A number of studies have looked at the relationship between hepatic iron concentration (HIC) and liver injury in NAFLD. George *et al*. showed that HIC was associated with increased fibrosis in 51 patients with NASH.[80] Three subsequent and similar studies, however, have failed to reproduce these results.[61, 81, 82] Two much larger studies have looked at the association between hepatic iron (Perls') staining and liver histology in NAFLD with conflicting results. In a study of 587 Italian patients with NAFLD, Valenti *et al*. found that hepatocellular rather than reticulo-endothelial iron was associated with 1.7 fold increased risk of significant fibrosis compared to those without iron staining.[64] Reticulo-endothelial iron was found to have a trend towards an association with a lower risk of significant fibrosis. Nelson *et al*., however, found seemingly contradictory results, with reticulo-endothelial iron being associated with greater risk of advanced fibrosis, lobular inflammation and hepatocellular ballooning in the US cohort of 849 patients enrolled in the NASH Clinical Research Network (CRN) database.[83] In this study, the mean NAFLD Activity Score (NAS) [84] was 4.8 in the reticulo-endothelial iron staining group compared to 4.0 in the hepatocellular iron staining group. The exact reasons for this discrepancy between these two large well-designed studies is unclear, although it is noted that there were some differences between the Italian and US cohorts including the frequency of steatohepatitis and beta-globin mutations.[7]

One might argue, however, that the sum of the human data indicates that if hepatic iron does promote liver injury in NAFLD, then its effect is likely to be relatively small.

Adipose tissue iron and insulin resistance

In recent years, there has been increasing recognition of the role of adipose tissue dysfunction in the development of insulin resistance and NAFLD.[21] Adipose tissue is undoubtedly a significant endocrine organ.[85] It is comprised of adipocytes (fat cells), a mixture of cells categorized as the stromal-vascular fraction including reticuloendothelial cells, predominantly macrophages.[85] Central obesity and the metabolic syndrome are characterized by infiltration of bone marrow-derived macrophages into adipose tissue.[40, 86] Macrophage accumulation in adipose tissue is associated with obesity and the development of NAFLD.[21, 40] A loss of regulatory T-cells and an increase in CD8+ effector T-cells characterizes visceral adipose tissue in insulin resistance.[21, 87, 88] The net effect of this adipose tissue infiltration with immune cells is a state of systemic low grade inflammation that is mediated by a number of adipose tissue cytokines, termed adipokines.[85] Ectopic fat, such as omental (visceral) and epicardial or mediastinal fat, is dysfunctional tissue that is more likely to undergo inflammation.[89] In the case of visceral fat, this inflammation is particularly problematic with regards to liver physiology due to the direct transfer of adipokines to the liver via the portal vein.[16]

Adipokines are polypeptides that are expressed significantly in adipose tissue in a regulated manner.[16] Of these, a number of important macrophage derived adipokines appear to play an important role in the development of NAFLD. Both tumor necrosis factor alpha (TNFα) and interleukin-6 (IL-6) have a pro-inflammatory role that may contribute directly to liver pathology in an endocrine fashion, and also via paracrine mechanisms that influence the production of other adipokines from adipocytes.[21] Adipokines produced by adipocytes which have been shown to influence NAFLD pathogenesis include adiponectin, leptin, resistin, suppressor of cytokine signalling-3 (SOCS-3) and secreted frizzled related protein 5 (SFRP5).[16, 21]

Adipose tissue has been proposed as a site at which iron may have a major pathogenic role in NASH.[7] Unfortunately, to our knowledge, direct human data reporting iron concentrations in visceral adipose tissue and its significance in disease are lacking and this area represents both a target for future research and a technical challenge.

Evidence for the role of adipose tissue iron in NAFLD pathogenesis mainly comes indirectly from the association between adipocyte iron and insulin resistance. In 2012, Gabrielsen *et al*. demonstrated that adipocyte iron reduced adiponectin gene expression, serum adiponectin levels and glucose tolerance in an adipocyte-specific *Ferroportin* knockout mouse model.[17] Using the novel Ap2-Cre:Fpn$^{fl/fl}$ model they were able to selectively load iron into adipocytes. The model was developed following the observation that adipocytes are high expressers of ferroportin.[17] Using cultured pre-adipocytes (3T3-L1 cells) and chromatin immunoprecipitation (ChIP) analysis, iron was shown to alter acetylation and binding of the forkhead transcription factor Foxo1 to adiponectin gene promoter binding sites. In a human arm of the same study, they were able to demonstrate an inverse correlation between serum ferritin concentration and adiponectin that was independent of inflammation. This observation has subsequently been replicated in 492 Dutch individuals with risk factors for type II diabetes.[90] Moreover, in obese patients undergoing bariatric surgery, two gene expression markers of increased adipocyte iron loading: increased hepcidin gene (*HAMP)* mRNA expression and decreased transferrin receptor 1 (*Tfr1*) mRNA expression were associated with reduced quantities of *Adipoq* (adiponectin gene) mRNA.[91]

Iron-mediated dysregulation of two other adipokines has been demonstrated in rodent models. Dongiovanni *et al*. have shown that dietary iron loading in mice leads to increased expression of resistin via SOCS-3 which are mediators of insulin resistance.[19] Recently, data from mouse and 3T3-L1 cell culture models found that iron down-regulates the expression of the appetite-suppressing adipokine, leptin – a hormone strongly implicated in NAFLD pathogenesis.[16, 18] Intriguingly, this may help explain the symptom of anorexia in iron deficiency, although the significance of these findings in NAFLD is uncertain.

Adipose tissue iron has been shown to directly enhance lipolysis in isolated rat adipocytes and cultured 3T3-L1 cells.[92, 93] As adipose tissue is the predominant source of free fatty acid flux to the liver [43], this is potentially a very important mechanism of adipose tissue iron action in NAFLD, although these findings are yet to be demonstrated in animal models or humans. Potential mechanisms relating to adipose tissue iron in NAFLD pathogenesis are summarized in Table 2.1.

In summary, iron has been increasingly recognized as a regulator of adipose tissue function. Evidence supports a role for iron in the regulation of adipose tissue inflammation,

adipokine regulation and adipose tissue lipolysis. At present, most of the evidence supports a role for adipose tissue iron in the pathogenesis of insulin resistance and type II diabetes, although clearly these mechanisms may be highly relevant in NAFLD.

Iron-related genetic polymorphisms in NAFLD pathogenesis

The most common inherited disorder affecting the hepcidin-ferroportin axis is type I hereditary hemochromatosis.[5, 38] This usually results from homozygous p.C282Y mutation of *HFE* (HFE-hemochromatosis).[94] The additional insult of NAFLD acts as a co-factor for the development of liver injury in C282Y homozygotes with hereditary hemochromatosis.[6] In non-hemochromatotics, the broader significance of *HFE* gene mutations as co-factors in the pathogenesis of NAFLD has received intense interest in recent years. The two most significant *HFE* mutations in Caucasian populations are the p.C282Y and p.H63D mutations.[38]

Heterozygosity for the C282Y mutation is found in approximately 10-11% of individuals in Caucasian populations.[13, 95] C282Y heterozygosity is associated with a mild increase in serum iron markers, but not with overt hemochromatosis.[13]

Many studies have looked at the association between *HFE* gene mutations and the incidence of NAFLD, but with conflicting results. These studies may have been limited by inadequate statistical power and heterogeneity of the cohorts. In 2011, Hernaez *et al*. published the results of a meta-analysis of 13 case-control studies specifically aimed at determining the association between *HFE* gene mutations and NAFLD.[96] In contrast to a previous meta-analysis by Ellervic *et al*., [14] they found no association between the C282Y/C282Y genotype and NAFLD. Similarly the presence of neither the C282Y mutation nor the H63D mutation resulted in an increased risk of NAFLD in Caucasians. In a sub-analysis of three studies of non-Caucasians, an association was found between the presence of the H63D mutation and the presence of NAFLD.[96]

A limitation of the meta-analysis, as noted by its authors, is that it was not able to determine whether *HFE* gene mutations might have a disease modifying role in subjects after they have developed NAFLD.[96] This study appears to show that *HFE* gene mutations are generally no more common in subjects with NAFLD than in those without, however, the investigators were unable to determine whether those patients with NAFLD and *HFE* gene mutations are more likely to develop steatohepatitis and progressive liver injury than those without mutations.

The issue concerning the effect of heterozygous mutations in progression to NASH was highlighted by an analysis of *HFE* mutations within the NASH CRN cohort.[97] This is a well-defined cohort of patients with biopsy proven NAFLD. Subjects with the H63D mutation had higher steatosis grades and NAS than their wild-type controls. However, those NAFLD patients with C282Y mutations had lower rates of hepatocyte ballooning and steatohepatitis.

Our group has previously shown that mice with homozygous knockout of the *Hfe* gene develop severe steatosis, steatohepatitis and early fibrosis when fed a high fat diet, whereas wild-type mice develop mild steatosis and no steatohepatitis or fibrosis when fed the same diet.[15] *Hfe* null mice had only modest increases in HIC, and it was proposed that the increased histologic injury seen in these animals may have been due to the lack of HFE protein rather than iron overload *per se*. *Hfe* null mice demonstrated dysregulated hepatic lipid metabolism with increased transcription of genes associated with *de novo* lipogenesis and reduced transcription of those associated with fatty acid oxidation.[15]

A number of other non-*HFE* iron-loading polymorphisms have been proposed as modulators of NAFLD pathogenesis.[7, 98] Of these, the A736V polymorphism of the *Trans-membrane protease serine-6 (TMPRSS6)* gene has been studied in patients with NAFLD. The *TMPRSS6* gene encodes for matriptase-2, an enzyme responsible for hemojuvelin cleavage that inhibits the bone morphogenetic protein-6 (BMP-6) pathway, thus reducing hepcidin expression and increasing duodenal iron absorption.[38, 98] Of 216 Italian patients with NAFLD, 38% had the AA genotype, 47% AV and, 15% VV.[98] The VV genotype is associated with increased hepcidin expression and reduced iron loading and in this study was associated with a trend (p=0.05) towards a reduction in hepatocyte ballooning.[98]

In summary, human and animal model data support a role for a co-toxic liver injury in the setting of hereditary hemochromatosis and NAFLD. Other more mild iron loading phenotypes such as heterozygous *HFE* gene mutations and polymorphisms of *TMPRSS6* may have disease modifying roles in NAFLD, although their effect is likely to be small.

Clinical trials of iron reduction therapy

Although associations of modest iron overload with NAFLD and diabetes appear reasonably well established, causality is difficult to determine using these studies alone.

The most useful information with which to more directly assess causality comes from human studies that have assessed the response to iron removal by venesection.

Venesection has been shown to improve glucose tolerance in healthy individuals and improve insulin sensitivity in type II diabetics with a high serum ferritin concentration.[99, 100] Moreover, in patients with the metabolic syndrome, venesection has been shown to improve metabolic syndrome parameters, including reduced blood pressure, blood glucose, glycosylated hemoglobin (HbA1C) and low-density lipoprotein/high density lipoprotein (LDL/HDL) ratio.[101] In patients with NAFLD and carbohydrate intolerance, venesection to near iron deficiency (decrease in serum ferritin from 299 ±41µg/L to 15±1µg/L) not only improved insulin sensitivity, as measured by fasting glucose, insulin and homeostatic model assessment-insulin resistance (HOMA-IR) score, but also improved serum alanine aminotransferase levels from 61 ± 5U/L to 32 ± 2U/L.[102]

Two randomized controlled trials investigating venesection efficacy in NAFLD have recently been published. In a study of 38 Italian patients with NAFLD and hyperferritinemia, participants were randomized to venesection versus no venesection with liver biopsy before and after treatment.[103] Of the 38 enrolled participants, 21 underwent liver biopsy at the end of treatment. Despite the small numbers, histological improvement, defined by an improvement in NAS, was seen in 8 of 12 participants in the venesection group compared to 2 of 9 participants in the control group (p=0.04).[103]

The largest randomized study of venesection in NAFLD to date involved 74 Australian participants with NAFLD.[104] These included patients with sonographically detected NAFLD and a wide range of serum ferritin concentration, including many within the normal range. Non-invasive assessment was performed to assess response to randomized therapy of either venesection with lifestyle advice versus lifestyle advice alone. There was no observed effect of venesection on hepatic steatosis determined by magnetic resonance imaging, serum ALT or CK-18 fragments. Somewhat surprisingly, there was also no effect on static and dynamic measures of glucose homeostasis including the HOMA-IR score and insulin sensitivity index.[104]

Overall, although there are promising results from small studies, venesection cannot currently be recommended as a suitable therapy for the majority of patients with NAFLD.[105] However, whether there are sub-groups of non-hemochromatotic NAFLD patients with increased iron that would benefit from venesection, remains to be determined by further studies.

Iron metabolism in NAFLD

So far, we have discussed the effect of iron on the pathogenesis of NAFLD and insulin resistance. It is also necessary to consider to what extent NAFLD and associated conditions, such as insulin resistance and obesity, might themselves mediate iron metabolism.

Serum hepcidin levels are typically elevated in individuals with NASH.[106] As this in itself fails to explain iron loading in NASH, one might consider that dysregulated iron metabolism occurs in NASH independently of hepcidin. In this regard, *Transferrin receptor-1* (*Tfr1*) has been shown to be upregulated as a consequence of a high fat diet in mice which may lead to hepatocellular uptake in NAFLD despite already increased hepatocellular iron.[107] Also, divalent metal transporter 1 (DMT-1), which is responsible for import of iron from the duodenal lumen into enterocytes is up-regulated in patients with NASH, despite increased serum hepcidin.[108] Another intriguing finding is that increased red cell fragility in response to a high fat diet in rabbits leads to increased erythrophagocytosis.[109] This may explain increases in hepatic reticuloendothelial iron that have been observed in some NASH cohorts.[83]

It seems likely that elevated hepcidin in NASH is either a reflection of hepatocellular inflammation or simply that increased iron, which induces hepcidin, pre-dates the development of NASH. Indeed, hepcidin expression appears to be directly enhanced by insulin and down-regulated in the setting of insulin resistance, thus indicting a possible mechanism for iron loading as an early event in the pathogenesis of NAFLD and type II diabetes.[110] Furthermore, it has been observed that hepcidin is expressed in white adipose tissue and is increased in obesity.[23] Although the contribution of adipose tissue-derived hepcidin to the serum hepcidin pool is uncertain, this is another potential factor that may explain increased serum hepcidin in NASH. Further complexity in these relationships arises when one considers that iron deficiency has been shown to be associated with obesity and in women with obesity and NAFLD.[111, 112] Together, these findings suggest that the interaction between iron and lipid metabolism is multi-faceted. It seems that ‘just enough’ but ‘not too much’ iron may be critical in preventing dysfunctional lipid metabolism.

If one accepts a causal role for iron in NASH pathogenesis, then variations in dietary iron may explain much of the spectrum of iron loading in NASH. Although there is no specific evidence relating iron intake to NASH pathogenesis in humans, increased dietary iron,

particularly from red meat, seems to predispose individuals to the development of insulin resistance and type II diabetes.[113-115]

Conclusions

In summary, there is considerable evidence that links increased iron stores with insulin resistance and NAFLD. This includes a number of studies that have identified serum ferritin concentration as a predictor of liver injury. Hepatic iron itself is attractive culprit for liver injury, although the cellular location of iron within the liver may vary between genetically distinct populations. Increasingly, adipose tissue iron has been linked with adipose tissue dysfunction, including the dysregulation of adipokines, enhanced adipose tissue lipolysis and adipose tissue inflammation. These are plausible candidate mechanisms that may link adipose tissue iron to liver injury. However, assessment of adipose tissue iron concentrations in individuals with well characterized NAFLD remains a goal for future studies.

Iron-related genetic polymorphisms, such as those of the *HFE* gene, may contribute to NAFLD pathogenesis, although it would appear that, other than for individuals with hereditary hemochromatosis, the effect of these polymorphisms, is likely to be small. The complexity of these relationships between iron and NAFLD is further increased when one considers the possibility that NAFLD itself is likely to have a number of effects on iron metabolism.

Finally, venesection studies have offered a unique opportunity with which to assess causality of iron loading in the pathogenesis of NAFLD. The available data suggest that venesection is unsuitable as a general treatment for all patients with NAFLD. Therefore, the key for future human studies will be to determine whether a subset of patients with NAFLD can be identified that might still benefit from therapeutic manipulation of iron homeostasis.

Chapter 3 : Heterozygous *Hfe* gene deletion leads to impaired glucose homeostasis but not liver injury in mice fed a high calorie diet

As described in Chapter 2, numerous human studies have evaluated the links between *HFE* gene mutations and NAFLD. It has previously been shown that homozygous deletion of *Hfe* in mice leads to a far greater severity of liver injury than wild-type mice when exposed to a high calorie diet.[15] The effects of heterozygous *Hfe* deletion, analogous to commonly observed heterozygous mutations have not been well studied in animal models of NAFLD. In this chapter, the effects of heterozygous *Hfe* gene deletion in a dietary mouse model of NAFLD are studied.

This chapter is published in Physiological Reports.

Britton LJ, Jaskowski L, Bridle KR, Santrampurwala N, Reiling J, Musgrave N, Subramaniam VN, Crawford DHG
Heterozygous Hfe gene deletion leads to impaired glucose homeostasis but not liver injury in mice fed a high calorie diet.
Physiological Reports. 4 (12), e12837, 2016

Heterozygous Hfe gene deletion leads to impaired glucose homeostasis but not liver injury in mice fed a high calorie diet

Laurence Britton[1,2,3,4], Lesley Jaskowski[1,2,4], Kim Bridle[1,2], Nishreen Santrampurwala[1,2,4], Janske Reiling[1,2,3,5], Nick Musgrave[6], V. Nathan Subramaniam[4*], Darrell Crawford[1,2*]

1. Gallipoli Medical Research Foundation, Greenslopes Private Hospital, Greenslopes, Queensland, Australia
2. The University of Queensland, Herston, Queensland, Australia
3. Princess Alexandra Hospital, Queensland, Australia
4. QIMR Berghofer Medical Research Institute, Herston, Queensland, Australia
5. Maastricht University, Maastricht, The Netherlands
6. Sullivan and Nicolaides Pathology, Greenslopes Private Hospital, Greenslopes, Queensland, Australia

*Joint senior authors

Abstract

Background & Aims: Heterozygous mutations of the *HFE* gene have been proposed as co-factors in the development and progression of non-alcoholic fatty liver disease (NAFLD). Homozygous *Hfe* deletion previously has been shown to lead to dysregulated hepatic lipid metabolism and accentuated liver injury in a dietary mouse model of NAFLD. We sought to establish whether heterozygous deletion of *Hfe* is sufficient to promote liver injury when mice are exposed to a high calorie diet (HCD). **Methods:** Eight-week-old wild type and *Hfe*$^{+/-}$ mice received eight weeks of a control diet or HCD. Liver histology and pathways of lipid and iron metabolism were analyzed. **Results:** Liver histology demonstrated that mice fed a HCD had increased NAFLD activity score (NAS), steatosis and hepatocyte ballooning. However, liver injury was unaffected by *Hfe* genotype. Hepatic iron concentration (HIC) was increased in *Hfe*$^{+/-}$ mice of both dietary groups. HCD resulted in a hepcidin-independent reduction in HIC. *Hfe*$^{+/-}$ mice demonstrated raised fasting serum glucose concentrations and HOMA-IR score, despite unaltered serum adiponectin concentrations. Downstream regulators of hepatic *de novo* lipogenesis (pAKT, SREBP-1, *Fas*, *Scd1*) and fatty acid oxidation (*AdipoR2*, *Pparα*, *Cpt1*) were largely unaffected by genotype. **Conclusions:** Heterozygous *Hfe* gene deletion is associated with impaired iron

and glucose metabolism. However, unlike homozygous *Hfe* deletion, heterozygous gene deletion did not affect lipid metabolism pathways or liver injury in this model.

Background

Non-alcoholic fatty liver disease (NAFLD) is increasingly common in the developed and developing world, affecting around 30% of many adult populations [116, 117]. The advanced form of the disease, non-alcoholic steatohepatitis (NASH) can lead to life-threatening complications including liver failure and liver cancer [2]. At present, effective treatment strategies to halt or reverse the natural history of NASH are lacking. Co-factors such as type II diabetes mellitus and iron overload have been implicated in NASH pathogenesis and represent readily treatable therapeutic targets [3, 7]. A greater understanding of the mechanisms by which such co-factors promote NASH disease progression is essential in order to develop effective treatments.

Iron overload due to homozygous p.C282Y mutation of *HFE* is responsible for the majority of cases of hereditary hemochromatosis seen worldwide [118]. Heterozygous p.C282Y mutations are found in approximately 11% of Caucasian populations and are associated with increased iron stores, but not with liver disease in the absence of an additional co-factor [13]. In a large meta-analysis, *HFE* gene mutations have been shown to convey an increased risk of non-alcoholic steatohepatitis [14]. Amongst individuals with NAFLD, the presence of the heterozygous p.H63D mutation of *HFE* has been shown to be associated with more advanced histological injury as assessed by the NAFLD activity score [97].

Liver injury in both hemochromatosis and NASH is characterized by the presence of oxidative stress [48, 118]. Insulin resistance, itself associated with oxidative stress, is commonly observed both in individuals with NASH and also in those with hemochromatosis [3, 34]. Given the prevalence of *HFE* gene mutations and shared pathogenic mechanisms with NASH, they have received intense interest in recent years as potential co-factors in NAFLD disease progression.

Previous work from our group has demonstrated that mice with homozygous *Hfe* deletion which are fed a high calorie diet (HCD) develop steatohepatitis and early fibrosis [15]. This effect of diet is not seen in wild type controls which develop only simple steatosis. In this model, *Hfe* null mice demonstrated up-regulation of gene expression of *de novo* lipogenesis pathways and down-regulation of fatty acid oxidation pathways. This imbalance of fatty acid synthesis and oxidation, may explain the liver injury seen in these

Hfe null mice. However, the mechanisms by which *Hfe* deletion might dysregulate hepatic lipid metabolism remain to be defined.

These findings led us to consider whether a partial deficiency of functional HFE, as seen in those with heterozygous C282Y and H63D mutations, might be sufficient to dysregulate hepatic lipid metabolism and promote liver injury in NAFLD. In this paper, we sought to explore the mechanisms of interaction between heterozygous *HFE* gene mutations and non-alcoholic fatty liver disease. We hypothesized that heterozygous *Hfe* deletion promotes dysregulated hepatic lipid metabolism as seen in the homozygous model. To test this hypothesis, we used a high calorie diet model of NAFLD in mice with and without heterozygous deletion of *Hfe*.

Methods

Experimental Animals: Eight-week-old male C57BL6/J *Hfe*$^{+/-}$ mice (bred at the QIMR Berghofer Medical Research Institute, Brisbane, Australia) and wild-type (WT) littermate controls were assigned to receive a control diet (CD) or a high calorie (40.5% sucrose, 23.5% fat, 0.19% cholesterol by weight) diet (HCD), for eight weeks (n=10 per group). The constituents of these diets are summarized in Table 3.1. Both diets contained 1.3μmol/g iron. The high calorie diet is analogous to a 'Western' style diet, containing a high content of fat, simple carbohydrates and cholesterol [15]. Both diets were supplied by Specialty Feeds, Glen Forrest, Western Australia. All animals were cared for in accordance with the NHMRC code for the care and use of animals for scientific purposes and with approval of the Animal Ethics Committee of the QIMR Berghofer Medical Research Institute. Mice were housed in a temperature controlled environment (23°C) with a 12:12 hour light: dark cycle. Mice had *ad libitum* access to diet and water.

Table 3.1: Major components of experimental diets

Dietary Component	Control Diet (CD)	High Calorie Diet (HCD)
Protein (% weight)	19.4%	19.4%
Total fat (% weight)	7.0%	23.0%
Total carbohydrate (% weight)	61.7%	50%
Digestible energy (MJ/kg)	16.1	20
Cholesterol (% weight)	0%	0.19%
Casein (acid) (g/kg)	200	200
Sucrose (g/kg)	100	405
Canola oil (g/kg)	70	50
Cellulose (g/kg)	50	50
Wheat starch (g/kg)	404	50
Dextrinized starch (g/kg)	132	0
Cocoa butter (g/kg)	0	50
Hydrogenated vegetable oil (g/kg)	0	131

Sixteen-week-old mice were sacrificed by general anesthesia with intraperitoneal injection of ketamine and xylazine, following a five hour fast. Blood was collected by cardiac puncture and serum was stored at -80°C. Livers were excised, and pieces of tissue were either dried at 100°C for 72 hours for hepatic iron concentration determination, fixed in formalin for histology or snap frozen in liquid nitrogen and stored at -80°C. Small bowel enterocytes were collected as previously described [119, 120]. In brief, 10 cm sections of proximal small bowel were cut longitudinally then washed in ice cold phosphate buffered saline (PBS). Samples were then gently rotated for 30 minutes at 4ºC in 1.5mM ethylenediaminetetraacetic acid (EDTA) in PBS. The gut tissue was removed and the remaining sample containing enterocytes was centrifuged at 500 x g to pellet the enterocytes.

Histological assessment: Formalin fixed samples were embedded in paraffin. Sections were stained with hematoxylin and eosin (H&E) for assessment of liver injury. Sirius Red staining was used to detect the presence of hepatic fibrosis. Histological scoring was performed by an expert histopathologist blinded to the study groups according to criteria described by Kleiner et al [84].

Hepatic iron concentration: Oven dried liver samples were weighing 4-9mg were added to 300µL of concentrated nitric acid. Duplicate samples for each liver were then digested in a heated sand bath. Chromagen reagent was prepared (0.1% banthophenanthroline sulphate, 1% mercaptoacetic acid). One part chromagen reagent was added to five parts saturated sodium acetate to make working chromagen reagent immediately prior to use. When fully digested, the volume of each sample was determined by pipette and 25µL was added to 125µL working chromagen reagent. Absorbance was measured at 540nm on a plate reader, Tecan infinite F200, Tecan, Switzerland. The iron concentration by dry weight was determined with reference to an iron standard (Iron standard for AAS, Sigma, St. Louis, USA).

Serum analysis: Serum alanine aminotransferase (ALT) was measured on a Beckman (DxC800) General Chemistry Automated Analyzer (Beckman Coulter, Fullerton, USA). Serum glucose and insulin were measured on a Cobas Integra 400 Chemistry Automated Analyzer (Roche Diagnostics, Basel, Switzerland).

RNA extraction and real-time quantitative PCR (RT-qPCR): RNA was extracted from tissue homogenates using QIAZOL reagent (Qiagen, Hilden, Germany). After treatment with deoxyribonuclease 1, cDNA was synthesized from 1µg RNA, using superscript III reverse transcriptase (Invitrogen, Mulgrave, Australia). RT-qPCR was performed in a ViiA 7 real-time PCR machine (Invitrogen) with a Quantifast SYBR Green master mix (Qiagen) and thermal cycling as follows: 95ºC for 5 minutes then 40 cycles at 95ºC for 10 seconds followed by 60ºC for 30 seconds prior to a melt curve analysis for validation. Relative mRNA expression was determined by calibration of Ct values to a standard curve of dilutions of a pooled mix of cDNA samples. Expression was then normalized to geometric mean of three reference genes Glyceraldehyde 3-phosphate dehydrogenase (*Gapdh*), Basic transcription factor-3 (*Btf3*) and Beta-2 microglobulin (*B2-mg*). Primer sequences that were used are shown in table 3.2.

Table 3.2: RT-qPCR primer sequences (5' to 3')

	Forward primer	**Reverse primer**
Hamp1	TTGCGATACCAATGCAGAAG	GGATGTGGCTCTAGGCTATGTT
Dmt1	CCAGCCAGTAAGTTCAAGGATC	GCGTAGCAGCTGATCTGGG
Hephaestin	CCGACCTTACACCATTCACC	GGACAGAATCATCCGCTTTC
Fas	TACCAAGCCAAGCACATTCG	TGGCTTCGGCATGAGA
AdipoR2	TACACACAGAGACGGGCAAC	TGGCTCCCAAGAAGAACAAG
Pparα	CATGTGAAGGCTGTAAGGGCTT	TCTTGCAGCTCCGATCACACT
Cpt1	AGACCGTGAGGAACTCAAACCTA	TGAAGAGTCGCTCCCACT
Gapdh	TCCTGCACCACCAACTGCTTAGC	GCCTGCTTCACCACCTTCTTGAT
Btf3	TGGCAGCAAACACCTTCACC	AGCTTCAGCCAGTCTCCTTAAAC
B2-mg	CTGATACATACGCCTGCAGAGTTAA	ATGAATCTTCAGAGCATCATGAT

Western blotting: Serum adiponectin levels were determined by western blotting. Samples of 1:1000 serum (5µL) were electrophoresed in 2% Agarose (in Tris-Glycine) gels (Lonza, Basel, Switzerland) at 70V for 60 minutes. Protein levels of phosphoAKT (pAKT) and sterol regulatory element binding protein-1 (SREBP-1) were determined using western blotting of liver tissue extracts. Protein concentration was quantified using a Pierce BCA Protein Assay Kit (Thermo Scientific, Rockford, USA). 30µg of protein from whole liver protein extracts (pAKT) and 20µg of protein from liver nuclear extracts (SREBP-1) were electrophoresed in 10% sodium dodecyl sulfate-10% polyacrylamide gels for 10 minutes at 75V then 50 minutes at 150V. Samples were then transferred onto polyvinylidene fluoride (PVDF) membranes (BioRad, Hercules, USA) at 100V for 60 mins. Membranes were blocked in 5% skim milk before immunostaining with primary antibodies. Secondary antibody binding was performed using horseradish peroxidase (HRP) antibodies (see supplementary information). Visualization was performed using a standard chemiluminescent kit (Supersignal West Femto, Thermo Scientific, Waltham, USA) on a 4000MM pro Image Station (Carestream Health, Inc., New York, USA). pAKT and SREBP-1 band net intensity were normalized to the reference proteins GAPDH and Histone-H3 respectively. Primary and secondary antibodies used for Western blots were as follows: Adiponectin: (MAB3608, Millipore) 1:10,000, Goat anti-mouse HRP (Invitrogen) 1:200,000; pAKT: (sc-7985-R, Santa Cruz) 1:1000, Goat anti-rabbit HRP (Invitrogen) 1:200,000**;** SREBP-1: (sc-367, Santa Cruz) 1:500, Goat anti-rabbit HRP (Invitrogen). 1:100,000**;** GAPDH: (MAB374, Millipore) 1:150,000, Goat anti-mouse HRP (Invitrogen) 1:100,000;

Histone-H3: (FL-136, sc10809, Santa Cruz) 1:100, Goat anti-rabbit HRP (Invitrogen). 1: 6000. All samples were processed concurrently using three gels with a minimum of three samples per group on each gel.

Statistical analysis: Statistical analysis was performed using GraphPad Prism 6 software (GraphPad, San Diego, CA, USA). For normally distributed continuous data, groups were compared using two-way ANOVA based on diet and genotype. For instances in which a significant interaction existed between diet and genotype, two pre-defined post-hoc comparisons to evaluate the effect of genotype for each diet were performed using Sidak's multiple comparisons test. These comparisons were: i) WT CD vs *Hfe*$^{+/-}$ CD and ii) WT HCD vs *Hfe*$^{+/-}$ HCD. In cases in which a significant interaction did not occur, p values relating to overall effect by two-way ANOVA of diet and genotype are reported. As initial body weight was measured prior to dietary intervention, an analysis between the two genotypes (n=20 per group) was performed using an unpaired Student's t-test.

For continuous data that were not normally distributed, a Kruskal-Wallis test was performed. When the results of this test were significant ($p<0.05$), post-hoc comparisons to evaluate the effect of genotype were performed using Dunn's multiple comparisons test (group comparisons as for Sidak's, above). Data for continuous variables are represented graphically with box and whisker plots, demonstrating the maximum, minimum, 25th and 75th centile and median values. Categorical data were analyzed by Fisher's exact test and represented in tabular form.

Results

Weight gain between 8 and 16 weeks of age was largely comparable between genotypes except for a small increase in weight gain in WT HCD fed mice compared to their *Hfe*$^{+/-}$ counterparts (13.1g vs 11.0g, p=0.04, Sidak's multiple comparison test after two-way ANOVA). (figure 3.1A and 3.1B). This effect may be related to a higher initial weight at 8 weeks in WT mice. (28.4g vs 26.0g, p=0.016). The higher initial weight is unlikely to be a true genotype effect as a difference was not seen between the two CD groups. All four groups of mice (CD and HCD) had been fed only CD diet up until this stage. Mean initial weight for all WT mice (n=20) was 27.5g, compared to 26.9g for *Hfe*$^{+/-}$ mice (n=20) p=0.39 (Student's t-test).

Figure 3.1: Body weight and serum ALT.

(A) Initial body weight (8 weeks). An interaction between diet and genotype was present (p=0.0044, two-way ANOVA). Post hoc analysis found increased weight in WT mice fed a HCD compared to *Hfe*$^{+/-}$ mice (p=0.016, Sidak's multiple comparisons test). No significant changes were seen in CD mice. (B) Weight gain (8 to 16 weeks). An interaction between diet and genotype was present (p=0.040, two-way ANOVA). Post hoc analysis found increased weight gain in WT mice fed a HCD compared to *Hfe*$^{+/-}$ mice (p=0.040, Sidak's multiple comparisons test). No significant changes were seen in CD mice. (C) Serum alanine aminotransferase (ALT) is not influenced by diet or genotype. A significant interaction by two-way ANOVA was present (p=0.047). However, differences between genotype (Sidak's multiple comparisons test) were not significant for either mice fed control diet or HCD. (n= 9-10 per group).

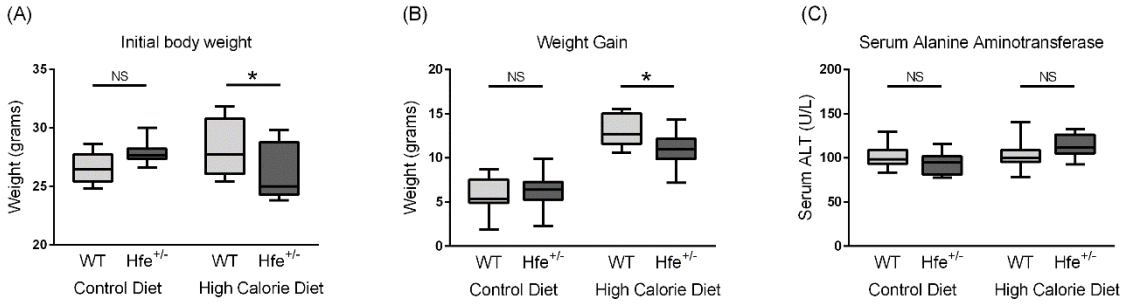

Diet, but not *Hfe* genotype influences liver injury in this model. There was no observed genotype effect on serum ALT (figure 3.1C). Mice fed HCD of both genotypes developed steatosis without overt steatohepatitis (figure 3.2). Table 3.3 shows the histological scoring of liver sections. NAFLD activity score (NAS) (p=0.003), steatosis (p<0.001) and hepatocyte ballooning (p=0.038) were associated with experimental group by Fisher's exact test. These associations evidently relate to diet rather than genotype. No more than minimal fibrosis was seen in any of the groups (data not shown).

Figure 3.2: High calorie diet leads to increased hepatic steatosis and ballooning degeneration in *Hfe*$^{+/-}$ mice.

Light microscopy of representative liver sections stained with hematoxylin and eosin are shown (original magnification x 100). (A) WT CD. (B) *Hfe*$^{+/-}$ CD. (C) WT HCD. (D) *Hfe*$^{+/-}$ HCD.

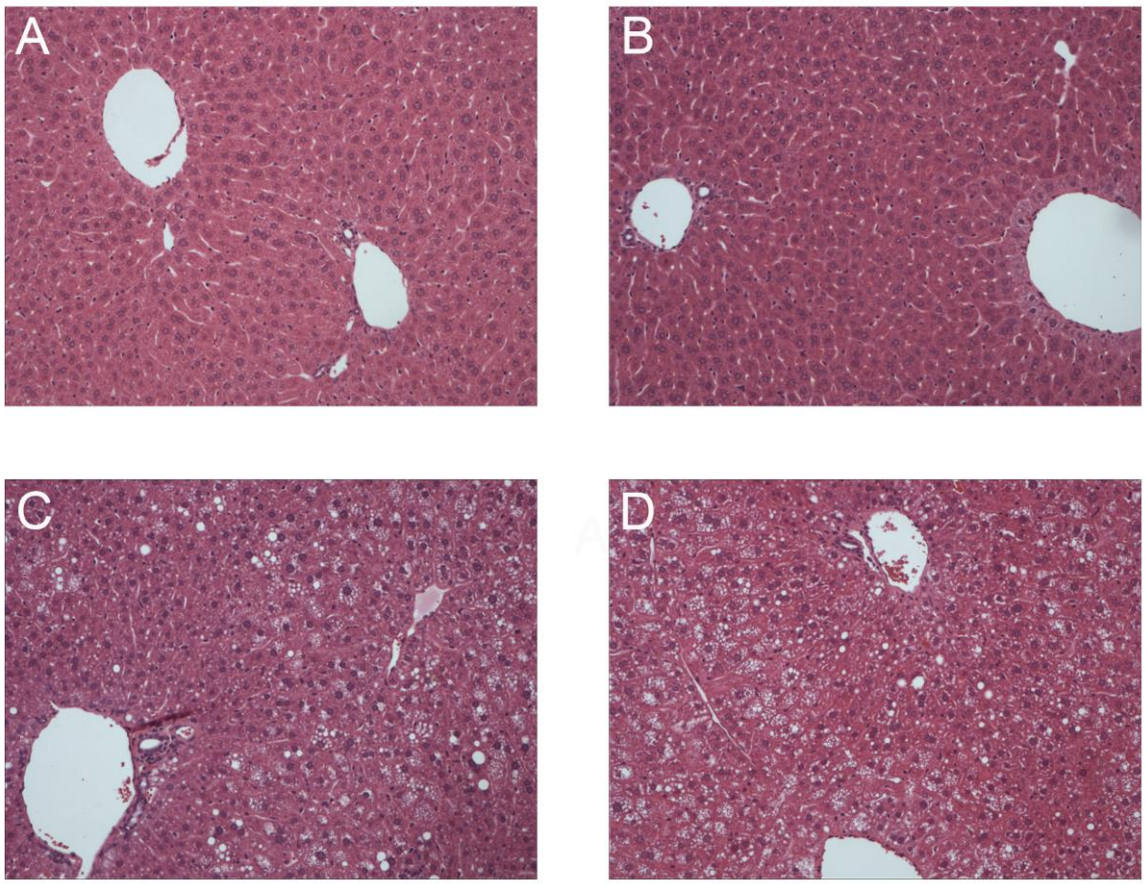

Table 3.3: High calorie diet, but not heterozygous *Hfe* gene deletion leads to increased hepatic steatosis, ballooning degeneration and NAS score.

Number of mice (%) with NAS (≥2), any macrovesicular steatosis (≥ grade 1), lobular inflammation (≥ grade 1), or ballooning (≥ grade 1). P-value is the result of Fisher's exact test. (n=10 per group)

	Control diet		**High Calorie Diet**		
	WT	***Hfe*$^{+/-}$**	**WT**	***Hfe*$^{+/-}$**	**p-value**
NAS (≥2)	0 (0%)	0 (0%)	5 (50%)	5 (50%)	0.003
Steatosis (Yes)	0 (0%)	0 (0%)	8 (80%)	8 (80%)	<0.001
Lobular Inflammation (Yes)	4 (40%)	3 (30%)	6 (60%)	6 (60%)	0.54
Ballooning (Yes)	0 (0%)	0 (0%)	4 (40%)	2 (20%)	0.038

Hepatic iron concentration (HIC) is increased in *Hfe*$^{+/-}$ mice in both dietary groups, consistent with the expected phenotype (figure 3.3A). *Hamp1* is the gene encoding hepcidin, the master regulator of iron homeostasis. When *Hamp1* is expressed as a ratio of HIC, expression was found to be approximately 50% lower in *Hfe*$^{+/-}$ mice across both dietary groups (figure 3.3C). This observation is consistent with haploinsufficiency of the HFE protein in *Hfe*$^{+/-}$ mice and supports HFE being the predominant regulator of *Hamp1* expression in this model.

Figure 3.3: High calorie diet induced reduction in hepatic iron concentration (HIC) occurs independently of hepcidin.

(A) Hepatic Iron Concentration. HCD was associated with reduced HIC (p<0.0001, two-way ANOVA). *Hfe*$^{+/-}$ mice had increased HIC compared to WT mice (p<0.0001, two-way ANOVA). (B) Hepatic *Hamp1* mRNA expression. *Hamp1* was lower in animals fed HCD (p=0.0012, two-way ANOVA). Gene effect was not significant (NS). (C) Hepatic *Hamp1* mRNA/HIC. *Hfe*$^{+/-}$ mice had lower *Hamp1*/HIC ratios (p=0.0003, 2way ANOVA). Diet effect was NS. (D) Gut cell *Dmt1* mRNA expression. Diet effect and gene effect were both NS (two-way ANOVA). (E) Gut cell *Hephaestin* mRNA expression. *Hfe*$^{+/-}$ mice had lower *Hephaestin* expression than WT mice (p=0.015). Diet effect was NS (two-way ANOVA). (n= 6-10 per group).

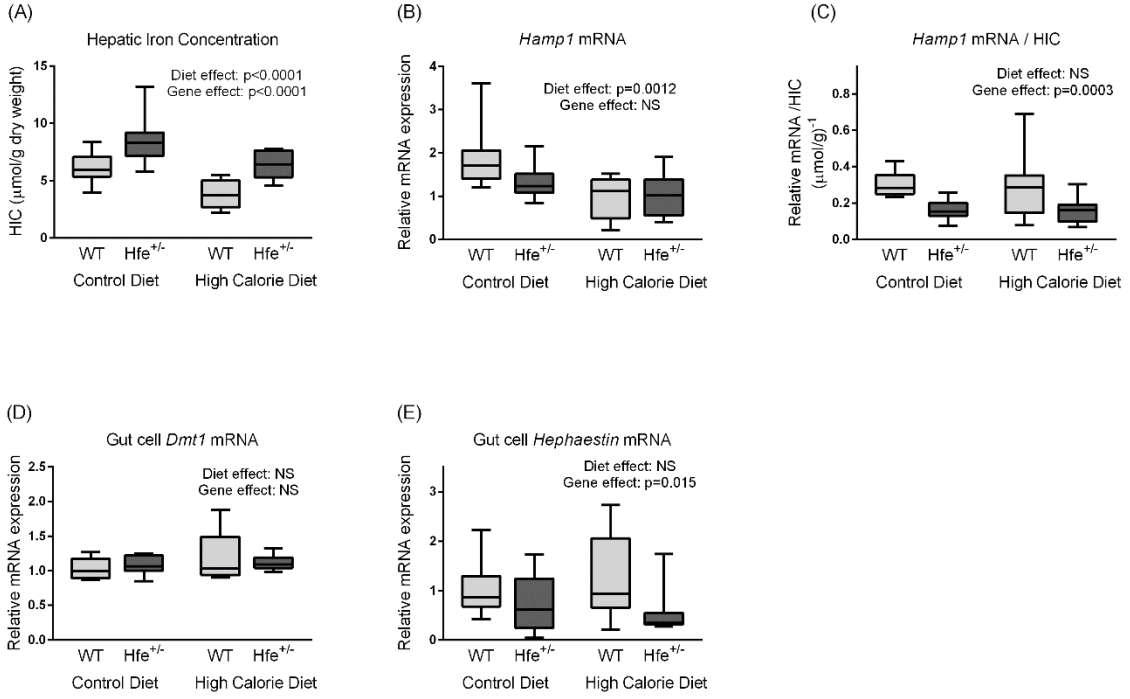

High calorie diet induced reduction of HIC occurs independently of hepcidin. HIC was significantly reduced by HCD in both genotypes (p<0.0001, two-way ANOVA) (figure 3.3A). The explanation for this is unclear. *Hamp1* mRNA expression was lower in HCD-fed mice (diet effect p=0.0012, two-way ANOVA, figure 3.3B). The *Hamp1*/HIC demonstrate that *Hamp1* expression when normalized to HIC is unaffected by diet (figure 3.3C). As the hepcidin-ferroportin axis did not appear to be the cause of the reduced HIC, we sought to evaluate two further regulators of intestinal iron absorption, the divalent metal transporter-1 (DMT1) and Hephaestin. There was no significant diet effect at the mRNA level for either of these by two-way ANOVA (figures 3.3D, 3.3E).

***Hfe*$^{+/-}$ mice display impaired glucose homeostasis.** As glucose and insulin are established drivers of hepatic *de novo* lipogenesis [121], we measured their fasting serum concentrations. Serum glucose was significantly higher in *Hfe*$^{+/-}$ than WT animals (genotype effect p=0.0007, two-way ANOVA). 8.1 vs 7.3 mmol/L in CD fed mice and 8.0 vs

7.2 mmol/L in HCD fed mice (figure 3.4A). A trend towards a similar effect was seen for serum insulin although this did not reach statistical significance (figure 3.4B). HOMA-IR score, which is the product of serum glucose, serum insulin and a constant, has been shown to be a useful static measure of insulin resistance in the fasting state [122]. HOMA-IR was significantly higher in *Hfe*$^{+/-}$ mice fed both CD (p=0.038) and also HCD (p=0.039) using Dunn's multiple comparison test after a significant Kruskal-Wallis test (p=0.0024) (figure 3.4C). Serum adiponectin has previously been shown to be regulated by iron in mice and is a known key determinant of insulin resistance [17]. However, we did not find any significant effect of genotype on total serum adiponectin (figures 3.4D, 3.4E). Moreover, when we looked specifically at the active form, high molecular weight (HMW) adiponectin, we again found no genotype effect irrespective of whether we analyzed absolute HMW adiponectin serum concentration or HMW adiponectin as a fraction of total adiponectin.

Figure 3.4: *Hfe*$^{+/-}$ mice have impaired glucose homeostasis irrespective of diet.

(A) Serum glucose. Serum glucose was higher in *Hfe*$^{+/-}$ mice compared to WT mice (p=0.0007), Diet effect was NS (two-way ANOVA). (B) Serum Insulin (mIU/L). Presented on logarithmic (base 10) scale. A difference between groups was present p=0.004 (Kruskal-Wallis test). Post hoc comparisons by genotype for CD and HCD mice were both NS (p=0.057, p=0.084 respectively by Dunn's multiple comparison test). (C) HOMA-IR. Presented on logarithmic (base 10) scale. A difference between groups was present p=0.0024 (Kruskal-Wallis test). *Hfe*$^{+/-}$ was associated with increased HOMA-IR score for mice fed CD (p=0.038) and HCD (p=0.039) (Dunn's multiple comparison test). (D, E) Immunoblotting for total serum adiponectin (D) densitometry, (E) representative blots. HMW = high molecular weight adiponectin. LMW= Low molecular weight adiponectin. Diet and gene effects were both NS (two-way ANOVA). (n= 9-10 per group).

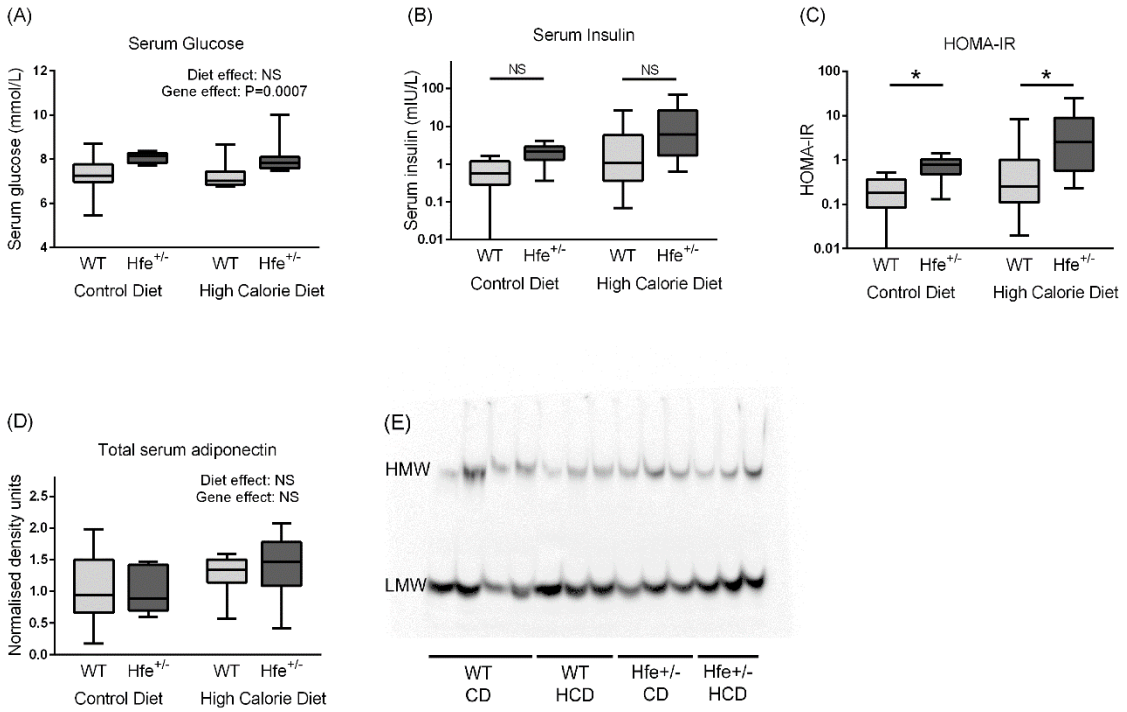

Despite increased serum glucose and HOMA-IR score, downstream regulators of *de novo* lipogenesis and fatty acid oxidation are largely unaffected by heterozygous *Hfe* deletion (figure 3.5). The active form of serine/threonine kinase AKT, phospho AKT, which is a central regulator of insulin signaling to lipogenesis pathways, was entirely unaltered by diet or genotype (figures 3.5A, 3.5C). Similarly, nuclear extract quantities of sterol regulatory element binding protein-1 (SREBP-1), the main transcription factor responsible for regulation of *de novo* lipogenesis were also unaffected by genotype (figures 3.5B, 3.5C). HCD diet however was associated with an increase in nuclear SREBP-1 protein, which may be substrate driven. mRNA quantities of fatty acid synthase (*Fas*) and stearoyl coA desaturase- 1 (*Scd1*) which are enzymes involved in hepatic lipogenesis and are downstream targets of SREBP-1 were also unaffected by genotype (figures 3.5D, 3.5E). Similarly there was no effect of *Hfe* heterozygosity on mRNA quantities of three key regulators of fatty acid oxidation; adiponectin receptor-2 (*Adipo R2*), peroxisome proliferator activated receptor alpha (*Pparα*), and carnitine palmitoyl transferase-1 (*Cpt1*), except for a small increase in *Cpt1* expression in $Hfe^{+/-}$ mice fed a HCD ($p=0.040$, Sidak's multiple comparisons test) (Figure 3.6A, 3.6B, 3.6C).

Figure 3.5: Hepatic *de novo* lipogenesis pathways are not up-regulated despite hyperglycemia.

(A) Immunoblotting densitometry of pAKT (whole liver protein extracts) normalized to GAPDH. Diet and genotype effect were both NS (two-way ANOVA). (B) Immunoblotting densitometry of SREBP-1 (nuclear protein extracts) normalized to Histone-H3. HCD was associated with increased nuclear SREBP-1 (p=0.022). Gene effect was NS (two-way ANOVA). (C) Representative immunoblots for pAKT, GAPDH, SREBP-1, Histone-H3. (n= 9-10 per group). (D) Hepatic fatty acid synthase (*Fas*) mRNA expression. Diet and genotype effect were both NS (two-way ANOVA). (E) Hepatic stearoyl coA desaturase- 1 (*Scd1*) mRNA expression. HCD was associated with increased *Scd1* expression. Gene effect was NS (two-way ANOVA).

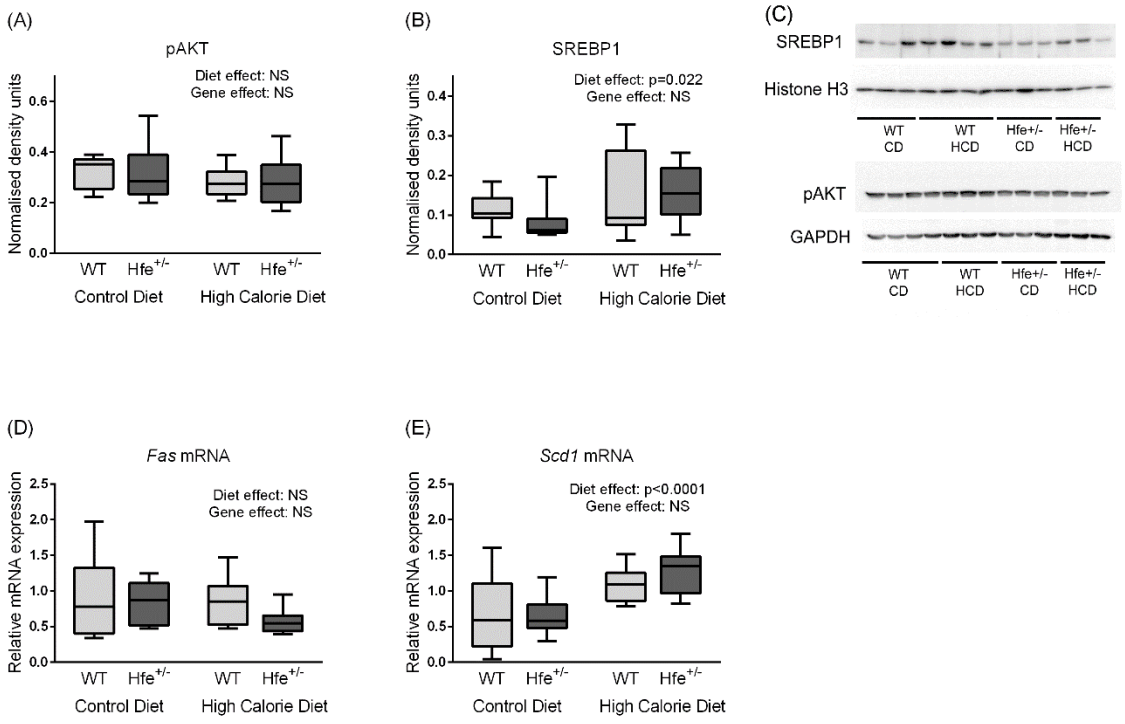

Figure 3.6: Hepatic lipid metabolism mRNA

(A) Hepatic adiponectin receptor-2 (*Adipo R2*) mRNA expression. HCD was associated with increased *AdipoR2* expression (p=0.0039). Gene effect was NS (two-way ANOVA). (B) Hepatic peroxisome proliferator activated receptor alpha (*Pparα*) mRNA expression. *Pparα* expression was increased by HCD. Gene effect was NS. (C) Hepatic carnitine palmitoyl transferase-1 (*Cpt1*) mRNA expression. There was a significant interaction between diet and genotype (p=0.045). Post hoc analysis found increased *Cpt1* expression due to *Hfe*$^{+/-}$ in HCD fed mice (p=0.040). In CD fed mice the results are NS (Sidak's multiple comparisons test). (n=10 per group).

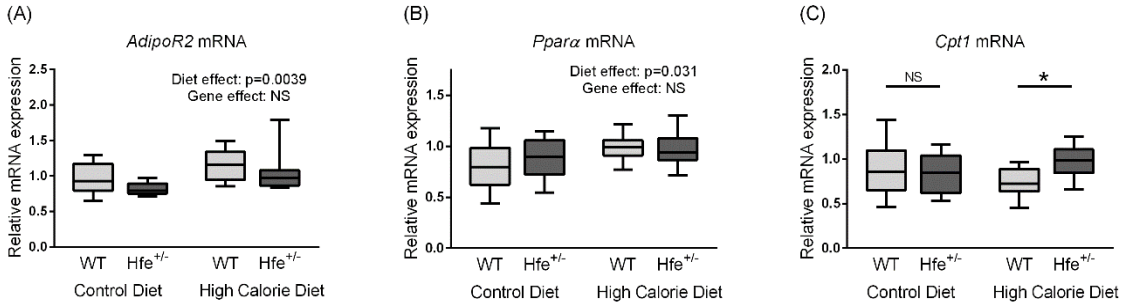

Discussion

In this study, we have demonstrated that heterozygous *Hfe* gene deletion in our mouse model of NAFLD leads to impaired glucose homeostasis in the fasted state, characterized by raised serum glucose concentrations and HOMA-IR scores. Despite this, the dysregulation of hepatic lipid metabolism and histological evidence of increased liver injury seen previously in $Hfe^{-/-}$ mice were not seen in $Hfe^{+/-}$ mice.

Increased serum glucose in $Hfe^{+/-}$ mice is a notable finding and is significant in relation to HFE's role in insulin sensitivity, type II diabetes mellitus and NAFLD [97, 123]. This study however was not primarily designed to investigate glucose homeostasis. Undoubtedly, dynamic measures of glucose homeostasis such as glucose and pyruvate tolerance testing with hyperinsulinemic-euglycemic clamp studies would help future studies to characterize the extent and specific location of insulin resistance in this model.

The links between iron, insulin resistance and type II diabetes have been extensively studied [34]. Two large longitudinal cohort studies have demonstrated increased risk of diabetes associated with hyperferritinemia [55, 57]. These associations remained valid even after accounting for known confounders such as inflammation. Furthermore, therapeutic phlebotomy as a method of iron depletion has been shown in small studies to improve glycemic control in non-diabetic, pre-diabetic and diabetic subjects [99-101].

Somewhat counterintuitively, previous studies have suggested enhanced insulin sensitivity in homozygous *Hfe* null mice [54, 124]. This has been proposed to be due to internalization of adipocyte ferroportin resulting in adipocyte iron loading and down-regulation of the expression of the insulin sensitizing adipokine, adiponectin [17]. This effect however was not seen in our model, as heterozygous $Hfe^{+/-}$ deletion did not appear to be sufficient to interfere with serum adiponectin levels.

The findings of our study are relevant if one considers the human data regarding *HFE* mutations and type II diabetes mellitus risk. A large meta-analysis that reviewed studies describing *HFE* gene polymorphisms and the risk of type II diabetes concluded that the heterozygous H63D mutation was associated with increased risk of diabetes [123]. In the context of this human data, our study provides a clear framework and suitable model for future animal studies exploring the mechanistic links between HFE and type II diabetes.

Amongst individuals with NAFLD, the presence of heterozygous H63D mutation has been associated with higher steatosis grades and NAS score [97]. Given that H63D has less iron loading potential than the C282Y mutation, this raises the intriguing possibility of an iron-independent role for the HFE protein in macronutrient metabolism that might protect against diabetes and NASH.

Heterozygous *Hfe* deletion did not appear to influence liver injury in this model, but it may be possible that histological differences between *Hfe*$^{+/-}$ and WT mice would only become evident in older mice with a more prolonged exposure to HCD and greater hepatic iron loading. Alternatively, it may be that these alterations in lipid and glucose metabolism are simply insufficient to impact on liver injury over even a prolonged period of time. It was suggested in previous studies of *Hfe*$^{-/-}$ mice that liver injury may have been attributed directly to a deficiency of Hfe protein rather than iron overload per se. Given the lack of genotype effect on liver injury seen in the *Hfe*$^{+/-}$ model, it is not possible to confirm this hypothesis. Further studies are planned to investigate the effect of an iron deficient diet in *Hfe*$^{-/-}$ animals in order to address this issue.

An interesting finding in this study was the effect of both diet and genotype on hepatic iron concentration (HIC). Increased hepatic iron in *Hfe*$^{+/-}$ mice is consistent with reduced stimulation of hepcidin-ferroportin axis in the setting of HFE deficiency. Humans with heterozygous C282Y mutations have been shown to have increased levels of serum ferritin, a marker of tissue iron stores, when compared to wild type controls [13]. The lower HIC observed with HCD is consistent with other previous studies [15, 125]. Whether lower HIC in association with HCD might be a protective or injurious response is difficult to determine. However, the lack of dietary effect on *Hamp1* mRNA when normalized to HIC suggests that hepcidin response remains appropriate in this model. Similarly, we found no dietary effect on the mRNA levels of two other regulators of iron absorption, the enterocyte iron transporter DMT1 and the ferroxidase, Hephaestin, despite a previous report of dysregulation of the mRNA transcripts of these genes in response to a high fat diet [125]. Recently Orr *et al* have demonstrated a repartitioning of iron from the liver to adipose tissue in the setting of a high fat diet [24]. This may explain the reduced HICs with HCD noted in our study. This will be further evaluated in future studies (Chapter 5).

In conclusion, we have demonstrated impaired glucose and iron homeostasis with heterozygous *Hfe* gene deletion in a mouse model of NAFLD. The genetic defect however was not associated with increased liver injury or impaired hepatic lipid metabolism.

Chapter 4 : Hepatic iron concentration correlates with insulin sensitivity in non-alcoholic fatty liver disease

The previous chapter demonstrated that heterozygous *Hfe* gene deletion in mice leads to impaired iron and glucose homeostasis. In order to further explore the relationships between iron and insulin resistance, data and human serum samples from a randomized, controlled trial of venesection in NAFLD were utilised.[104] Firstly associations between measures of iron status, serum ferritin, hepatic iron concentration (HIC) and multiple measures of insulin resistance were studied. Secondly, the effect of iron depletion through venesection on six adipokines with potential relevance to iron's role in NAFLD pathogenesis was determined.

This chapter is published in Hepatology Communications.

Britton LJ, Bridle KR, Reiling J, Santrampurwala N, Wockner L, Ching H, Stuart KA, Subramaniam VN, Jeffrey G, St Pierre T, House M, Gummer J, Trengove R, Olynyk J, Crawford DHG, Adams LA

Hepatic iron concentration correlates with insulin sensitivity in non-alcoholic fatty liver disease

Hepatology Communications 2018 Apr 27;2(6):644-653

Hepatic iron concentration correlates with insulin sensitivity in non-alcoholic fatty liver disease

Laurence Britton[1,2,3,4], Kim Bridle[1,2], Janske Reiling[1,2,5], Nishreen Santrampurwala[1,2,4], Leesa Wockner[4], Helena Ching[6], Katherine Stuart[1,3], V. Nathan Subramaniam[4,7], Gary Jeffrey[6,8], Tim St Pierre[9], Michael House[9], Joel Gummer[10], Robert Trengove[10], John Olynyk[11,12], Darrell Crawford[1,2], Leon Adams[6,8]

1. Gallipoli Medical Research Institute, Greenslopes Private Hospital, Greenslopes, Queensland, Australia
2. The University of Queensland, Herston, Queensland, Australia
3. Department of Gastroenterology, Princess Alexandra Hospital, Queensland, Australia
4. QIMR Berghofer Medical Research Institute, Brisbane, Queensland, Australia
5. Department of Surgery, NUTRIM School of Nutrition and Translational Research in Metabolism, Maastricht University, Maastricht, The Netherlands
6. Medical School, Faculty of Health Sciences, University of Western Australia, Crawley, Australia
7. Institute of Health and Biomedical Innovation and School of Biomedical Sciences, Queensland University of Technology, Kelvin Grove, Queensland, Australia
8. Department of Hepatology, Sir Charles Gairdner Hospital, Perth, Western Australia
9. School of Physics, University of Western Australia, Crawley, Western Australia, Australia.
10. Separation Science and Metabolomics Laboratory (Metabolomics Australia, Western Australia node), Murdoch University, Murdoch, Western Australia.
11. Department of Gastroenterology, Fiona Stanley and Fremantle Hospital Group, Western Australia
12. School of Health and Medical Sciences, Edith Cowan University, Joondalup, Western Australia

Abstract

Rodent and cell-culture models support a role for iron-related adipokine dysregulation and insulin resistance in the pathogenesis of non-alcoholic fatty liver disease (NAFLD), however substantial human data is lacking. We examined the relationship between measures of iron status, adipokines and insulin resistance in NAFLD patients in the presence and absence of venesection. This study forms part of the IIRON2 study, a prospective randomized controlled trial of venesection for adults with NAFLD. Paired serum samples at baseline and six months (end of treatment) in controls (n=28) and venesection patients (n=23) were assayed for adiponectin, leptin, resistin, retinol binding protein-4, TNFα and IL-6 using a Quantibody customized multiplexed ELISA array. Hepatic iron concentration (HIC) was determined using MR FerriScan. Unexpectedly, analysis revealed a significant positive correlation between baseline serum adiponectin concentration and HIC, which strengthened after correction for age, gender and body mass index (rho 0.36, p=0.007). In addition there were significant inverse correlations between HIC and measures of insulin resistance; Adipo-IR, serum insulin, serum glucose, HOMA-IR, HbA1C and hepatic steatosis whereas a positive correlation was noted with insulin sensitivity index. Changes in serum adipokines over six months did not differ between the control and venesection groups. **Conclusion:** HIC positively correlates with serum adiponectin and insulin sensitivity in patients with NAFLD. Further study is required to establish causality and mechanistic explanations for these associations and their relevance in the pathogenesis of insulin resistance and NAFLD.

Background

The epidemic of obesity in both the developed and developing world has led to a major rise in the prevalence of non-alcoholic fatty liver disease (NAFLD). NAFLD is estimated to be present in 20-30 percent of the adult population.[28] Non-alcoholic steatohepatitis, the aggressive form of NAFLD, predisposes individuals towards liver failure and hepatocellular carcinoma.[30] Furthermore, NAFLD has been shown to be an independent risk factor for cardiovascular disease and type II diabetes.[2]

Unfortunately, currently available treatment options for NAFLD are largely ineffective and novel therapeutic targets are urgently needed for this disease. Iron has long been considered to have role in the pathogenesis of NAFLD and insulin resistance, a hallmark

feature of NAFLD.[7, 8, 34] Therefore, iron has been considered as a potential therapeutic target in NAFLD and type 2 diabetes mellitus.[7, 34]

In recent years, there has been considerable interest in the role of iron in adipose tissue biology and the regulation of adipokines.[7, 21] Adipokines are defined as "polypeptides that are secreted in the adipose tissue in a regulated manner".[16] Many of these adipokines have endocrine effects on the liver as well as local effects on adipose tissue.[16] Altered adipose tissue biology and dysregulation of adipokine synthesis may promote liver injury via increased insulin resistance and also by other direct and indirect effects on hepatic and adipose tissue lipid metabolism.[16] Studies in animals and tissue culture models have demonstrated an iron-induced dysregulation of the synthesis of three adipokines with such roles, namely adiponectin, leptin and resistin.[17-19]

Adiponectin is the most abundant adipokine in serum and has a number of hepato-protective effects in NAFLD.[16, 21] Iron has been shown to down-regulate adiponectin in a rodent model of selective adipocyte iron loading and also in cultured 3T3-L1 pre-adipocytes via decreased acetylation of the transcription factor FOX01.[17] More recently, it has been demonstrated that iron down-regulates the appetite-suppressing hormone, leptin in mice fed a high iron diet via iron-dependent activation of cAMP-responsive element binding protein (CREB).[18] Two other adipokines, resistin and retinol binding protein-4 (RBP-4), have been associated with insulin resistance [16] and iron has been proposed as a regulator of serum concentrations of both of these hormones.[19, 20] Tumor necrosis factor-alpha (TNFα) and interleukin-6 (IL-6) are cytokines secreted from adipose tissue as adipokines as well as from other tissues.[16] Both have important roles in the induction of insulin resistance in NAFLD and type II diabetes[16, 126, 127] and iron has been shown in cell culture studies to promote a pro-inflammatory phenotype in macrophages.[75]

To date, studies regarding iron and the regulation of adipokines in humans are relatively sparse. Recently, a randomized controlled trial of 274 adults with dysmetabolic iron overload syndrome showed that venesection did not affect serum adiponectin levels, however other adipokines were not assessed.[128] Venesection in a cohort of six patients with type 2 diabetes led to a reduction in serum levels of RBP-4.[20]

At present therefore, there is a clear need for more comprehensive human data to determine whether iron-adipokine interactions observed in animal studies might translate

to humans. We hypothesized that iron is a key determinant in the regulation of insulin sensitivity and a number of adipokines relevant to NAFLD pathogenesis. To investigate these relationships further, we analyzed the relationships between hepatic iron concentration and serum ferritin with markers of insulin resistance and serum concentrations of six target adipokines. We also assessed the effect of iron removal by venesection on serum levels of these adipokines.

The IIRON2 study is a multi-center, prospective, randomized, controlled trial evaluating the effect of venesection on liver injury in adults with NAFLD.[104] As a component of this larger study, this report describes the relationships between baseline iron loading and measures of insulin resistance as well as the effect of venesection and lifestyle advice versus lifestyle advice alone on serum concentrations of adiponectin, leptin, resistin, RBP-4, TNFα and IL-6.

Methods

Participants

Subjects were recruited from hepatology clinics at the Sir Charles Gairdner and Fremantle Hospitals in Western Australia and Greenslopes Private Hospital, Queensland, Australia between November 2010 and December 2012, by the physicians involved in the study (LA, JO, DC and KS).[104] Subjects were adults with hepatic steatosis evident on ultrasonography or computed tomography scan and serum ferritin >50 ng/ml. Exclusion criteria included the presence of an *HFE* hemochromatosis genotype (C282Y/C282Y or C282Y/H63D), liver disease other than NAFLD, ischemic heart disease, uncontrolled diabetes (HbA1C>8.0%) or evidence of decompensated liver disease. Detailed inclusion and exclusion criteria have been previously described.[104] The current study also excluded those screened with hemochromatosis range HIC (greater than two times the upper limit of normal) in order to avoid bias in parametric correlation analyses. The IIRON2 study was registered with the Australia New Zealand Clinical Trials Registry (Registration no. ACTRN12610000868088). This registration included an ‘a priori’ assessment of serum adipokine levels as a secondary endpoint (secondary endpoint 4). Written informed consent was obtained from all participants. The study protocol conforms to the ethical guidelines of the 1975 declaration of Helsinki and was approved by the human research

ethics committees of the Sir Charles Gairdner, Fremantle and Greenslopes Private Hospitals.

Randomization

Participants were randomized, using a randomization sequence generated by the study research coordinator from a computerized random number generator, to venesection with lifestyle advice (venesection group) or lifestyle advice alone (control group) at a ratio of 1:1 as previously described.[104] Allocation concealment prior to randomization was achieved using numbered sealed opaque envelopes. Assignment was performed by the research coordinators. All subjects received dietary advice regarding the institution of a hypocaloric diet from an accredited dietician and all received standardized advice regarding exercise. Participants in the venesection group underwent two to three weekly venesections targeting a serum ferritin of <45ng/ml.

Clinical and laboratory assessment

A thorough clinical assessment including history and physical examination was performed at baseline, three months and at six months (end of study). Standard laboratory parameters were measured including liver function tests, serum triglycerides, high density lipoprotein (HDL-cholesterol), free (non-esterified) fatty acids (FFA), glucose, insulin, glycosylated hemoglobin (HbA1C), 75g oral glucose tolerance test, transferrin saturation, serum ferritin and full blood count. Hepascore, a validated serum measure of hepatic fibrosis in NAFLD [129] was performed at the Western Australia state referral laboratory (Pathwest, Queen Elizabeth II Medical Centre, Nedlands, Australia). Serum cytokeratin-18 (CK-18) fragments were measured using an m30 Aptosense ELISA kit (Peviva, Nacka, Sweden).

Serum concentrations of adiponectin, leptin, resistin, RBP-4, TNFα and IL-6 were measured using a customized multiplexed Quantibody enzyme-linked immunosorbent assay (ELISA) array (Human Obesity Array Q3, Raybiotech, Norcross, USA). Assays of participant serum samples at 1:2 dilution and adipokine control dilutions for a standard curve were performed in quadruplicate by Jomar Life Research, Scoresby, Australia according to the manufacturer's instructions. Hepcidin-25 was isolated from patient serum by solid phase extraction, and measured by liquid chromatography quadrupole time-of-

flight mass spectrometry (LC-qTOF-MS) as previously described.[130-132] Quantitation was by reference to a synthetic hepcidin-25 ($^{13}C_{18}$,$^{15}N_3$) peptide internal standard (Peptides International, Inc., Kentucky, USA).

Imaging studies

Hepatic steatosis and hepatic iron concentration (HIC) were measured using non-invasive magnetic resonance imaging (MRI) methods on a 1.5T Avanto scanner (Siemens Medical Systems, Erlagen, Germany). Hepatic steatosis was quantified, as a volumetric percentage, using a validated opposed phase, in-phase gradient echo protocol.[133] A validated MRI method (FerriScan) was used to determine HIC.[134]

Statistical analysis

Comparison of baseline variables between groups was performed using two-tailed Student's t-test for continuous variables and Pearson's Chi-squared or Fisher's exact test, as appropriate, for categorical variables. Baseline correlation analyses were performed using Pearson's correlation. As the dependency between adipokines and measures of iron is unknown, bivariate correlation analysis was used to detect associations. The relationships between serum adipokine concentrations, measures of insulin resistance, serum ferritin and HIC after correction for body mass index (BMI), age and gender were assessed using a partial correlation analysis. The relationships between serum hepcidin and surrogates of insulin resistance were assessed using a partial correlation analysis correcting for HIC.

For each of the six adipokines, comparisons between the venesection and control groups of the change of serum concentration were made using a two-sided independent-sample t-test. A further analysis of this data was performed using analysis of covariance (ANCOVA) with correction for BMI, age and gender.

Results

Participant characteristics.

Seventy-four participants were randomized in the study.[104] This cohort was used to analyze baseline relationships of measures of insulin resistance and serum adipokines

with measures of iron status. The characteristics of this cohort are summarized in Table 4.1. Of these, 60 patients had serum stored at baseline available for measurement of serum adipokine concentrations. Fifty-one also had serum available from the end of the study and this cohort was used in the analysis comparing the effect of venesection (n=23) versus control (n=28) as shown in Figure 4.1. The baseline characteristics of the participants from each randomized group with available paired sera are outlined in Table 4.2. Baseline characteristics including serum adipokine concentrations were not significantly different between groups.

Table 4.1: Baseline characteristics of randomized participants.

Data is presented as mean and standard deviation except for diabetes and male gender, for which the total number of participants and percentage of participants is presented.

Characteristic (n=73)	**Mean (standard deviation)**
Age, years	51.3 (10.8)
Male gender (%)	43 (59%)
BMI, kg/m^2	31.4 (5.0)
Waist circumference, cm	105 (13)
Diabetes (%)	13 (18%)
ALT, IU/L	72 (56)
Hepascore	0.33 (0.26)
Glucose, mmol/L	6.1 (2.1)
Serum ferritin, ng/mL	507 (442)
Transferrin saturation, %	31.6 (13.5)
Hepatic iron concentration, mmol/kg	23.0 (11.3)
Hepatic steatosis, % by volume	18.1 (10.9)

Figure 4.1: Patient flow diagram for the analysis of venesection effect on serum adipokine concentrations

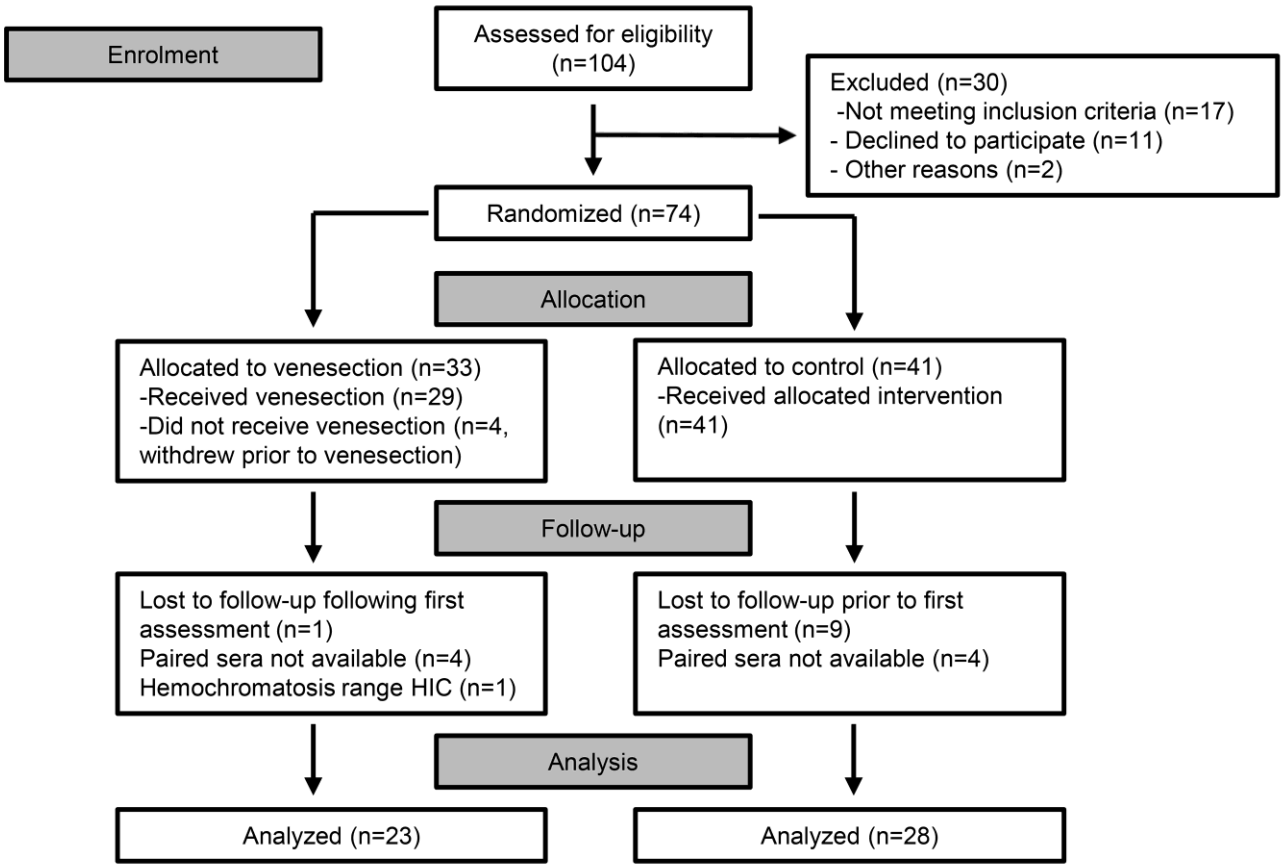

Table 4.2: Baseline characteristics of participants with available paired sera

Data is presented as mean and standard deviation except for diabetes, male gender and metabolic syndrome, for which the total number of participants and percentage of participants is presented. Values presented are mean values with standard deviation in parentheses except where indicated otherwise. p values are the result of unpaired t-tests unless indicated otherwise. * p <0.05, # Exact p value from Fisher's exact test, ‡ Pearson's Chi-squared test.

Characteristic	Control group (n=28)	Venesection group (n=23)	p value
Age, years	51.8 (11.3)	54.0 (9.7)	0.45
Male gender	18 (64%)	14 (61%)	0.80‡
BMI, kg/m^2	30.9 (5.3)	31.8 (4.4)	0.52
Waist circumference, cm	103.4 (13.9)	108.5 (11.3)	0.17
Diabetes	5 (18%)	4 (17%)	1.0 #
ALT, IU/L	65.0 (37.7)	81.6 (74.0)	0.31
AST, IU/L	41.8 (20.5)	47.4 (36.6)	0.49
Bilirubin, µmol/L	13.8 (5.5)	14.0 (6.5)	0.92
Alkaline Phosphatase, IU/L	84.5 (19.9)	89.2 (24.8)	0.45
Albumin, mg/dl	45.0 (3)	43.5 (2.6)	0.054
CK-18, U/L	287.2 (286.9)	367.8 (322.5)	0.36
Hepascore	0.29 (0.2)	0.42 (0.3)	0.059
Triglycerides, mmol/L	1.74 (0.9)	1.63 (0.8)	0.65
HDL-cholesterol, mmol/L	1.16 (0.3)	1.07 (0.3)	0.26
Free fatty acids, mmol/L	0.32 (0.2)	0.38 (0.2)	0.28
Glucose, mmol/L	5.64 (0.8)	6.16 (2.3)	0.27
Insulin, mU/L	15.6 (12)	14.1 (6.8)	0.60
HbA1C, %	5.89 (0.7)	6.10 (1.2)	0.46
HOMA-IR	4.24 (4.1)	4.07 (2.9)	0.86
ISI	3.44 (3.4)	3.55 (2.9)	0.91

Hemoglobin, g/L	152.7 (13.7)	149.2 (12.1)	0.34
Platelet, $x10^9$/dL	216.7 (33.8)	231.6 (99.2)	0.46
Ferritin, ng/mL	448.1 (388.2)	587.2.1 (353.1)	0.19
Transferrin saturation, %	31.6 (11.1)	33.4 (14.0)	0.63
Hepatic iron concentration, mmol/kg	22.1 (10.2)	24.6 (12.7)	0.44
Hepatic steatosis, %	17.0 (12.7)	18.0 (8.6)	0.76
Metabolic syndrome	17 (61%)	16 (70%)	0.57#
Adiponectin, ng/ml	538.4 (249.8)	471.2 (216.7)	0.32
Leptin, ng/ml	19.5 (18.8)	22.7 (14.2)	0.50
Resistin, ng/ml	7.55 (2.6)	8.01 (2.0)	0.49
RBP-4, ng/ml	42.8 (20.1)	38.4 (12.7)	0.37
TNFα, pg/ml	292.2 (395.4)	249.2 (336.6)	0.68
IL-6, pg/ml	114.9 (171.4)	114.2 (136.3)	0.99

Correlation of measures of iron loading with baseline serum adipokine concentrations

The 61 participants with available baseline serum were assessed to evaluate the relationships between serum adipokine concentrations with two baseline measures of iron status, serum ferritin and HIC (Table 4.3). All participants had serum ferritin measured and HIC was available for 57 of the 61 participants. A single participant with hemochromatosis-range HIC (99mmol/kg) was excluded from the analysis. HIC was corrected for steatosis percentage volume as determined by MRI in order to provide a true, comparable iron concentration in the aqueous (non-lipid) fraction of the liver. Baseline serum hepcidin data was available for 37 of the randomized participants.

Table 4.3: Correlation between baseline serum ferritin, HIC and serum adipokine concentrations

*p<0.05, df = degrees of freedom

		Pearson's correlation		Partial correlation, corrected for age, gender and BMI	
		Ferritin n=60	**HIC n=57**	**Ferritin df=55**	**HIC df=52**
Adiponectin	rho *p*	-0.06 0.67	+0.26 0.048*	+0.02 0.90	+0.36 0.007*
Leptin	rho *p*	-0.20 0.13	-0.20 0.13	-0.01 0.92	-0.12 0.38
Resistin	rho *p*	-0.01 0.93	-0.04 0.77	+0.10 0.46	+0.05 0.73
RBP-4	rho *p*	+0.05 0.68	+0.11 0.44	+0.07 0.60	+0.14 0.31
TNFα	rho *p*	+0.07 0.58	-0.04 0.79	+0.10 0.45	-0.02 0.90
IL-6	rho *p*	+0.07 0.59	-0.09 0.50	+0.06 0.65	-0.10 0.46

Baseline serum ferritin was not associated with serum concentrations of any of the six adipokines. HIC however, showed a significant positive correlation with serum adiponectin (p=0.048, rho= +0.26, Table 4.3, Figure 4.2(a)), but not with the other five adipokines. In the cohort, six subjects were taking the insulin sensitizing drug, metformin. No other insulin sensitizing drugs were in use amongst the cohort. In particular, no subjects were using thiazolidinediones. As metformin might increase serum adiponectin concentrations [135], an analysis of the correlation between HIC and adiponectin was performed after excluding those subjects taking metformin. In this analysis, the association between HIC and serum adiponectin lost statistical significance, (n= 51, rho= +0.25, p= 0.08), however significance was maintained after correction for age, BMI and gender with partial correlation analysis (df= 46, rho= +0.34, p= 0.02). BMI correlated with serum leptin concentration (p<0.0001, rho=0.585), but not with other adipokines (data not shown). Baseline serum ferritin and HIC were correlated (n=65, rho=+0.41, p=0.001).

Figure 4.2: Relationships between HIC and insulin sensitivity

HIC and a) adiponectin, b) adipo-IR, c) percentage hepatic steatosis, d) HOMA-IR, e) HbA1C, f) insulin sensitivity index (ISI)

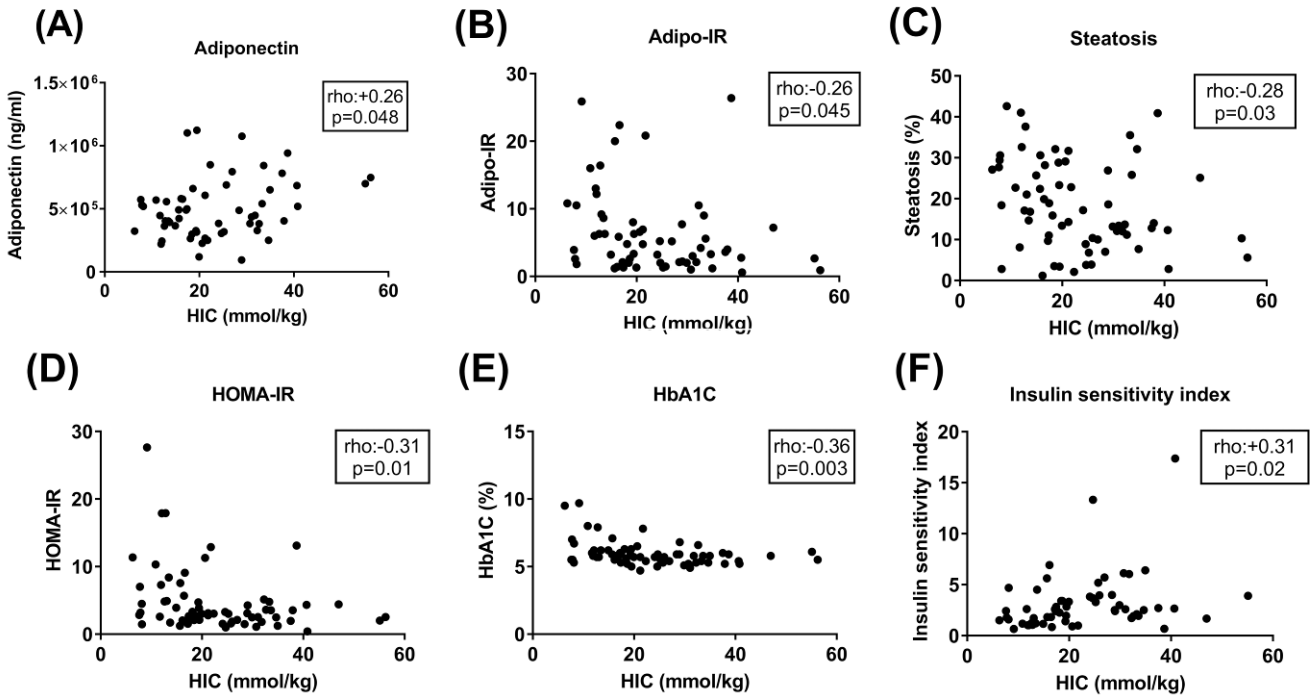

Correlation analysis of the baseline data was repeated for all adipokines using partial correlation adjusting for three potential confounders: baseline age, gender and BMI (Table 4.3). This correction strengthened the positive relationship between serum adiponectin and HIC (p=0.007, rho= +0.36). There remained no association between HIC and the other five adipokines. When also corrected for the same factors, there was no significant correlation between serum ferritin and the six adipokines. An analysis of the correlation between adiponectin and HIC in non-diabetics and particularly in diabetics is limited by sample size. In non-diabetics, there was no significant correlation between adiponectin and HIC (n=49, rho=+0.21, p=0.15), however after correction for age, gender and BMI, partial correlation remained just significant (df=43, rho=+0.33, p=0.0496).

Correlation of HIC with measures of insulin resistance

Next, we sought to determine whether the association between HIC and adiponectin was an isolated finding or whether HIC is associated with measures of insulin resistance. We found that HIC negatively correlated with six surrogates of insulin resistance relating to different sites of insulin action. These were: Adipo-IR [136] percentage hepatic steatosis, serum insulin, serum glucose, homeostatic model assessment of insulin resistance

(HOMA-IR)[122] and HbA1C (Table 4.4 and Figure 4.2(b-e)). Furthermore, the insulin sensitivity index (ISI)[137] was significantly positively correlated with HIC (Table 4.4 and Figure 4.2(f)). After correction for age, gender and BMI by partial correlation, all associations remained significant except for Adipo-IR (Table 4.4).

In order to determine whether insulin might mediate hepcidin response, we analyzed the relationships between hepcidin and the seven surrogates for insulin resistance, using a partial correlation analysis, correcting for HIC (Table 4.4). We found that serum insulin and serum hepcidin levels positively correlated (df=29, rho=+0.37, p=0.04). However, there were no significant relationships between serum hepcidin and the other seven surrogates for insulin resistance.

Table 4.4: Correlation between HIC and hepcidin with measures of insulin resistance

* p<0.05, df = degrees of freedom

	HIC (Pearson's correlation)			**HIC (partial correlation, correction for age, gender and BMI)**			**Serum hepcidin (partial correlation corrected for HIC)**		
	n	**rho**	**p**	**df**	**rho**	**p**	**df**	**rho**	**p**
Adipo-IR	62	-0.26	0.045*	57	-0.23	0.08	29	+0.14	0.46
Steatosis(%)	65	-0.28	0.03*	60	-0.28	0.03*	29	+0.09	0.63
Insulin	65	-0.26	0.04*	60	-0.28	0.03*	29	+0.37	0.04*
FFAs	62	-0.21	0.10	57	-0.14	0.29	29	-0.34	0.06
Glucose	65	-0.31	0.01*	60	-0.26	0.04*	29	-0.12	0.53
HOMA-IR	65	-0.31	0.01*	60	-0.30	0.02*	29	+0.30	0.10
HbA1C	64	-0.36	0.003*	59	-0.31	0.01*	29	+0.09	0.63
ISI	59	+0.30	0.02*	54	+0.28	0.04*	24	+0.05	0.80

* p<0.05, df = degrees of freedom

Serum adipokine concentrations in response to venesection

Subjects in the venesection group underwent a median of 7 venesections (range 2-19). This is roughly equivalent to 1.58g of iron (range 450mg to 4.28g). [118] Change in body mass index (BMI) during the study did not differ between groups (-0.67kg/m^2 (control group) vs +0.24kg/m^2 (venesection group), p=0.08, Student's t-test). BMI, serum triglycerides, HDL, LDL cholesterol, HOMA-IR and ISI were not significantly different between groups at the end of the study.

Serum adipokine concentrations did not significantly change between baseline and six months for each of the six adipokines in each group except for a 63pg/ml (26%) rise in serum TNFα in the venesection group (*p*=0.048). When comparing the difference in absolute change of serum concentration for each adipokine between the control and venesection groups, there were no significant differences (Figure 4.3). An ANCOVA analysis was performed correcting for baseline body mass index, age and gender and no significant differences between groups were observed for each of the six adipokines (data not shown).

Figure 4.3: Change in serum adipokine concentrations over six months

Mean change is represented as a percentage of the baseline mean for each adipokine. No significant differences were observed for each adipokine between the control (n=28) and venesection groups (n=23). Values represented are mean absolute change in serum adipokine concentration with error bars to represent standard error of the mean. Measured serum concentration of TNFα and IL-6 was below the lower limit of detection of the assays in 11 (of 102) and 23 (of 102) samples respectively. In these instances, the lower limit of detection value was used for statistical analysis. A analysis in which zero values were used instead of the lower limit of detection values, did not substantially alter the results (data not shown)

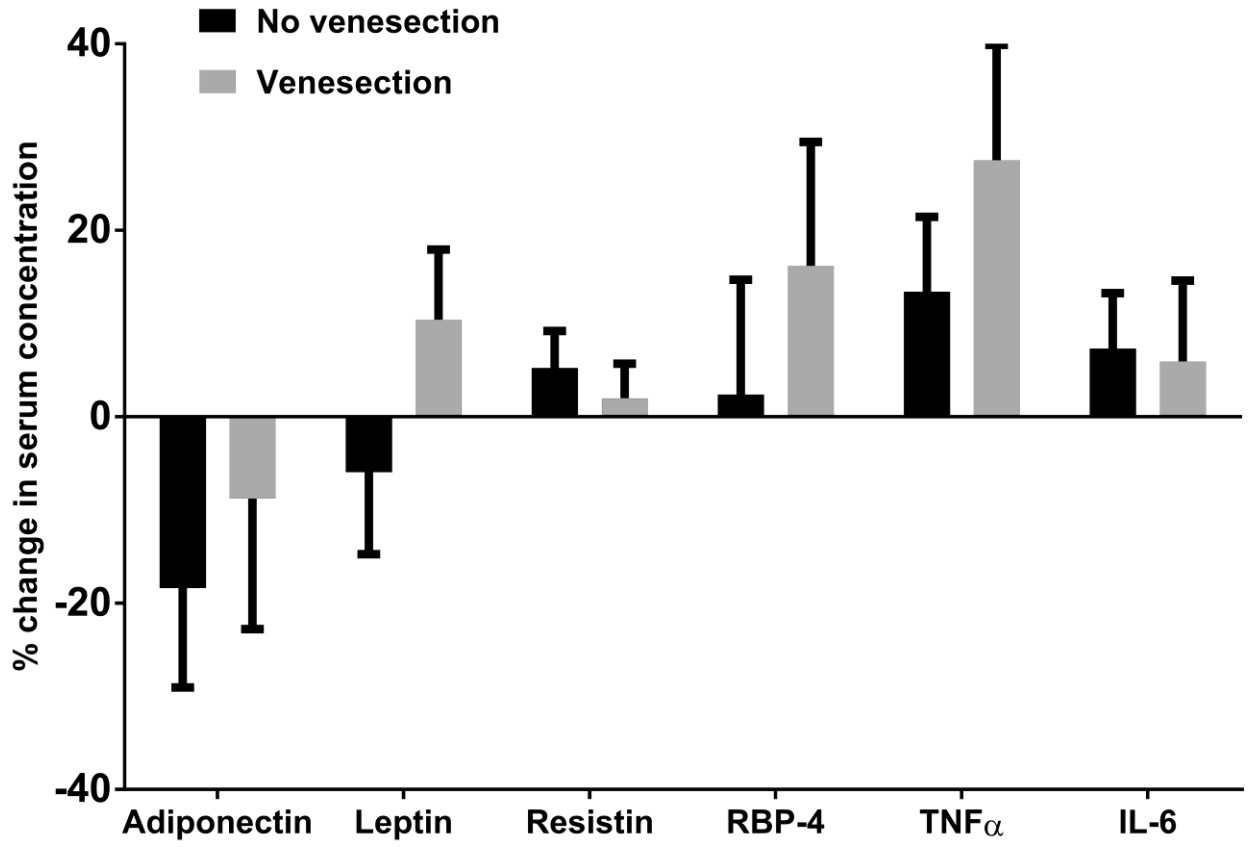

Discussion

In this prospective, randomized, controlled clinical trial, we have shown that venesection does not alter the serum concentrations of six key adipokines in participants with NAFLD. To our surprise however, we demonstrated a significant positive relationship between HIC and serum adiponectin concentration in this cohort. This observation was strengthened further after correction for age, gender and BMI. Furthermore, we have shown that HIC negatively correlated with multiple measures of insulin resistance. We looked at eight surrogate measures of insulin resistance and their relationship to iron. In all cases, except for FFAs, a significant relationship was found associating enhanced insulin sensitivity with

increasing HIC. These data suggest that HIC inversely predicts insulin resistance in the periphery (adipose tissue and skeletal muscle) as well as within the liver.

Notably, in keeping with our findings, a cross-sectional study of 80 Italian patients with biopsy-proven NAFLD, found that the Oral Glucose Sensitivity Index increased with increasing HIC.[61] Furthermore, a recently published randomized controlled study by Lainé *et al* of 274 participants with dysmetabolic iron overload and significantly elevated HIC (>50mmol/kg) found that venesection was associated with significantly increased serum insulin and HOMA-IR scores over time[128]. We found no difference between groups in HOMA-IR scores, ISI or change in HOMA-IR or ISI over time.[104] This remained the case in sub-group analyses of diabetics and non-diabetics (data not shown). Although we did not find that venesection altered insulin resistance, the longer duration of venesection (12 months versus 6 months) and higher baseline HIC in the Lainé study may account for the change in insulin resistance in that study. It is therefore worth considering however that there may be subgroups of patients with NAFLD that may develop altered adipokine concentrations in response to venesection, possibly over a longer duration of treatment.

Our findings add weight to the possibility of a causal relationship between iron and insulin sensitivity in individuals with NAFLD. These results suggest that hepatic iron loading below the hemochromatosis range (less than two times the upper limit of normal, normal range 3-33mmol/kg[138]) may actually be beneficial in terms of insulin sensitivity. In contrast, the association between excess hepatic iron seen in hemochromatosis and insulin resistance and diabetes is well established.[34] Pathologic iron overload from hereditary hemochromatosis can cause diabetes through both insulin deficiency from beta-cell loss in the pancreas as well as insulin resistance.[34] Our data, coupled with these observed relationships between hemochromatosis and insulin resistance suggest that a ‘sweet-spot’ of HIC for maximal insulin sensitivity exits, above and below which, increased insulin resistance is observed.

An alternative explanation for the relationship between HIC and insulin sensitivity might be that insulin or some aspect of insulin resistance might regulate iron homeostasis. In order to explore this possibility further we looked at serum hepcidin concentrations and their relationship to our eight measures of insulin sensitivity. Hepcidin is the key regulator of systemic iron absorption through its effect on small bowel enterocyte iron export.[36, 38]

Hepcidin is predominantly produced by hepatocytes and is transcriptionally regulated by a number of factors, including hepatic iron.[36, 38] As such, we examined the markers of insulin resistance in relation to hepcidin after correction for HIC. We found that serum hepcidin levels positively correlated with serum insulin. This could indicate that insulin signaling may play a role in hepcidin regulation, whereby insulin resistance leads to reduced intestinal iron absorption. However, as the other measures of insulin resistance were not associated with serum hepcidin levels, a direct link would seem unlikely.

We found that serum concentrations of the insulin sensitizing adipokine, adiponectin, positively correlate with HIC. This may in part explain the relationship between iron and insulin sensitivity in this cohort. However, adipokines by definition, are cytokines that are synthesized in adipose tissue and therefore adipocyte, or adipose tissue, iron concentrations are likely to be most important with respect to iron-adipokine interactions. Indeed, HIC may not be an accurate surrogate measure of adipose tissue iron. Rodent data have shown that a high fat diet leads to a redistribution of iron from the liver to adipose tissue with a four-fold increase in adipocyte iron concentration and a two-fold reduction in HIC.[24] Human studies demonstrate that obesity is associated not only with iron deficiency, but paradoxically also with increased sub-cutaneous and visceral adipose tissue iron.[22, 111, 112] Furthermore, increased adipocyte iron leading to a reduction in adiponectin expression has been demonstrated in a variety of mouse and adipocyte culture models.[17] Taken together, it may be possible in NAFLD that iron redistributes from the liver to adipose tissue, thus contributing to insulin resistance and a reduction in serum adiponectin.

In this study, we have measured HIC, as a well validated surrogate for total body iron stores.[139] We corrected HIC for percentage steatosis volume, in order to give a truer, more physiologically relevant HIC that is reflective of iron concentration in the aqueous (non-lipid) fraction of the liver. By doing this, we have demonstrated that it is not simply HIC dilution by lipid that erroneously explains the relationships between iron, steatosis and other measures of insulin resistance. It should be noted that this HIC correction is a conservative approach to the data that weakens the associations observed compared to when un-corrected HIC is used (data not shown).

Contrary to our findings, a number of other studies have indicated a positive association between serum adiponectin and measures of human iron stores.[17, 90, 140] These

studies may be limited by the choice of surrogate for HIC. In all three studies, inverse correlations were noted between serum ferritin and serum adiponectin, however this only reached statistical significance in two of the studies. [17, 90]. These are interesting observations that were not seen in our cohort. However, although serum ferritin undoubtedly correlates with HIC, it is clearly an imprecise measure of HIC. Our data show that despite strong statistical significance ($p<0.001$), the association itself is not strong ($r^2= 0.17$), indicating that only 17% of the variance in serum ferritin is attributable to HIC. Ryan *et al*, have recently reported an inverse association between liver iron and serum adiponectin. [140] However, the MRI T2* values, used as an inverse surrogate for HIC, were not corrected for volume of hepatic steatosis. In addition there may have been a greater degree of liver injury in the Ryan et al cohort with 35.3% of individuals reported as having tissue elastography measurements indicative of bridging fibrosis or cirrhosis. These factors may, in part, explain the disparity between the two cohorts.

A weakness of our study is that it presupposes that venesection mobilizes adipose tissue iron as it does for other tissues. Although it is increasingly clear that adipocytes utilize much of the iron metabolism apparatus that is used in other tissues, such as transferrin receptor 1, hepcidin and ferroportin, we are not aware of any human data that has addressed the degree to which adipose tissue iron is mobilized by venesection.[17, 23]

Another limitation of our study is the lack of liver histology. It is likely that there was degree of heterogeneity of liver injury among participants studied. In addition, the lack of liver histology does not allow for determination of the relative distribution of iron between hepatocytes and reticuloendothelial cells. This may be critical to iron's impact within the liver as reticuloendothelial iron has been shown to be associated with apoptosis and a greater risk of hepatocellular ballooning, steatohepatitis and advanced fibrosis in humans with NAFLD. [74, 83]

A strength of this study is that it represents an 'a priori' assessment as part of a randomized, controlled trial. Our study failed to demonstrate any effect of venesection on serum concentrations of the six adipokines studied. It is possible that our study may be underpowered for some of the adipokines as these were secondary endpoints for which the study was not prospectively powered.

A number of avenues for future work in this field present themselves. Firstly, obtaining human adipose tissue samples for the determination of adipose tissue and adipocyte iron concentrations would be technically challenging but likely highly informative. A pragmatic approach to this would be obtaining visceral adipose tissue samples in patients undergoing laparoscopic cholecystectomy. Coupled with an in depth assessment of insulin resistance and serum adipokine concentrations, ideally using hyperinsulinemic-euglycemic clamps, relationships between insulin resistance and adipose tissue iron concentrations could be readily evaluated in a cross-sectional cohort such as this. Another approach, would be to perform a study in which insulin resistance, using hyperinsulinemic-euglycemic clamp studies and serum adipokine concentrations were assessed before and after and the infusion of intravenous iron.

In conclusion, we have found a lack of effect of venesection on serum concentrations of six important adipokines in patients with NAFLD. We have however demonstrated significant correlations between hepatic iron, serum adiponectin and multiple surrogate measures of insulin sensitivity. The causality of these relationships remains uncertain. Mechanistic explanations for the relationships between iron metabolism and insulin resistance are targets for future studies.

Chapter 5 : Ferroportin expression in adipocytes does not contribute to iron homeostasis or metabolic responses to a high calorie diet

The previous two chapters have demonstrated seemingly conflicting observations between a human and an animal study regarding the associations between hepatic iron and insulin resistance in NAFLD. Chapter 3 showed that mild increases in iron in the context of heterozygous *Hfe* gene deletion in mice are associated with impaired glucose homeostasis. In humans with NAFLD however, increased hepatic iron concentration appears to be associated with increased insulin sensitivity. In this chapter, the theme of mild increases in iron in insulin resistance and NAFLD pathogenesis is explored further. It is increasingly evident that the key site of iron's impact on insulin resistance and NAFLD may centre upon its effects on adipocyte biology.[7, 17, 18, 34] In this chapter, a model of selective knockout of the iron exporter ferroportin in adipocytes is developed, focusing on the effects on adipocyte iron metabolism, glucose homeostasis and liver injury.

This chapter is published in Cellular and Molecular Gastroenterology and Hepatology

Britton LJ, Jaskowski L, Bridle KR, Secondes E, Wallace D, Santrampurwala N, Reiling J, Miller G, Mangiafico S, Andrikopoulos S, Subramaniam VN*, Crawford DHG
Adipocyte-specific Ferroportin knockout in mice: no effect on iron accumulation or metabolic response to fast food diet
Cellular and Molecular Gastroenterology and Hepatology 5 (3) 319-331 Mar 2018

Ferroportin expression in adipocytes does not contribute to iron homeostasis or metabolic responses to a high calorie diet

Laurence Britton[1,2,3,4], Lesley-Anne Jaskowski[1,2], Kim Bridle[1,2], Eriza Secondes[4,5], Daniel Wallace[4,5], Nishreen Santrampurwala[1,2], Janske Reiling[1,2,6], Gregory Miller[2,7], Salvatore Mangiafico[8], Sofianos Andrikopoulos[8], V. Nathan Subramaniam[4,5*], Darrell Crawford[1,2*]

1. Gallipoli Medical Research Institute, Greenslopes Private Hospital, Greenslopes, Queensland, Australia
2. The University of Queensland, Herston, Queensland, Australia
3. Department of Gastroenterology, Princess Alexandra Hospital, Queensland, Australia
4. QIMR Berghofer Medical Research Institute, Brisbane, Queensland, Australia
5. Institute of Health and Biomedical Innovation and School of Biomedical Sciences, Queensland University of Technology (QUT), Kelvin Grove, Queensland, Australia
6. Department of Surgery, NUTRIM school of Nutrition and Translational Research in Metabolism, Maastricht University, Maastricht, the Netherlands
7. Envoi Pathology, Kelvin Grove, Queensland, Australia
8. Department of Medicine, Austin Hospital University of Melbourne, Heidelberg, Victoria, Australia

*Joint Senior Authors

Abstract

Background & Aims: Iron has an increasingly recognized role in the regulation of adipose tissue function, including the expression of adipokines involved in the pathogenesis of non-alcoholic fatty liver disease (NAFLD). The cellular iron exporter, ferroportin, has been proposed as being a key determinant of adipocyte iron homeostasis. Methods: We studied an adipocyte-specific ferroportin (*Fpn1*) knockout (FKO) mouse model, using an *Adipoq*-Cre recombinase driven *Fpn1* deletion and fed mice according to the fast food diet model of non-alcoholic steatohepatitis. Results: We demonstrated successful selective deletion of *Fpn1* in adipocytes, but found that this did not lead to increased adipocyte iron stores as measured by atomic absorption spectroscopy or histologically quantified iron granules after staining with DAB enhanced Perls' stain. Mice with adipocyte-specific *Fpn1* deletion did not demonstrate dysregulation of adiponectin, leptin, resistin or retinol-binding protein-

4 (RBP-4) expression. Similarly, adipocyte-specific *Fpn1* deletion did not affect insulin sensitivity during hyperinsulinemic-euglycemic clamp studies or lead to histological evidence of increased liver injury. We have however shown that the fast food diet model of non-alcoholic steatohepatitis generates an increase in adipose tissue macrophage infiltration with crown-like structures, as seen in humans, further validating the utility of this model. Conclusions: Ferroportin may not be a key determinant of adipocyte iron homeostasis in this knockout model. Further studies are needed to determine the mechanisms of iron metabolism in adipocytes and adipose tissue.

Background

Non-alcoholic fatty liver disease (NAFLD) affects around one billion people worldwide [1]. Many of these individuals develop non-alcoholic steatohepatitis (NASH) and hepatic fibrosis, which can lead to liver failure and hepatocellular carcinoma [2, 30, 31]. Treatments that effectively alter the natural history of this disease are lacking and a greater understanding of its pathogenesis is essential in order to develop such therapies. Dysfunctional adipose tissue has been shown to be central to the pathogenesis of insulin resistance and NAFLD [21]. Adipose tissue serves as the predominant source of liver fat in NAFLD and is the source of adipokines that have significant roles in the regulation of liver injury [16, 43].

Iron is an essential element in cellular metabolism, but has also been implicated in a wide range of human disease [36]. It has been reported that adipocytes within adipose tissue utilize the same apparatus for iron metabolism as other cell types, such as transferrin receptor 1 (Tfr1), hepcidin and ferroportin, [17, 22, 141]. Recent data support a role for iron in the regulation of adipose tissue function. Adipose tissue iron has been proposed as having roles in the pathogenesis of NAFLD as well as type 2 diabetes mellitus [7, 34]. Studies have implicated adipose tissue iron in the dysregulation of four key adipokines in NAFLD: adiponectin, leptin, resistin and retinol binding protein-4 (RBP-4) [17-20, 22]. Furthermore, iron has been shown to increase lipolysis in isolated rat adipocytes [142].

It has been proposed that the cellular iron-exporter ferroportin is a key determinant of adipocyte iron metabolism [17]. Gabrielsen *et al* demonstrated the down-regulation of adiponectin in response to iron across a range of *in vivo* and *in vitro* models [17]. The authors employed an *AP2-Cre:Fpn1*$^{fl/fl}$ model of selective adipocyte ferroportin deletion as a model of adipocyte iron loading. However, results of direct measurement of adipocyte

iron were not presented and an iron-loading phenotype was inferred solely on the basis of reduced *Tfr1* mRNA quantities [143]. *Tfr1* mRNA quantification remains, at best, an indirect surrogate for iron loading that has not been well validated in adipocytes. Furthermore, the *AP2* gene has been shown to be significantly expressed in other cell types, notably macrophages [26, 27, 144]. As such, the importance of ferroportin in adipocyte iron handling requires further validation. The *Adipoq*-Cre model which utilizes a BAC transgene Cre recombinase in the promoter region of the adiponectin gene has been shown to have greater adipocyte specificity than the *AP2*-Cre and is considered to be a superior model of selective adipocyte-specific gene deletion [26, 27].

In this study, we sought to determine whether ferroportin regulates adipocyte iron metabolism by selectively knocking out *Fpn1* in adipocytes using an *Adipoq*-Cre recombinase mouse model. We utilized the fast food diet model, as described by Charlton *et al*, as a model for non-alcoholic steatohepatitis in these mice [25]. This paper investigates the role of ferroportin in the handling of iron by adipose tissue. In addition, we examine the effect of adipocyte-specific ferroportin deletion on glucose metabolism and liver injury using the fast food diet model of NASH. We also evaluate the utility of the fast food diet model as a model for adipose tissue dysfunction in NASH.

Methods

Experimental Animals

Mice with loxP fragments inserted in exons 6 and 7 of the mouse Ferroportin gene (*Fpn1*$^{fl/fl}$ mice) on a 129/SvEvTac background were a kind gift of Prof Nancy Andrews, Duke University, Durham, USA [145]. *Fpn1*$^{fl/fl}$ mice were backcrossed for at least eight generations onto a C57BL/6 background. Male *Fpn1*$^{fl/fl}$ mice were then crossed with female heterozygous C57BL/6 *Adipoq*-Cre$^{+/-}$ mice expressing Cre recombinase under the control of *Adipoq* (adiponectin gene) promotor regions on a BAC transgene (Jackson Laboratory, Bar Harbor, USA) [27]. This generated both *Adipoq-Cre:Fpn1*$^{fl/fl}$, adipocyte-specific ferroportin knockout (FKO) and *Fpn1*$^{fl/fl}$ (Flox) littermate control mice.

After weaning, mice were housed singly. Sixteen week-old male mice were randomly assigned, using a computerized random allocation sequence generator, to receive either control diet or fast food diet for 25 weeks until the end of the experiment [25]. Control diet mice were provided with drinking water and fast food diet mice were supplied with 42g/L high fructose corn syrup (23.1g/L fructose, 18.9g/L glucose, Chem-supply, Gillman,

Australia) in the drinking water [146]. Diets were supplied by Specialty Feeds (Glen Forrest, WA, Australia). Mice had *ad libitum* access to diet and water (control diet) or high fructose corn syrup in water (fast food diet). The key constituents of the diets are outlined in Table 5.1.

Table 5.1: Major components of experimental diets

Dietary component	Control diet	Fast food diet
Protein (% weight)	13.6	17.4
Total fat (% weight)	4.0	20
Total digestible carbohydrate (% weight)	64.8	48.2
Digestible energy (MJ/kg)	15.1	18.6
Cholesterol (% weight)	0	0.15
Casein (acid) (g/kg)	140	180
Sucrose (g/kg)	100	341
Clarified butter (ghee) g/kg	0	200
Wheat starch (g/kg)	472	82
Dextrinized starch (g/kg)	155	0
Iron (mg/kg)	75	75
High fructose corn syrup in drinking water (g/L)	0	42

At 41 weeks of age, mice were weighed. After a five hour fast, mice received an intraperitoneal injection of either 0.75 mU/g humulin R insulin (Eli-Lilly, Indianapolis, USA) in sterile 0.9% sodium chloride (0.15 mU/µL), (Pfizer, New York, USA) or 5 µL/g 0.9% sodium chloride alone. After ten minutes, mice were sacrificed as previously described [147].

Whole liver and epididymal fat pad weights were recorded. Liver and epididymal fat pad samples were fixed in formalin for histology. Liver samples were snap frozen in liquid nitrogen and stored at -80 ^{o}C. Liver and spleen samples were dried at 110 ^{o}C for 72 hours for measurement of tissue iron concentration. Blood was collected by cardiac puncture and serum was stored at -80 ^{o}C. Adipocytes were isolated from epididymal fat pads following collagenase-dispase digestion as previously described and stored at -80 ^{o}C [144].

All experiments were performed with approval from the Animal Ethics Committee of the QIMR Berghofer Medical Research Institute and were conducted in accordance with the

NHMRC code for the care and use of animals for scientific purposes. Mice were housed in a temperature controlled environment (23 ^{o}C) in a 12:12 hour light: dark cycle. All authors had access to the study data and reviewed and approved the final manuscript.

Glucose tolerance tests

Glucose tolerance tests were performed one week prior to sacrifice, at 40 weeks of age. After a five hour fast, mice were given 1 g/kg glucose via the intraperitoneal route. Tail vein sampling was performed at 0, 15, 30, 60 and 120 minutes and blood glucose was measured using an Accu-Chek Performa II hand-held glucometer (Roche, Basel, Switzerland).

Hyperinsulinemic-euglycemic clamp studies

Hyperinsulinemic–euglycemic clamps were performed as previously described in 6 hour-fasted mice [148]. An initial two minute-priming dose of insulin (150 mU/kg/min) was followed by a constant infusion at a rate of 15 mU/kg/min. Maintenance of euglycemia was achieved by a variable infusion of 25% glucose solution. Steele's steady-state equation was used to calculate glucose turnover.

Tissue iron concentration

Hepatic and splenic iron concentrations were measured as previously described [147]. Adipocyte iron concentration was performed on isolated adipocytes by atomic absorption spectroscopy (AAS). Approximately 100 mg of adipocytes for each animal were weighed and then dried down at 60 ^{o}C for 60 hours and 100 µL concentrated nitric acid was added. Samples were then incubated at 60 ^{o}C for 30 minutes, before dilution 1:5 with zero standard (0.2% nitric acid). Standards over a range of 0-25 µmol/L were prepared using iron pure single element standard 1000 mg/L iron in 2% nitric acid (Perkin Elmer, Waltham, USA). All samples (including standards, quality control and analytical samples) were further diluted 1:3 with 10g/L palladium matrix modifier for graphite furnace AAS (Merck Millipore, Darmstadt, Germany). AAS was performed at a wavelength of 372nm using an AA280Z, Zeeman Atomic Absorption Spectrometer (Varian, Palo Alto, USA) with a GTA 120 Graphite Tube Atomizer (Agilent Technologies, Santa Clara, USA). Zeeman background correction was used. The final results were expressed per gram wet weight.

RNA extraction, real time quantitative (RT-qPCR) and DNA electrophoresis

RNA was extracted from liver and adipocyte homogenates using Trisure reagent (Bioline, London, UK). Samples were treated with DNAse 1 (Invitrogen, Carlsbad, USA) and cDNA was synthesized from 1 µg RNA (liver) and 500 ng RNA (adipocytes) using a Sensifast cDNA synthesis kit (Bioline). For RT-qPCR, a ViiA7 real-time PCR machine (Invitrogen) with a SensiFAST SYBR Lo-ROX Kit was used (Bioline). Samples underwent thermal cycling as follows: 95 ^{o}C for 2 minutes then 40 cycles at 95 ^{o}C for 5 seconds followed by 63 ^{o}C for 20 seconds prior to a melt curve analysis. Relative mRNA expression was determined by calibration of Ct values to standard curve of pooled cDNA samples and normalized to the geometric mean of three reference genes (basic transcription factor-3 (*Btf3*), glyceraldehyde-3-phosphate dehydrogenase (*Gapdh*) and beta-2-microglobulin (β*2-mg*) for liver samples and RNA Polymerase II Subunit A (*Polr2a*), *Beta-actin* and hypoxanthine guanine phosphoribosyl transferase (*Hprt*) for adipocyte samples. Primer sequences are provided in Table 5.2.

Table 5.2: RT-qPCR primer sequences (5' to 3')

	Forward primer	**Reverse primer**
Tfr1	GAGGCAGACCTTGCACTCTT	TGACTGAGATGGCGGAAAC
Fpn1	GCCACTGCGATCACAATCC	TGGAGTTCTGCACACCATTGAT
Hamp1	TTGCGATACCAATGCAGAAG	GGATGTGGCTCTAGGCTATGTT
Adiponectin	GGAGATGCAGGTCTTCTTGG	TCCAGGCTCTCCTTTCCTG
Leptin	GCAGTGCCTATCCAGAAAGTCC	GGAATGAAGTCCAAGCCAGTGAC
Resistin	CATGCCACTGTGTCCCATCGAT	ACTTCCCTCTGGAGGAGACTGT
Rbp-4	TGTAGCCTCCTTTCTCCAGCGA	ACAGGTGCCATCCAGATTCTGC
B2-mg	CTGATACATACGCCTGCAGAGTTAA	ATGAATCTTCAGAGCATCATGAT
Btf-3	TGGCAGCAAACACCTTCACC	AGCTTCAGCCAGTCTCCTTAAAC
Gapdh	TCCTGCACCACCAACTGCTTAGC	GCCTGCTTCACCACCTTCTTGAT
Polr2a	AGCTGGTCCTTCGAATCCGC	CTGATCTGCTCGATACCCTGC
Beta-actin	CATTGCTGACAGGATGCAGAAGG	TGCTGGAAGGTGGACAGTGAGG
Hprt	GGACTGATTATGGACAGGA	GAGGGCCACAATGTGATG
Hmox1	CACTCTGGAGATGACACCTGAG	GTGTTCCTCTGTCAGCATCACC

For confirmation of adipocyte-specific ferroportin knockout, 10µl of adipocyte *Fpn1* DNA amplification product, created using primers flanking exons 6 and 7 (Table 5.2) (thermal

cycling: 95 ^{o}C for 2 minutes then 40 cycles at 95 ^{o}C for 5 seconds followed by 63 ^{o}C for 45 seconds) was mixed with 2 µl of 6X DNA loading buffer (New England Biolabs, Ipswich, USA). Samples were electrophoresed at 110 V for 40 minutes in a 1.5% agarose gel (Bioline) mixed with Sybr safe buffer (Invitrogen). The products were visualized on an ImageQuant LAS 500 machine (GE Healthcare Life Sciences, Little Chalfont, UK).

Immunoblotting

Eight µL of 1:1000 mouse serum was electrophoresed on 2% Metaphor Agarose gels (Lonza, Basel, Switzerland) for 75 minutes at 75 V. Protein was transferred onto polyvinylidene fluoride (PVDF) membranes (Biorad, Hercules, USA) over 60 minutes at 100 V. Blocking was performed using 5% skim milk powder. A 1:10,000 dilution of primary antibody against adiponectin (MAB3608, Merck Millipore) was applied to the membranes. A 1:50,000 dilution of goat anti-mouse horseradish peroxidase antibody (Invitrogen) was applied as secondary antibody. Visualization was performed using a Supersignal West Femto chemiluminescent kit (Thermo Fisher Scientific, Waltham, USA) on an ImageQuant LAS 500 machine (GE Healthcare Life Sciences).

Histological assessment and hepatic hydroxyproline assays

Formalin fixed samples of liver and epididymal fat pad (EFP) were embedded in paraffin. Liver sections were stained with Hematoxylin and Eosin (H&E) for assessment of steatohepatitis and Sirius Red for assessment of fibrosis. Scoring was performed according to criteria established by Kleiner et al [84]. Further liver sections were stained with Oil Red O and percentage area stained was measured using ImageJ software, version 2. EFP sections were stained with H&E and the absolute count of macrophage clusters over ten high power fields (x400) was determined. Additional EFP sections were stained with 3,3'-diaminobenzidine (DAB) enhanced Perls' stain and Eosin counterstain. The average count of iron granules within adipocytes in five adjacent high power fields (x400 magnification) was determined. Small iron granules were counted individually (score=1), granules filling the whole cell scored 10. All histological assessments were performed by an expert histopathologist blinded to study group. Photomicrographs were created using a MicroPublisher 3.3 RTV camera (Q Imaging, Surrey, Canada) and a Biological System Microscope CX41 (Olympus, Tokyo, Japan). Hepatic hydroxyproline assay was performed as previously described.[149]

Statistical analysis

Statistical analysis was performed using GraphPad Prism software, version 7.03 (GraphPad, San Diego, USA). Hyperinsulinemic-euglycemic clamp data and glucose concentrations during glucose tolerance tests were analyzed using two-tailed Student's t-tests. For liver histology scoring, Mann-Whitney tests were used to compare genotypes for each diet. For all remaining data, two-way ANOVA was used to assess the effect of diet and genotype. If a significant interaction ($p<0.05$) was found, Sidak's multiple comparison's test was used to compare between genotypes for each diet and between diets for each genotype. In cases in which no interaction was found, *p* values for the diet and genotype effect are indicated. Data presented on box and whisker plots show bars representing the median and interquartile range with whiskers representing the maximum and minimum values.

Results

Fast food diet was associated with increased body, liver and epididymal fat pad weights. Initial body weight was comparable across all four groups (all non-significant (NS), Sidak's multiple comparisons test, data not shown). Consistent with the description of the fast food diet model [25], mice fed with the fast food diet had greater final body weight ($p<0.0001$) and liver weight ($p<0.0001$, two-way ANOVA) (Fig. 5.1). EFP weight was higher in both genotypes with fast food diet ($p=0.0001$ Flox mice, $p<0.0001$ FKO mice, Sidak's multiple comparisons test) (Fig. 4.1).

Figure 5.1: Tissue and body weights.

(A) Total body weight. Total body weight was increased in in animals fed the fast food diet (FFD), $P<0.0001$, genotype effect was not significant (NS, two-way ANOVA) (B) Liver weight. Liver weight was increased in animals fed FFD, $P<0.0001$, gene effect was NS, (two-way ANOVA) (C) Epididymal fat pad (EFP) weight. There was a significant interaction between diet and genotype effects ($P=0.03$, two-way ANOVA). Post-hoc analysis demonstrated lower EFP weight in FKO mice compared to Flox mice fed FFD ($P=0.02$) and increased weight with FFD diet for both Flox and FKO mice ($P=0.0001$ and $P<0.0001$ respectively, Sidak's multiple comparisons test) n = 8-12 per group.

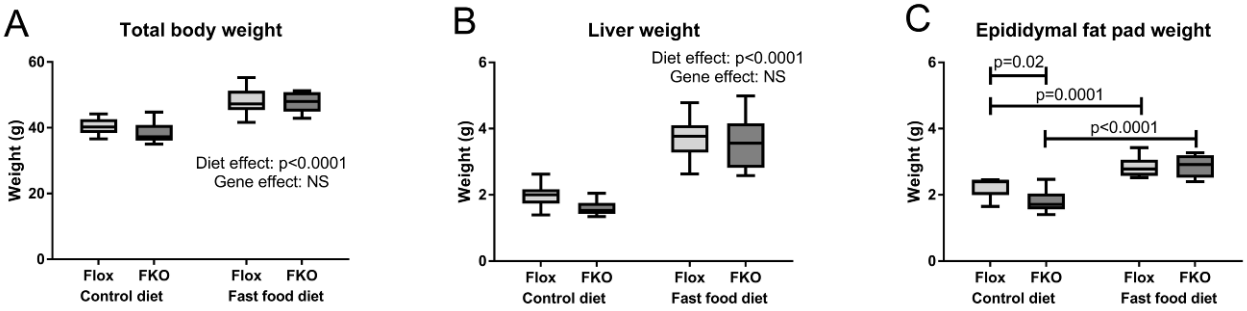

FKO mice demonstrate successful selective adipocyte knockout of ferroportin in adipocytes, but not in other tissues. *Fpn1* primers targeting sequences in exons 5 and 8 which flank the *Fpn1* loxP sites predicted amplification products of 1048 base pairs (bp) for the intact gene and 163bp for Cre-recombinase-deleted *Fpn1* gene. DNA electrophoresis of *Fpn1* qRT-PCR products from isolated adipocytes demonstrated a clear 163 bp band in all 20 samples of FKO mice and no 163bp band in all 24 samples in Flox mice, indicating adipocyte *Fpn1* deletion in FKO, but not in Flox mice. A representative gel is shown in Fig. 5.2A. In all liver samples, Flox (n=9), FKO (n=8) and all spleen samples Flox (n=7), FKO (n=14), the 163 bp band was absent whereas a 1048 bp band was present indicating a lack of Cre recombinase effect in liver and spleen, irrespective of genotype.

Figure 5.2: Adipocyte-specific ferroportin knockout does not alter adipocyte iron phenotype.

(A) Representative DNA electrophoresis blot of adipocyte *Fpn1* RT-PCR products showing the predicted 163bp band in adipocytes from FKO but not Flox mice. (B) *TfR1* mRNA expression. Diet and genotype effects were both NS (two-way ANOVA) (n = 8-12 per group). (C) Adipocyte iron concentration. Diet and genotype effects were both NS (two-way ANOVA) (n = 8-12 per group). (D) Quantified adipocyte iron granules. Mean count of granules of iron in five adjacent high power fields (x400 magnification). Diet and genotype effects were both NS (two-way ANOVA) (n = 8-12 per group). (E-H) Perls' staining of epididymal fat pads. Representative light microscopy sections are shown of Eosin and DAB enhanced Perls' stained sections of epididymal fat pads with arrows indicating small iron granules (x 400 magnification) (E) Flox control diet. (F) Flox fast food diet. (G) FKO control diet. (H) FKO fast food diet (n = 7-12 per group).

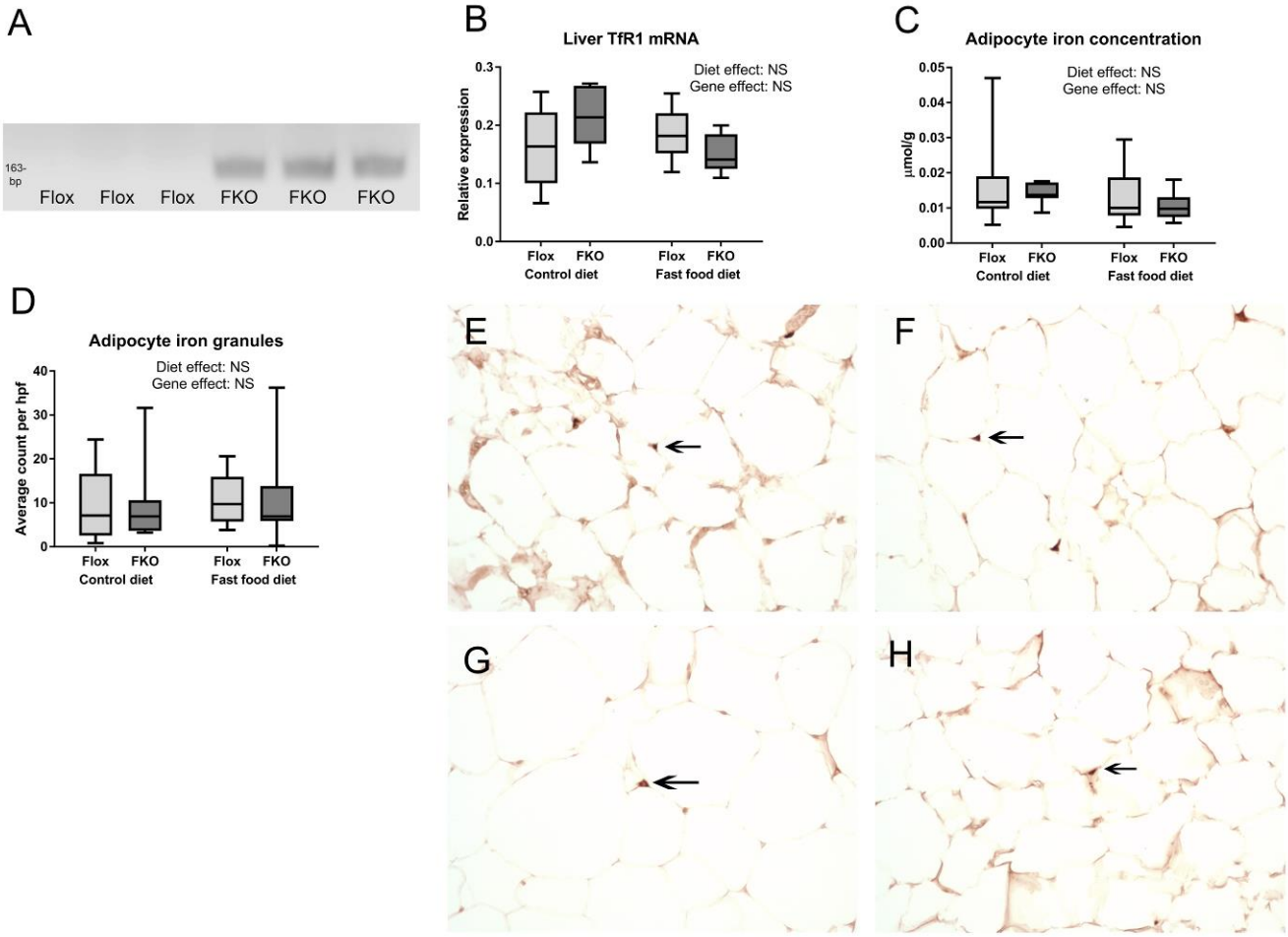

Adipocyte-specific ferroportin deletion does not alter adipocyte iron phenotype. All three measures of adipocyte iron loading in adipocytes consistently showed no effect of *Fpn1* deletion on iron phenotype (Fig. 5.2B-H). Quantification of *Tfr1* mRNA as an inversely related surrogate for cellular iron concentration found no genotype effect (NS, two-way ANOVA) (Fig. 5.2B). Similarly, adipocyte iron concentration by atomic absorption spectroscopy was not altered by *Fpn1* deletion (NS, two-way ANOVA) (Fig. 5.2C). Histologic assessment of adipocyte iron granules using DAB-enhanced Perls' stain found

that iron granule numbers were not increased in FKO mice (NS, two-way ANOVA) (Fig. 5.2D-H).

Fast food diet leads to reduced tissue iron concentrations via a hepcidin-independent mechanism. Hepatic iron concentration (HIC) was reduced by fast food diet in FKO mice (p<0.0001, Sidak's multiple comparison test) (Fig. 5.3A). Reduced HIC with fast food diet does not appear to be explained by an increase in *Hamp1* (encoding hepcidin) mRNA, as *Hamp1* mRNA levels were substantially reduced in fast food diet mice in both genotypes (p<0.0001, two-way ANOVA) (Fig. 5.3B). As HIC is an established regulator of hepcidin transcription [36, 38], we normalized *Hamp1* mRNA to HIC and found markedly reduced *Hamp1*/HIC levels with fast food diet, likely indicating an appropriate compensatory *Hamp1* response to reduced HIC (p<0.0001, two-way ANOVA) (Fig. 5.3C). Splenic iron concentration was also reduced by fast food diet (p<0.0001, two-way ANOVA) (Fig. 5.3D).

Figure 5.3: Fast food diet leads to reduced tissue iron concentrations via a hepcidin-independent mechanism

(A) Hepatic iron concentration (HIC). There was a significant interaction between diet and genotype (*P*=0.03, two-way ANOVA). Post hoc analysis demonstrated significantly lower HIC in FKO animals fed fast food diet compared to control diet (*P*<0.0001, Sidak's multiple comparisons test). (B) Hepatic *Hamp1* mRNA expression. Hepatic *Hamp1* mRNA was reduced by fast food diet (*P*<0.0001). Genotype effect was NS. (two-way ANOVA). (C) Hepatic *Hamp1* mRNA/HIC. Hepatic *Hamp1* mRNA/HIC ratio was reduced by fast food diet (*P*<0.0001). Genotype effect was NS. (two-way ANOVA). (D) Splenic iron concentration. Splenic iron concentration was reduced by fast food diet (*P*<0.0001). Genotype effect was NS (two-way ANOVA) (n= 8-12 per group).

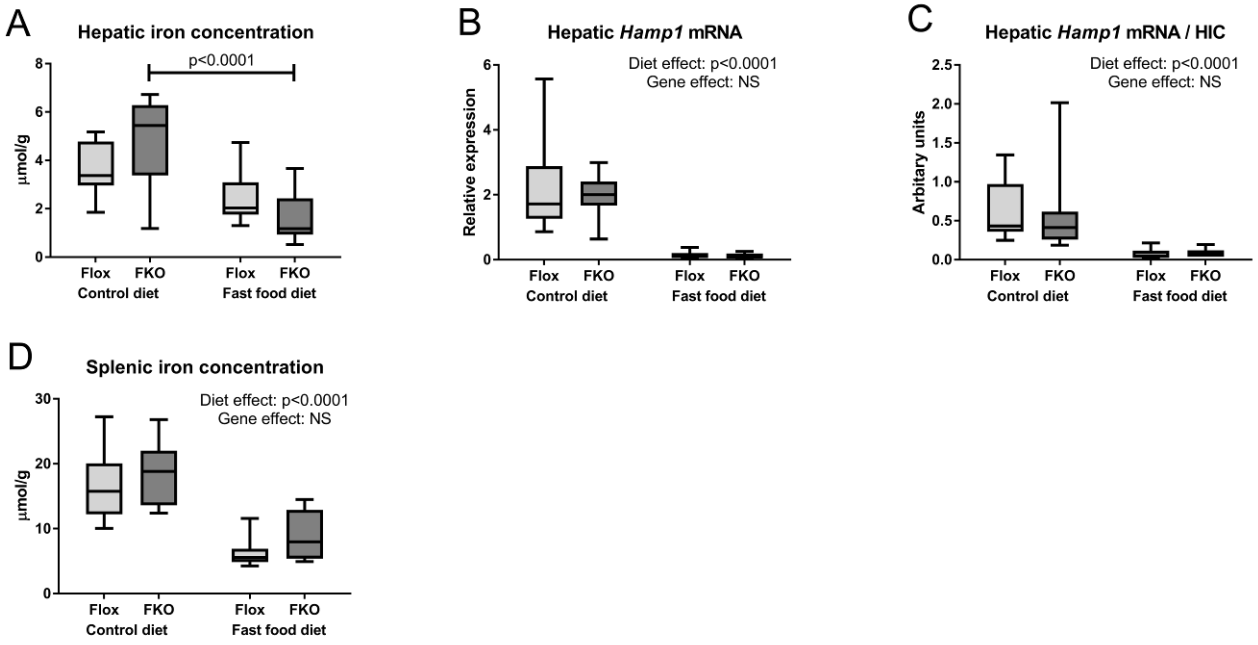

The fast food diet model is associated with adipose tissue macrophage accumulation. Clusters of macrophages, resembling crown-like structures [150] (as indicated by arrows in Fig. 5.4C, 5.4E) were frequently observed in adipose tissue sections from fast food diet-fed mice but not in their control diet counterparts ($p<0.0001$, two-way ANOVA). *Fpn1* deletion had no effect on the numbers of macrophage clusters (NS, two way ANOVA) (Fig. 5.4).

Figure 5.4: Fast food diet is associated with adipose tissue macrophage accumulation

(A) Number of macrophage clusters. Absolute count over ten high power fields. Macrophage clusters were increased by fast food diet (*P*<0.0001, two-way ANOVA). (B-E) Light microscopy of representative sections of Hematoxylin and Eosin stained epididymal fat pads (x 400 magnification). (B) Flox control diet. (C) Flox fast food diet. (D) FKO control diet. (E) FKO fast food diet. Arrows indicate examples of macrophage clusters. (n = 8-12 per group)

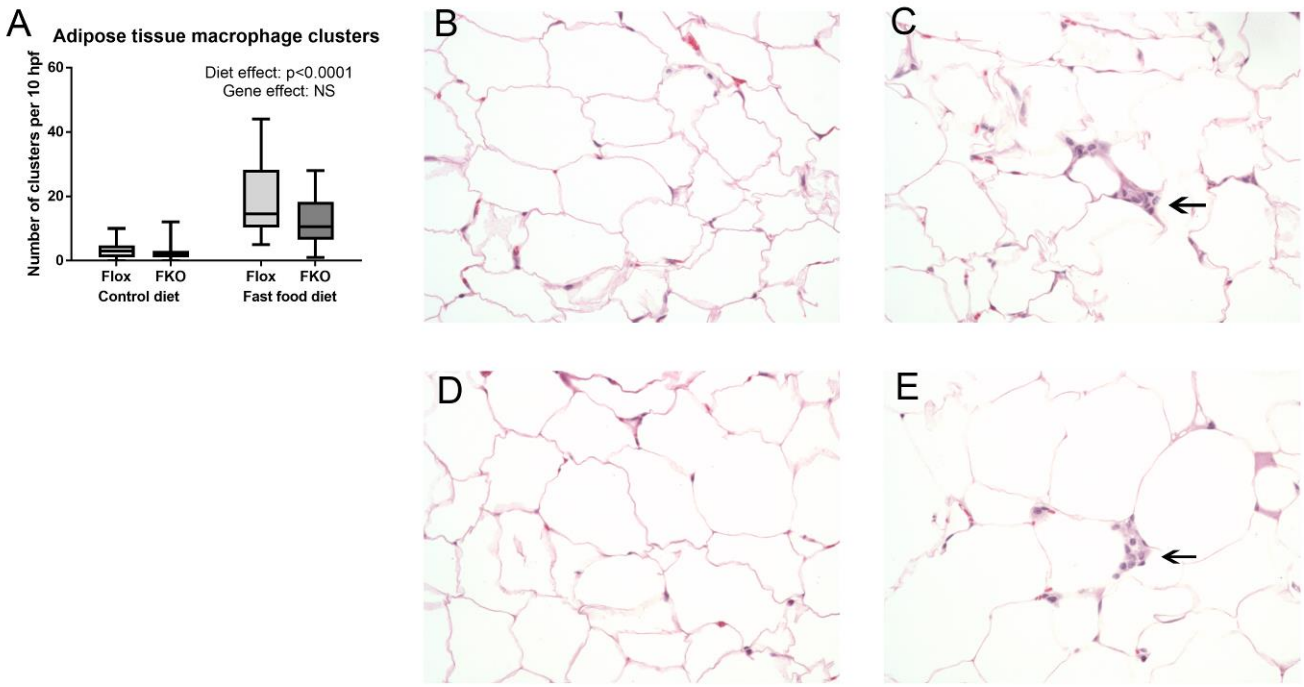

Adipokine expression is unchanged in FKO mice. There was no effect of *Fpn1* deletion on mRNA quantities of the four studied adipokines (adiponectin, leptin, resistin and RBP-4) in both non-insulin stimulated (basal, fasted state) animals (Fig. 5.5A-D) and in insulin stimulated animals (Fig. 5.6A-D) (all NS, two way ANOVA). Fast food diet led to increased *leptin* mRNA quantities in both basal-state and insulin stimulated animals ($p=0.03$ and $p=0.01$ respectively, two-way ANOVA). Fast food diet was associated with reduced *adiponectin* and *resistin* mRNA in insulin stimulated animals ($p=0.0003$ and $p=0.01$ respectively, two-way ANOVA). A reduction in *RBP-4* mRNA was seen in basal-state

animals (p=0.01, two way ANOVA) and insulin stimulated FKO animals (p=0.0008, Sidak's multiple comparisons test). Total serum adiponectin was unaffected by diet or genotype in basal-state and insulin-stimulated animals (NS in all cases, two way ANOVA) (Fig. 5.5E, F). There were also no significant differences with diet or genotype in basal state or insulin-stimulated animals for high molecular weight (HMW) adiponectin or HMW/total adiponectin ratios (all NS, two-way ANOVA, data not shown).

Figure 5.5: Adipokine expression is unchanged in FKO mice.

(A-D) Relative mRNA expression of the adipocyte fraction of epididymal fad pads for non-insulin stimulated animals. (A) *Adiponectin* mRNA. Diet and genotype effects were both NS (two-way ANOVA). (B) *Leptin* mRNA. Fast food diet was associated with increased *Leptin* mRNA (p=0.03, two-way ANOVA). (C) *Resistin* mRNA. Diet and genotype effects were both NS (two-way ANOVA). (D) *RBP-4* mRNA. Fast food diet was associated with decreased RBP-4 mRNA (p=0.01, two-way ANOVA). (E) Immunoblotting densitometry of total serum adiponectin (non-insulin stimulated only is represented here). Diet and genotype effects were both NS (two-way ANOVA). (n = 4-6 per group) (F) Representative immunoblots of serum adiponectin (presented blot includes both non-insulin and insulin stimulated animals as indicated: S=Saline (vehicle), I= Insulin).

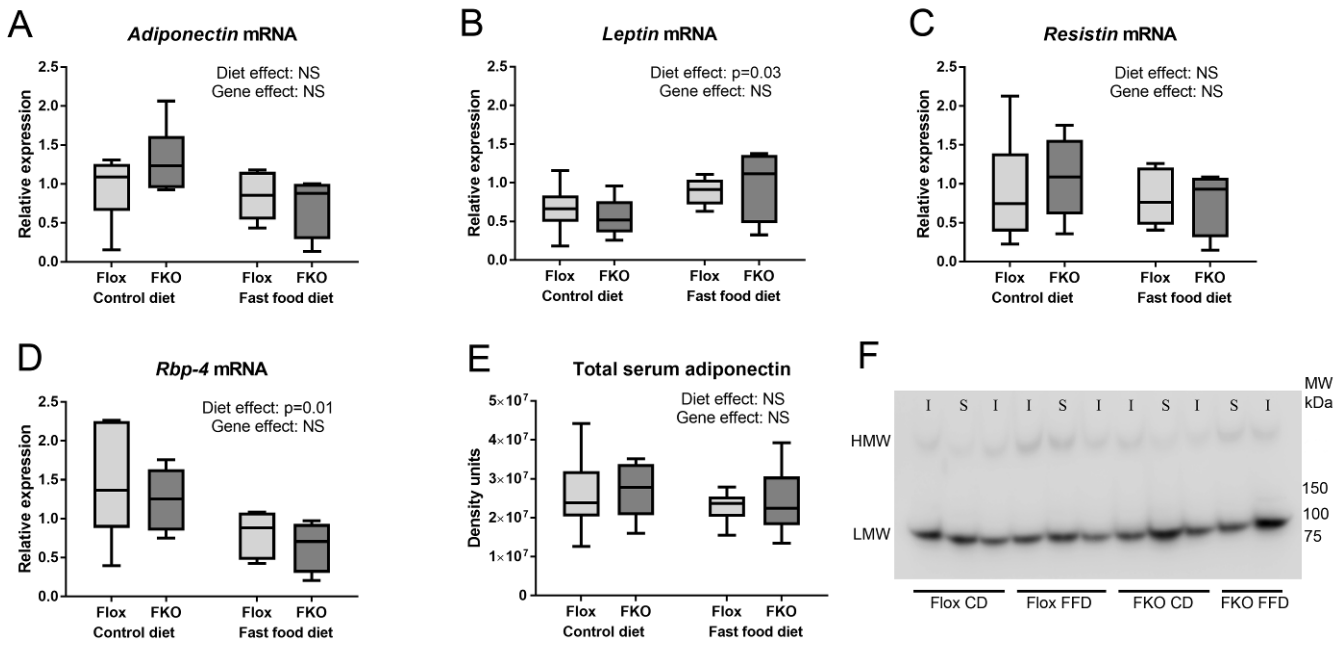

Figure 5.6: Adipokine expression is unchanged in insulin stimulated FKO mice

(A-D) Relative mRNA expression of the adipocyte fraction of epididymal fad pads (insulin stimulated state). (A) Adiponectin. *Adiponectin* mRNA was reduced by fast food diet (p=0.0003, two-way ANOVA). Genotype effect NS. (B) Leptin. *Leptin* mRNA was increased by fast food diet (p=0.01, two-way ANOVA). Genotype effect NS. (C) Resistin. *Resistin* mRNA was reduced by fast food diet (p=0.01, two way ANOVA). Genotype effect NS. (D) RBP-4. There was a significant interaction between diet and genotype (p=0.049). Post-hoc analysis found *RBP-4* mRNA was reduced by fast food diet among FKO animals (p=0.0008, Sidak's multiple comparisons test). In Flox mice the results were NS. (n= 4-6 per group).

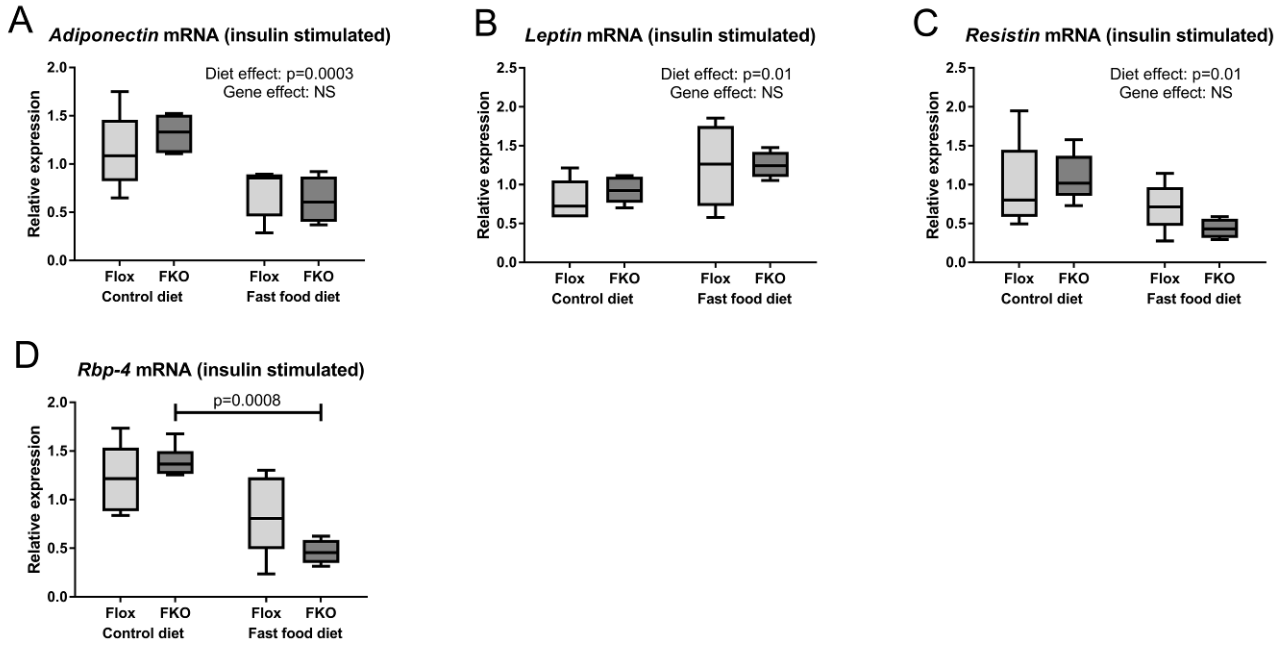

Adipocyte-specific ferroportin deletion does not influence glucose homeostasis. Intraperitoneal glucose tolerance tests found no significant differences in blood glucose concentrations for both diets at every time-point except 120 minutes (Fig. 5.7A, B). For control diet-fed Flox mice, mean glucose at 120 minutes was 16.1 mmol/L vs 12.8 mmol/L in FKO mice (p=0.02, Student's t-test). In fast food diet-fed Flox mice, mean glucose at 120 minutes was 13.8mmol/L vs 11.3mmmol/L in FKO mice (p=0.046, Student's t-test) (Fig. 5.7A, B). Area under the curve (AUC) was measured above the minimum glucose value of 7.7 mmol/L as a baseline. Both diet and genotype effects for AUC were non-significant (two-way ANOVA, data not shown). For hyperinsulinemic-euglycemic clamp studies performed on fast food diet-fed mice, mean body weight between the two groups was comparable 42.8 g (Flox) vs 43.4 g (FKO) (NS, Student's t-test, Fig. 5.7C). Flox mice had similar basal plasma glucose levels to FKO mice (9.3 vs 9.9 mmol/L) and clamp glucose levels (8.3 vs 8.4 mmol/L), both NS, Student's t-test (data not shown). Both groups of mice had substantial rises in mean plasma insulin levels during the clamp studies compared with basal levels (8.3 fold increase in Flox mice (15.7 vs 1.9 ng/ml) and

8.5 fold increase in FKO mice (19.8 vs 2.3 ng/ml), both p<0.0001, Student's t-test, data not shown). Overall, there was no evidence of an effect of FKO on glucose homeostasis. Mean glucose infusion rate was 122.9 µmol/min/kg in Flox mice vs 121.7 µmol/min/kg in FKO mice (NS, Student's t-test, Fig. 5.7D). Mean rate of whole body glucose disappearance was 202.5 µmol/min/kg in Flox mice vs 198.8 µmol/min/kg in FKO mice (NS, Student's t-test, Fig. 5.7E). Under clamp conditions of hyperinsulinemia, both groups to a similar extent, failed to suppress endogenous glucose production, a measure of hepatic gluconeogenesis, 79.6 µmol/min/kg in Flox mice vs 77.2 µmol/min/kg in FKO mice (NS, Student's t-test, Fig. 5.7F).

Figure 5.7: Adipocyte specific ferroportin deletion does not influence glucose homeostasis

(A + B) Glucose tolerance tests at 0, 15, 30, 60, 120 mins. Mean with 95% confidence intervals. * indicates p<0.05 at a single time-point (Student's t-test) (n = 8-12 per group). (A) Control diet (B) Fast food diet (C-F) Hyperinsulinemic-euglycemic clamp studies (n= 5 per group). Differences between Flox and FKO groups were all NS (Student's t-test). C) Body weight. (D) Glucose infusion rate. (E) Rate of whole body glucose disappearance. (F) Endogenous glucose production.

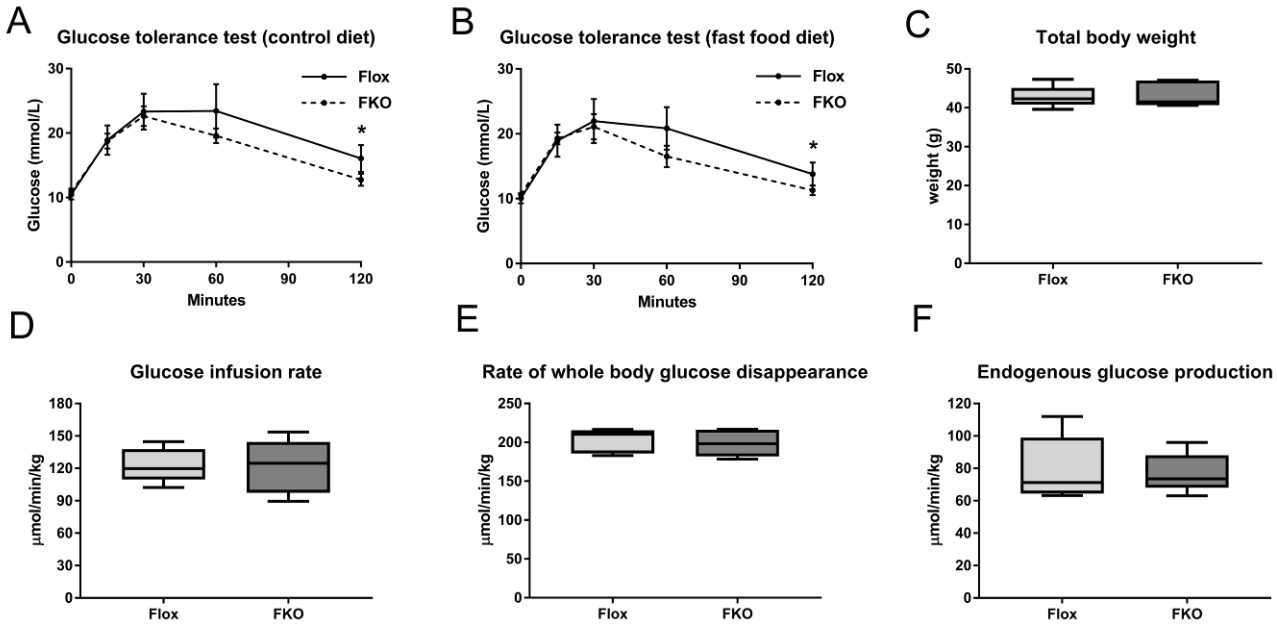

Fast food diet, but not adipocyte-specific ferroportin deletion, leads to steatohepatitis. Fast food diet in both genotypes led to steatohepatitis, characterized, by severe (grade 3) steatosis with lobular inflammation and prominent hepatocyte ballooning with perisinusoidal and periportal fibrosis. Control diet-fed mice of both genotypes typically had simple steatosis with few balloon cells and an absence of lobular inflammation and hepatic fibrosis. A summary of the histology findings is shown in Table 5.3 and representative liver sections stained with H&E are shown in Fig. 5.8. In both control diet

and fast food diet-fed animals, there were no significant differences between genotypes for steatosis grade, lobular inflammation, ballooning or fibrosis (all NS, Mann-Whitney tests). Increased percentage area of steatosis as quantified by Oil Red O staining was found in animals fed fast food diet (p=0.0001), whereas there was no difference between Flox and FKO genotypes (NS, both two-way ANOVA, Fig. 5.8E). Hepatic Heme oxygenase-1 (*Hmox1*) mRNA, a marker of oxidative stress response [151], was increased by fast food diet (p<0.001), but unaffected by genotype (NS, both two-way ANOVA, Fig. 5.8F). Hepatic hydroxyproline was significantly increased by fast food diet (p<0.001), but not by FKO (NS, two-way ANOVA, Fig. 5.8G).

Table 5.3: Increased liver injury with fast food diet, but not with *Fpn1* deletion.

NAFLD activity score (NAS). Median score (range) for NAS (score: 0-8), macrovesicular steatosis (grade 0-3), lobular inflammation (grade 0-3), ballooning (grade 0-2), fibrosis (grade 0-4). *P*-value is the result of Mann-Whitney tests comparing genotypes for each diet. (n = 8-12 per group)

	Control diet			**Fast Food Diet**		
	Flox	**FKO**	***P***	**Flox**	**FKO**	***P***
NAS (0-8)	4(0-6)	2 (0-5)	ns	6(5-7)	6(5-7)	ns
Steatosis (0-3)	2.5(0-3)	1.5(0-3)	ns	3(3-3)	3(3-3)	ns
Lobular inflammation (0-3)	0(0-1)	0(0-1)	ns	1(0-2)	1(0-2)	ns
Ballooning (0-2)	1.5(0-2)	0.5(0-2)	ns	2(2-2)	2(2-2)	ns
Fibrosis (0-4)	0(0-1)	0(0-2)	ns	2(1-2)	2(2-2)	ns

Figure 5.8: Fast food diet, but not genotype leads to steatohepatitis.

(A-D) Light microscopy of representative liver sections stained with Hematoxylin and Eosin (x 200 magnification). (A) Flox control diet (B) Flox fast food diet (C) FKO control diet (D) FKO fast food diet (E) Percentage area of liver sections stained with Oil Red O. Oil red O staining was increased by fast food diet (p=0.0001), but unaltered by genotype (NS, both two-way ANOVA) (F) Liver *Hmox1* mRNA. Fast food diet led to increased Hmox1 mRNA (p<0.001), but there was no genotype effect (NS, two way ANOVA). (G) Hepatic hydroxyproline. Hydroxyproline was increased by fast food diet (p<0.001) but was unaffected by genotype (NS, two-way ANOVA). (n=8-12 per group)

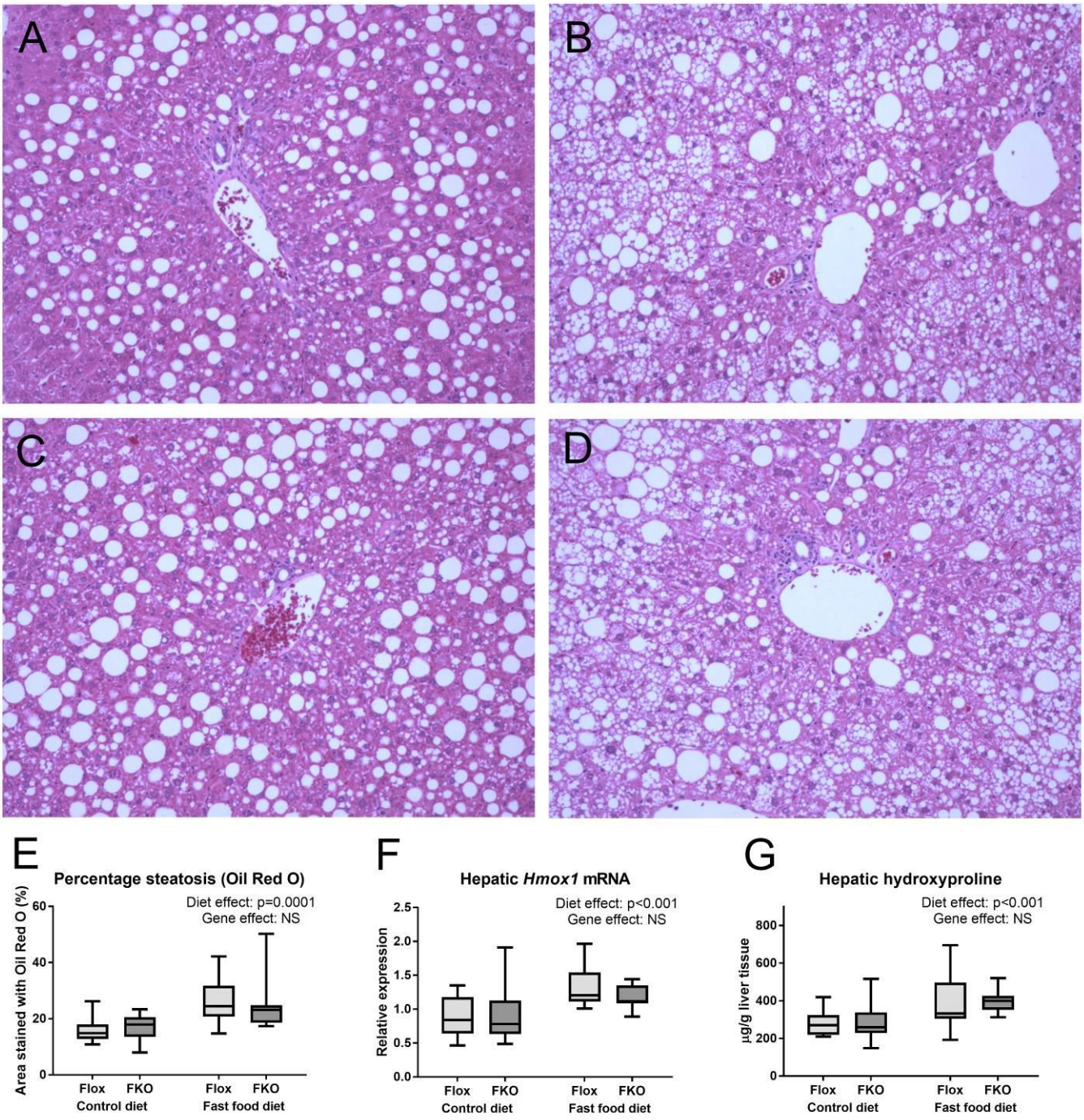

Discussion

In this study, we have demonstrated effective adipocyte-specific ferroportin deletion using an *Adipoq*-Cre recombinase model. Our study demonstrates three key findings. Firstly, ferroportin deletion did not result in any alteration of adipocyte iron phenotype, glucose homeostasis, adipokine regulation or liver injury. Secondly, we have shown that the fast food diet is associated with reduced hepatic and splenic iron concentrations with a compensatory hepcidin response. Thirdly, we confirm the fast food diet model's utility as a model for NASH and have identified adipose tissue macrophage infiltration which further validates this model.

We did not find an adipocyte iron loading phenotype despite successful *Fpn1* deletion in FKO mice. There are several possible explanations for this. Firstly, ferroportin may not have a significant role in adipocyte iron homeostasis. However, it is not known whether iron importers such as the divalent metal transporter-1 (DMT-1) or an unidentified alternative export mechanism may have more important roles in the regulation of iron content in adipocytes. Secondly, it is possible that the FKO mice would require a longer period of dietary iron loading to generate such a phenotype even in the absence of adipocyte ferroportin. As such, it may be difficult to determine the importance of adipocyte ferroportin to humans who may accumulate iron over many years.

Gabrielsen *et al* utilized the *AP2-Cre Fpn*$^{fl/fl}$ model and reported an iron loading phenotype on the basis of reduced quantities of adipocyte *Tfr1* mRNA leading to reduced adiponectin transcription and insulin resistance [17]. However, data regarding direct iron assay or histologic assessment of iron were not presented. *Tfr1* mRNA quantity is expected to be reduced in iron loaded cells due to a negative feedback mechanism involving iron-responsive elements in the *Tfr1* gene 3' untranslated region [143]. However *Tfr1* mRNA is a surrogate that is not well validated as a measure of iron loading and particularly not in adipocytes.

The disparity between the study by Gabrielsen *et al* and ours could relate to the difference in Cre recombinase site. In addition to its expression in adipocytes, the *AP2-Cre* has been reported to have some degree of expression in macrophages [26, 27, 144]. Although altered *Fpn1* mRNA quantities were not seen in splenic extracts by Gabrielsen et al, the *Adipoq-Cre* has been regarded as a more specific Cre recombinase for adipocytes [17, 26]. Differences between the two studies may also relate to a difference in mouse strain. The strain was reported as either "129/SvEvTac or C57BL6" by Gabrielsen *et al*.

Regardless, it appears that if Cre-lox models of adipocyte ferroportin deletion are to be used as models of adipocyte iron loading, then the iron loading phenotype needs to be more clearly demonstrated.

Glucose homeostasis was assessed in this study using intra-peritoneal glucose tolerance tests and hyperinsulinemic-euglycemic clamp studies. FKO mice had lower blood glucose concentrations at the 120 minute time-point, but not at other time-points or on the AUC analysis, suggesting that the significance of this result in isolation is doubtful, particularly given the lack of observed change in iron phenotype. Glucose infusion rate and other measures in the clamp studies found no difference between genotypes, indicating that adipocyte-specific ferroportin knockout does not affect insulin resistance in this model.

We have demonstrated reduced hepatic and splenic iron concentrations as a result of the fast food diet suggesting reduced body iron stores as a consequence of high calorie diet. The hormone hepcidin is considered the key regulator of body iron homeostasis [152]. Hepcidin production is reported to be raised in individuals with NAFLD [153]. It therefore might be expected that low HIC in these mice could be explained by increased *Hamp1* expression leading to reduced intestinal iron absorption following the internalization of enterocyte ferroportin [36]. However, *Hamp1* expression was markedly decreased in these mice suggesting appropriate *Hamp1* response to reduced hepatic iron stores and is consistent with previous studies [24, 125, 147, 154]. These findings are also in keeping with the established association between iron deficiency and obesity in humans [111, 112]. Orr *et al* have shown that a high fat diet led to iron repartitioning with a reduction in HIC and an increase in adipocyte iron concentration via an unknown mechanism, although this was not seen in our model [24]. In our study, it was not technically possible to accurately measure iron concentrations in the stromal vascular fraction of the adipose tissue, due to the very low volume of these samples, but this would undoubtedly be very useful information if this could be reliably determined in future studies.

The fast food diet model involves five months of exposure to a high calorie diet and high fructose corn syrup in drinking water in mice housed singly to mimic a sedentary lifestyle [25]. We have found this to be a reliable model for the generation of a phenotype of steatohepatitis and hepatic fibrosis as demonstrated by expert histological assessment and supported further by quantification of Oil Red O, *Hmox1* mRNA and hepatic hydroxyproline. Furthermore, the high residual endogenous glucose production during hyperinsulinemic clamp studies suggests profound insulin resistance in this model, which

is a highly appropriate feature for a model of human NASH. It was unexpected however that our mice fed control diet should develop significant amounts of simple steatosis. This may be partly explained by a number of factors including single housing leading to a sedentary existence and a relatively advanced age of the mice.

Adipose tissue macrophage infiltration is a hallmark of obesity and steatohepatitis in humans [21, 40]. We have shown that the fast food diet model generates a significant increase in adipose tissue macrophage infiltration with crown-like structures. This further validates the applicability of the fast food diet model for use in the study of NASH. We had considered that an increase in adipocyte iron in FKO mice might create an inflammatory state induced by oxidative stress and lead to macrophage infiltration. However, given the observed lack of effect of FKO on iron phenotype, it seems unsurprising that genotype did not affect macrophage infiltration in this model. In our study, we found that EFP weight was lower in FKO mice, although this was only seen in animals fed the control and not the fast food diet. In the context of unaltered iron phenotype and lack of effect in fast food diet fed mice, the significance of this result remains uncertain. When we studied adipokine expression in our model, we found increased adipocyte *leptin* mRNA and decreased *RBP-4* mRNA with fast food diet. These findings are broadly consistent with human studies of NASH, although conflicting reports exist in the literature [16, 155, 156].

In summary, our findings indicate that the physiological role of ferroportin in adipocytes may be limited and other factors involved in iron homeostasis may be more important in these cells. As adipocyte iron appears to play a key role in physiological process such as appetite regulation and pathophysiological process such as NAFLD and diabetes, a greater understanding of iron metabolism in these cells is clearly a target for future studies.

Chapter 6 : Iron inhibits the secretion of apolipoprotein E in cultured human adipocytes

The previous chapter sought to examine the role of *in vivo* adipocyte iron loading. In this chapter, focus shifts to an *in vitro* model. As discussed in detail in Chapter 2, there is an emerging body of evidence that associates adipose tissue iron with adipose tissue dysfunction relevant to NAFLD.[7, 34] In particular, a number of adipokines have been shown to be regulated by iron, however the overall effects of iron on the adipocyte secretome have not been established.[17, 18] In this chapter, the development of a model of iron loading in cultured human adipocytes is described. A proteomic approach to explore the effects of iron on the adipocyte secretome relevant to NAFLD is used.

This chapter is published as an abridged version (Research Letter) with detailed methods as supplementary material in Cellular and Molecular Gastroenterology and Hepatology. In this chapter the research is presented in its original, conventional manuscript form. The abridged version in press with Cellular and Molecular Gastroenterology and Hepatology is included as an Appendix, although the content is very similar.

Britton LJ, Bridle KR, Jaskowski L, He J, Ng C, Ruelcke J, Mohamed A, Reiling J, Santrampurwala N, Hill MM, Whitehead JP, Subramaniam VN, Crawford DHG
Iron inhibits the secretion of apolipoprotein E in cultured human adipocytes
Cellular and Molecular Gastroenterology and Hepatology 2018 Apr 16;6(2):215-217

Iron inhibits the secretion of apolipoprotein E in cultured human adipocytes

Laurence Britton[1,2,3,4], Kim Bridle[1,2], Lesley-Anne Jaskowski[1,2], Jingjing He[4], Choaping Ng[4,5], Jayde Ruelcke[6], Ahmed Mohamed[6,7], Janske Reiling[1,2,8], Nishreen Santrampurwala[1,2], Michelle Hill[6,7], Jonathan Whitehead[4,5], V. Nathan Subramaniam[9], Darrell Crawford[1,2]

1. Gallipoli Medical Research Institute, Greenslopes Private Hospital, Greenslopes, Queensland, Australia
2. The University of Queensland, Herston, Queensland, Australia
3. Department of Gastroenterology, Princess Alexandra Hospital, Queensland, Australia
4. Mater Research, Translational Research Institute, Woolloongabba, Queensland, Australia
5. School of Life Sciences, University of Lincoln, U.K
6. The University of Queensland Diamantina Institute, Faculty of Medicine, University of Queensland
7. QIMR Berghofer Medical Research Institute, Brisbane, Queensland, Australia
8. Department of Surgery, NUTRIM school of Nutrition and Translational Research in Metabolism, Maastricht University, Maastricht, the Netherlands
9. Institute of Health and Biomedical Innovation and School of Biomedical Sciences, Queensland University of Technology (QUT), Kelvin Grove, Queensland, Australia

Abstract

Background & Aims: Non-alcoholic steatohepatitis (NASH) is characterized by adipose tissue dysfunction with insulin resistance and the dysregulation of adipokines. Recent data indicate increased concentrations of iron in mouse model of obesity and a role for iron in the development of adipose tissue dysfunction, however the molecular mechanisms have not been established. Methods: To test the hypothesis that iron modulates adipokine release, we performed a quantitative proteomics analysis of the human Simpson-Golabi-Behmel Syndrome (SGBS) adipocyte secretome following 48 hours of treatment with ferric ammonium citrate. Results: Treatment with 100 μM iron significantly increased intracellular iron concentration, however cellular viability and total protein secretion were not altered. A total of 338 proteins were quantified by SILAC (stable isotope labelling with amino acids in cell culture). Iron treatment led to differential secretion of 60 of these proteins (>2-fold change and p-value <0.05). We focused on iron regulation of apolipoprotein E (ApoE)

secretion as ApoE has been shown to have a protective role in promoting adipogenesis and, in mice fed a Western diet, has been shown to protect against steatohepatitis. Interestingly, while iron reduced secreted ApoE by 58% (p=0.001) and 76% (p=0.007), as measured by SILAC and western blot respectively, iron treatment increased intracellular ApoE levels by more than 11-fold (p=0.0005), without causing a significant change in mRNA levels. Conclusions: These findings indicate that ApoE secretion is inhibited by iron, causing ApoE to accumulate within adipocytes. Identifying the molecular mechanisms of iron-induced inhibition of ApoE secretion from adipocytes may reveal novel therapeutic strategies for improving adipocyte function in NASH.

Background

Non-alcoholic fatty liver disease (NAFLD) is estimated to affect over one billion individuals worldwide.[1] It is mostly unclear at present, why some of these individuals develop liver failure or liver cancer and yet others do not. Greater insights into disease pathogenesis and regulation of liver injury will be essential in order to develop novel effective treatments. Much of the pathogenesis of NAFLD has been linked to dysfunctional adipose tissue.[21] Inflamed adipose tissue, characterized by macrophage infiltration, predisposes towards insulin resistance leading to dysregulated lipolysis of adipose tissue triglyceride by hormone sensitive lipase.[21, 42] This in turn increases free fatty acid flux to the liver and promotes hepatic steatosis and liver injury.[45, 46] In addition, adipose tissue, as a major endocrine organ, is responsible for the secretion of adipokines which are defined as “polypeptides that are secreted in the adipose tissue in a regulated manner.”[16] These adipokines can have local, paracrine effects on adipose tissue or endocrine effects on organs such as the liver.

Recent data have shown markedly increased adipocyte iron concentration in a high fat diet mouse model of obesity.[24] Furthermore, iron has been proposed as a key determinant of adipose tissue function and has been linked to the dysregulation of a number of adipokines.[17, 19] Of these, the insulin sensitizing and hepato-protective adipokine, adiponectin, has been shown in tissue culture and rodent models to be down-regulated at a transcriptional level by iron through altered acetylation of the forkhead transcription factor, Fox01.[17] Similarly, in a mouse model of dietary iron enrichment, serum concentrations of resistin, an adipokine associated with insulin resistance were increased via transcriptional up-regulation.[19] Iron has also been shown to increase lipolysis in *in vitro* models using both rat and mouse adipocytes.[92, 93] These effects on adipose tissue

biology point towards a potential pathogenic role of iron in the generation of insulin resistance and NAFLD. However, the effect of iron on the majority of proteins in the adipocyte secretome has not been studied.

In order to gain a greater understanding of the role of iron in adipokine dysregulation and identify novel treatment targets, we developed an *in vitro* human adipocyte model of cellular iron loading using differentiated Simpson-Golabi-Behmel Syndrome (SGBS) pre-adipocytes. We utilized stable isotope labelled amino acids in cell culture (SILAC) to characterize changes in the adipocyte secretome in response to iron. This technique has enabled direct comparison of quantities of individual proteins in the adipocyte secretome in response to iron using a proteomics approach. This study, therefore provides a detailed analysis of the effect of iron on the human adipocyte secretome as a tool for the identification of novel treatment targets in NAFLD.

Methods

SGBS differentiation and iron treatment

SGBS pre-adipocytes were a gift from Martin Wabitsch (University of Ulm, Germany) and were passaged, proliferated and differentiated at less than 50 generations in 12 well plates and 100 mm dishes as previously described.[157, 158] Cells were treated with 90 µg/ml heparin and 1 ng/ml fibroblast growth factor-1 (FGF-1) (both Sigma-Aldrich, St Louis, Missouri) throughout proliferation and differentiation. After 14 days of differentiation, cells were incubated with 0, 25, 100 or 500 µM ferric ammonium citrate (FAC) (Sigma- Aldrich) for 24 hrs. After this media was replaced with the same for a further 24 hrs to the end of experiment.

RNA extraction and real-time quantitative PCR (RT-qPCR)

RNA was extracted from treated SGBS adipocytes using a PureLink RNA mini kit (Invitrogen, Carlsbad, California). Complementary DNA was synthesized from 1 µg RNA using a Sensifast cDNA synthesis kit (Bioline, London, UK) after treatment with DNase 1 (Invitrogen). Samples underwent thermal cycling using a ViiA7 real-time PCR machine (Invitrogen) with a Sensifast SYBR Lo-ROX Kit (Bioline). The following protocol was used: 2 min at 95^{o}C, then 40 cycles of 5 sec at 95^{o}C alternating with 20 sec at 63^{o}C, followed by a melt curve analysis. Relative mRNA quantities were determined by calibration of Ct

values to standard curve of pooled cDNA samples. Results were normalized to Ct values of Cyclophillin.

Iron, cellular viability (MTS) and protein assays.

Iron levels were quantified using a chromagen reagent method, described by Kohyama et al.[159] Cellular viability was assessed using a CellTiter 96 AQueous One Solution Cell Proliferation Assay (Promega, Madison, Wisconsin) according to the manufacturer's instructions. Whole cell lysate and secretome samples underwent protein estimation using a Pierce BCA protein assay kit (Thermofisher Scientific, Waltham, Massachusetts).

SILAC proteomics

For SILAC labelling, SGBS pre-adipocytes were grown in SILAC DMEM: F12 media (Thermofisher Scientific) supplemented with dialyzed fetal bovine serum (Thermofisher Scientific,) and 22.81mg/L $^{2}H_{4}$-Lysine and 36.88mg/L $^{13}C_{6}$-Arginine (K4R6) or 22.81mg/L $^{13}C_{6}{}^{15}N_{2}$-Lysine and 36.88mg/L $^{13}C_{6}{}^{15}N_{4}$-Arginine (K8R10). Incorporation of labelled amino acids was confirmed by liquid chromatography tandem mass spectrometry (LC-MS/MS) on tryptic peptides prepared from whole cell lysates. Cell pellets were lysed in 8M urea in 100mM TEAB (Triethylamonium bicarbonate), and protein concentration estimated using Bradford assay (BioRad, Hercules, California). Thirty µg of cell lysate was reduced and alkylated by incubating samples for 30 min at 37^{o}C with 2.5mM TCEP (tris(2-carboxyethyl)phosphine) and then 5mM 2CAA (2-Chloroacetamide). Urea concentration was diluted to 1M with 100mM TEAB before adding 0.6 µg of trypsin. Samples were incubated overnight then acidified to 1% trifluoroacetic acid (TFA) and cleaned with OMIX C18 tips according to the manufacturers' protocol (Agilent, Santa Clara, California). LC-MS/MS and database searching was performed as described below. The percentage of peptides containing labelled amino acids was then calculated.

Labelled (>97%) cells underwent differentiation to adipocytes as described above. At day 14 post differentiation, cells were treated with vehicle (K4R6 cells) or 100 µM FAC (K8R10 cells) for a further 48 hours using exactly equal volumes of media, replacing the media after 24 hrs. Media for secretome analysis was collected from K4R6 and K8R10 cells and mixed 1:1 (v/v) before centrifugation at 600 x G at 4^{o}C for 10 min to remove cell debris. Supernatant was then concentrated using Amicon Ultra 15ml 10 kDa centrifugal filter units (Merck Millipore, Burlington, Massachusetts) in a fixed angle centrifuge at 5000 x G to provide approximately 1 ml samples of concentrated mixed secretome. Thirty □g of protein

was separated on 10% SDS-PAGE gels to 10 mm. Protein visualisation, excision of bands and in-gel trypsin digest were performed using a semi-automated method as described.[160] A band corresponding to the same molecular weight as transferrin (media additive) was removed prior to digestion in order to provide a protein sample exclusively secreted from cultured adipocytes.

Mass spectrometry

A Q Exactive Plus Orbitrap Mass Spectrometer (Thermofisher Scientific), coupled with Easy-nLC 1000 and EASY-spray ion source (both Thermofisher Scientific), was used to analyze the digested peptides. Samples were loaded onto an EASY-Spray PepMap RSLC C18 2 µm column (50 cm x 75 µm ID), with a Nanoviper Acclaim C18 guard (75 µm x 2 cm) (both Thermofisher Scientific). A 90 min method was run using a combination of Buffer A (0.1% Formic acid) and Buffer B (0.1% Formic acid: Acetonitrile). A two-step gradient was run comprising a 60 min gradient from 3% to 25% Buffer B and a 12 min gradient from 25% to 40% Buffer B. Flow rate was at 250 nL/min. The mass spectrometer was programmed to acquire a full mass spectrometry (MS) resolution of 70,000 with an ACG target of $3x10^6$ with a maximum injection time of 100 ms. The MS scan range was from 350 to 1400 m/z. MS/MS was set to acquire a resolution of 17,500 with an ACG target of $5x10^5$ and maximum injection time of 55 ms. The loop count was set to 20 with a dynamic exclusion after 30 sec.

Raw data was processed with Spectrum mill (Rev B.05.00.181 SP1, Agilent). Selected modifications included fixed carbamidomethylation of cysteine and SILAC labels (Arg 0-6-10 Da Lys 0-4-8 Da) and variable oxidized methionine. Results were searched against the Human Uniprot database (downloaded 06/01/2015).[161] Trypsin was selected as digest enzyme, with two maximum missed cleavages allowed. The precursor mass tolerance was set at +/- 20 ppm and product mass tolerance was +/- 20 ppm.

Immunoblotting

Western blotting using whole cell lysate samples (10 µg) and 5 µL concentrated secretome samples was performed as previously described.[147] A 1:500 dilution of primary antibody against Apolipoprotein E (ApoE) (sc-53570, Santa Cruz, Dallas, Texas) was applied to the membranes. A 1:100,000 dilution of goat anti-mouse horseradish peroxidase antibody (Invitrogen) was applied as secondary antibody. ApoE whole cell lysate densitometry was

normalized against densitometry using beta-actin as a reference protein (1:2000 primary antibody) (Cat No. 4967, Cell Signaling, Danvers, Massachusetts) and 1:20,000 goat anti-rabbit horseradish peroxidase antibody (Invitrogen).

Statistical analysis

For comparisons between the four concentrations of FAC, a one-way ANOVA analysis was used. In the event of a p value < 0.05, Dunnett's multiple comparison test was used to compare vehicle (0 μM FAC) with each of 25, 100 and 500 μM FAC treated cells. Mass spectrometry proteomic data were analyzed using the online Quantitative Proteomics P-value Calculator (QPPC) using no normalization and non-adjusted p-values.[162] For comparison of mRNA quantities and immunoblot densitometry between two groups, ratio paired t-tests were used. For enrichment analysis of significantly iron-regulated proteins, one-tailed Fisher's exact tests were used. All authors had access to the study data and have reviewed and approved the final manuscript.

Results

We first sought to identify a suitable media concentration of FAC that would load iron into differentiated adipocytes without compromising cellular viability. We found that compared to vehicle both 100 μM and 500 μM FAC caused significant increases in cellular iron concentration ($p=0.007$ and $p=0.006$ respectively, Figure 6.1(a)). There was no effect of iron loading on cellular viability (MTS) assay, total mRNA, total whole cell lysate protein or total secretome protein (Figure 6.1 (b-d)).

Figure 6.1: Optimization of iron loading in SGBS cells

(a) Iron assay, p=0.004 (one-way ANOVA), *indicates p<0.01 (Dunnett's multiple comparisons test compared to 0μM FAC, n=2 per group). (b) Total RNA (non-significant (NS) by one-way ANOVA, n=3 per group). (c) Total lysate protein (NS by one-way ANOVA, n=3 per group). (d) Total secretome protein (NS by one-way ANOVA, n=3 per group). (e) Viability assay (MTS) (NS by one-way ANOVA, n=3 per group).

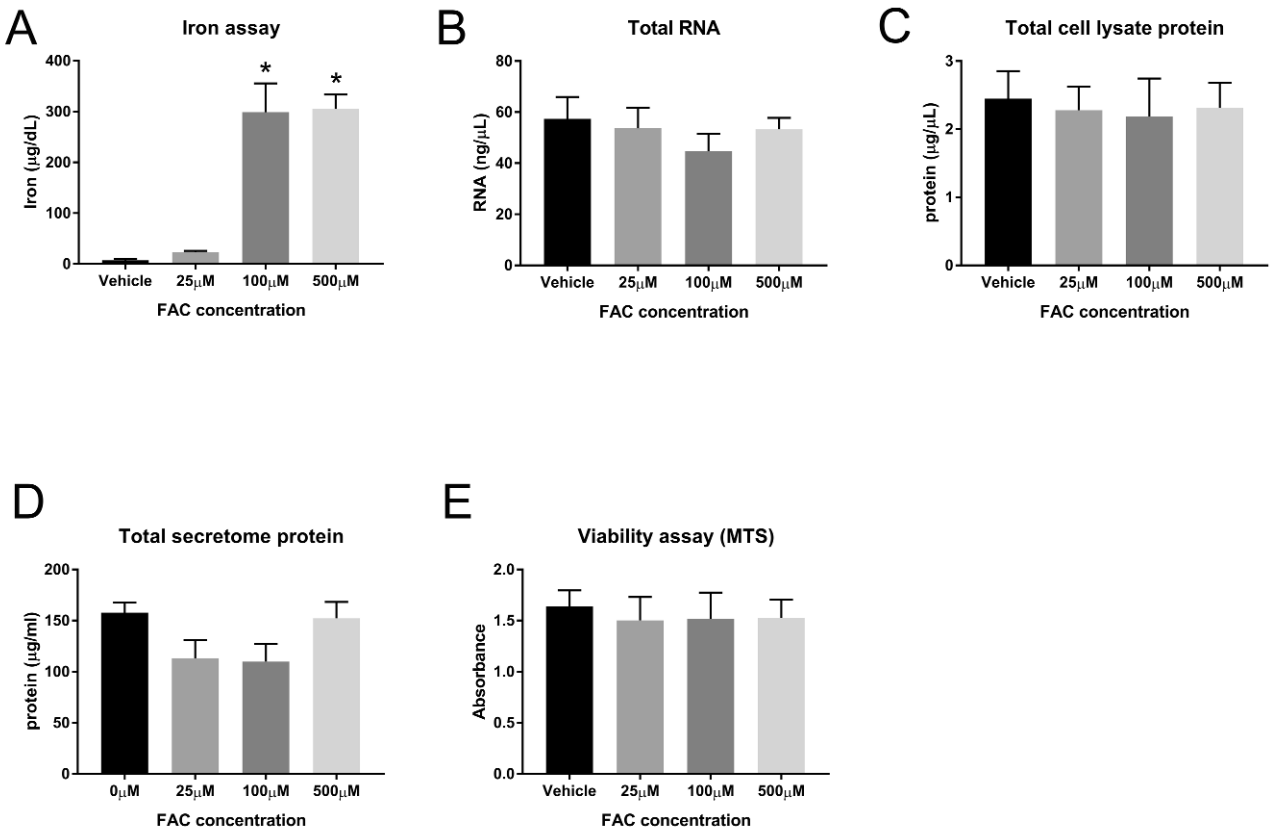

Given these findings, we selected 100 μM FAC as the concentration to compare with vehicle in the secretome SILAC proteomic analysis. An overview of the workflow for the SILAC experiment is shown in Figure 6.2. A total of 338 proteins were quantified in the adipocyte secretome by SILAC proteomics. These are represented graphically as a volcano plot in Figure 6.3 and summarized in Table 6.1.

Figure 6.2: SILAC workflow

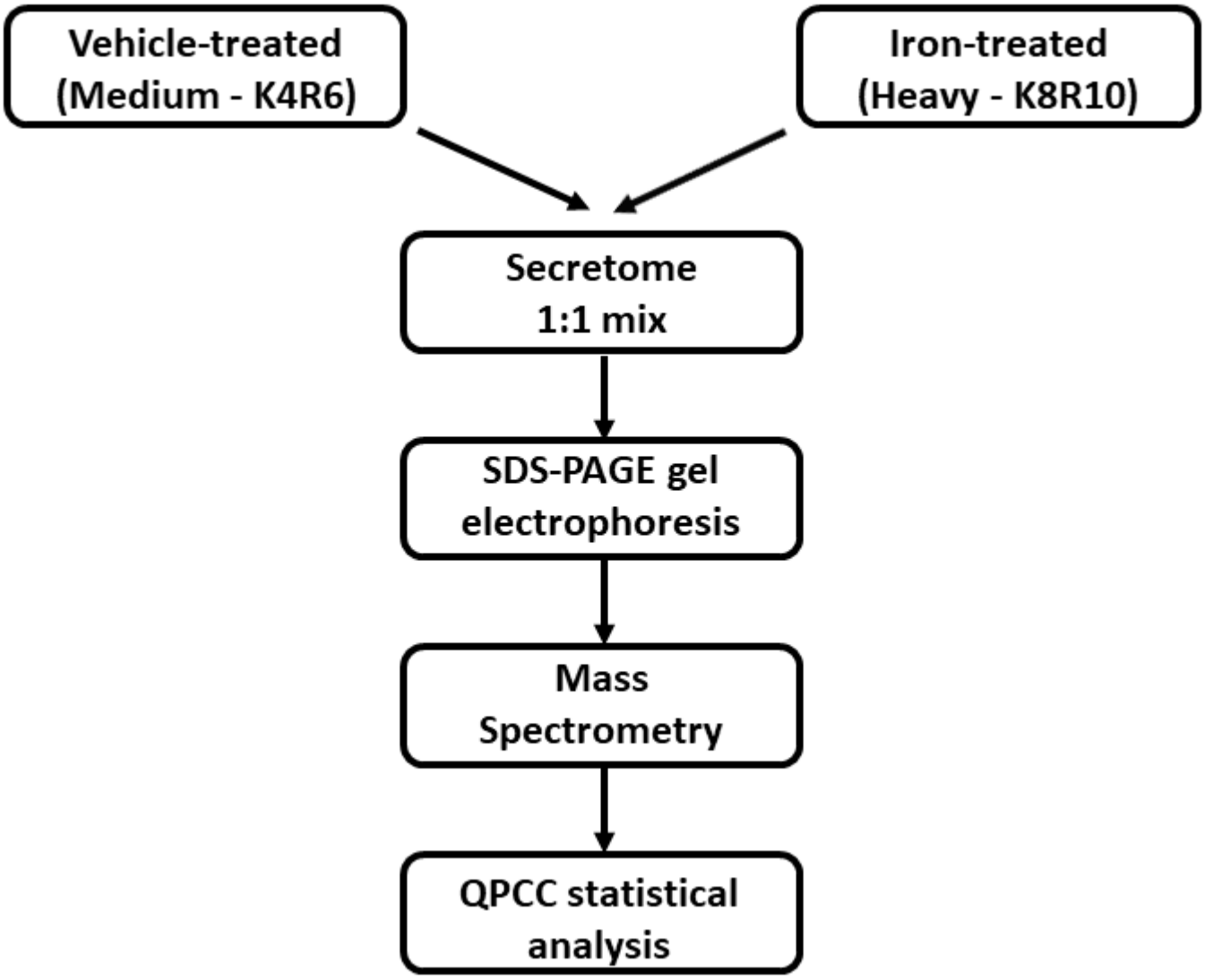

Figure 6.3: Volcano plot of relative signal intensity of proteins identified in the adipocyte secretome

The x-axis denotes log 2 of the ratio of iron treated/vehicle treated cells, with proteins to the left of zero representing those downregulated by iron and the those to the right representing up-regulation by iron. The y-axis denotes statistical significance with a line representing p-value of 0.05. Proteins above this line have p<0.05. Those proteins containing signal peptide (as determined by signal peptide annotations on the Uniprot database) are shown in red. Those without signal peptide are shown in blue.

Table 6.1: Summary of iron effects on the adipocyte secretome by SILAC proteomics.

Number of proteins with a greater than 2-fold change are shown in parentheses.

	Number of proteins down-regulated	Number of proteins up-regulated	Total (>2 fold change)
Significant (p<0.05)	61 (53)	11 (7)	72 (60)
Non-significant (p>0.05)	152	114	266
Total	213	125	338

To explore the relationships further between proteins that appear to be significantly dysregulated in the adipocyte secretome (greater than two-fold change and p<0.05), we performed a STRING network interaction analysis. This is represented graphically in Figure 6.4. This analysis highlighted central roles for Apolipoprotein E (APOE) and Adioponectin (ADIPOQ) which have been shown to have hepatoprotective effects in

NAFLD. However, major linked pathways of dysregulation relevant to NAFLD were not clearly identified.

Figure 6.4: STRING pathway analysis of secreted proteins.

STRING pathway network summary of secretome proteins with a greater than two fold change in signal intensity in response to iron and $p<0.05$. Each node represents an individual secretome protein, labelled by gene name (as indicated in Table 6.2). Line thickness of network edges indicates the strength of data supporting interactions between individual proteins.

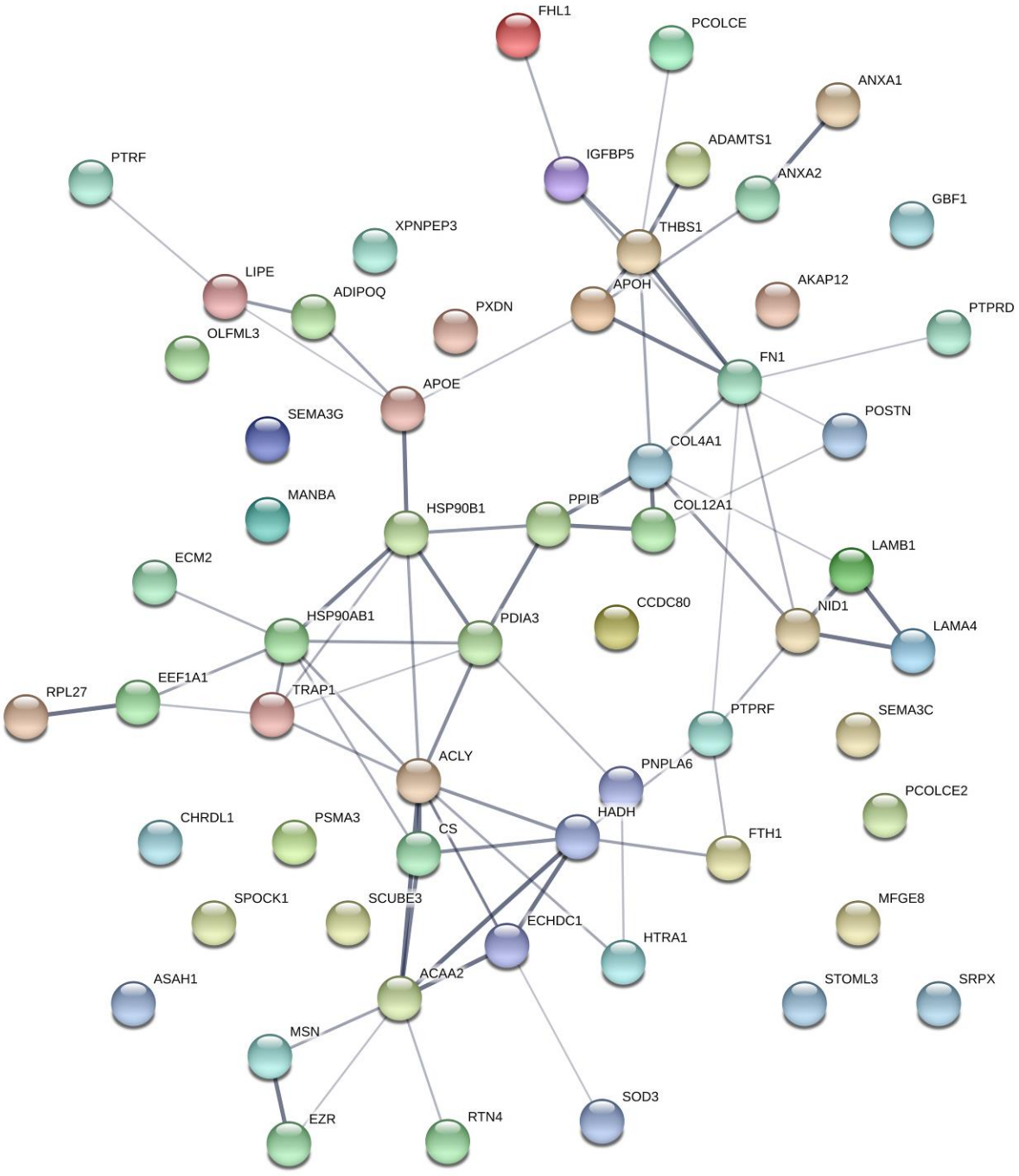

We then manually reviewed Uniprot database descriptions of the 60 proteins with both a greater than two-fold change in response to iron and p-value < 0.05. This generated a list of 20 proteins of interest (highlighted in bold in Table 6.2). These proteins of interest and their synonyms were then entered into a Pubmed title/abstract search in association with NAFLD and its synonyms. This identified three proteins as candidate intermediates for iron-induced adipose tissue dysfunction in NAFLD. These proteins were adiponectin, apolipoprotein E (ApoE) and annexin A1.

Table 6.2: List of SGBS secretome proteins with significantly altered signal intensity in response to iron.

Proteins shown have a greater than 2-fold change in signal intensity in response to iron, with a p-value <0.05. Proteins highlighted in bold represent the 20 proteins of interest after review of Uniprot protein descriptions.

Accession number	Gene name	Protein name	Mean signal intensity ratio (iron/vehicle)	Standard deviation	P value
Q8IX30	**SCUBE3**	**Signal peptide, CUB and EGF-like domain-containing protein 3**	**0.026**	**0.016**	**0.001**
P61353	RPL27	60S ribosomal protein L27	0.060	0.005	0.001
Q9NQH7	XPNPEP3	Probable Xaa-Pro aminopeptidase 3	0.076	0.004	0.001
P07996	**THBS1**	**Thrombospondin-1**	**0.083**	**0.047**	**0.001**
Q76M96	CCDC80	Coiled-coil domain-containing protein 80	0.090	0.031	0.001
P78539	SRPX	Sushi repeat-containing protein SRPX	0.096	0.620	0.001
Q9UHI8	ADAMTS1	A disintegrin and metalloproteinase with thrombospondin motifs 1	0.114	0.090	0.002
Q92538	GBF1	Golgi-specific brefeldin A-resistance guanine nucleotide exchange factor 1	0.118	0.024	0.004
Q15063	**POSTN**	**Periostin**	**0.121**	**0.149**	**0.001**
P08238	HSP90AB1	Heat shock protein HSP 90-beta	0.125	0.038	0.004
P24593	**IGFBP5**	**Insulin-like growth factor-binding protein 5**	**0.154**	**0.069**	**0.001**
Q15113	PCOLCE	Procollagen C-endopeptidase	0.155	0.088	0.001

		enhancer 1			
Q9NTX5	ECHDC1	Ethylmalonyl-CoA decarboxylase	0.158	0.068	0.001
P25788	PSMA3	Proteasome subunit alpha type-3	0.176	0.442	0.001
Q12931	TRAP1	Heat shock protein 75 kDa, mitochondrial	0.186	0.028	0.018
P04083	**ANXA1**	**Annexin A1**	**0.192**	**0.049**	**0.001**
P30101	PDIA3	Protein disulfide-isomerase A3	0.198	0.059	0.001
Q99985	**SEMA3C**	**Semaphorin-3C**	**0.199**	**0.225**	**0.001**
Q6NZI2	PTRF	Polymerase I and transcript release factor	0.210	0.134	0.001
Q8TAV4	STOML3	Stomatin-like protein 3	0.220	0.084	0.006
Q9UKZ9	PCOLCE2	Procollagen C-endopeptidase enhancer 2	0.226	0.030	0.001
Q05469	LIPE	Hormone-sensitive lipase	0.231	0.196	0.023
Q13642	FHL1	Four and a half LIM domains protein 1	0.263	0.006	0.029
P02749	APOH	Beta-2-glycoprotein 1	0.286	0.310	0.048
P02462	COL4A1	Collagen alpha-1(IV) chain	0.286	0.351	0.001
P15311	EZR	Ezrin	0.296	0.077	0.003
P42765	ACAA2	3-ketoacyl-CoA thiolase, mitochondrial	0.308	0.136	0.001
P68104	**EEF1A1**	**Elongation factor 1-alpha 1**	**0.309**	**0.215**	**0.001**
Q9NQC3	**RTN4**	**Reticulon-4**	**0.312**	**0.119**	**0.007**
Q8IY17	PNPLA6	Neuropathy target esterase	0.316	0.028	0.026
Q92743	HTRA1	Serine protease HTRA1	0.324	0.075	0.001
P08294	**SOD3**	**Extracellular superoxide dismutase [Cu-Zn]**	**0.339**	**0.027**	**0.005**
Q16836	HADH	Hydroxyacyl-coenzyme A dehydrogenase, mitochondrial	0.348	0.207	0.011
Q99715	COL12A1	Collagen alpha-1(XII) chain	0.348	0.183	0.001
P07355	**ANXA2**	**Annexin A2**	**0.354**	**0.111**	**0.001**
P26038	MSN	Moesin	0.362	0.110	0.034
P23284	PPIB	Peptidyl-prolyl cis-trans isomerase B	0.374	0.122	0.001
O94769	ECM2	Extracellular matrix protein 2	0.375	0.060	0.005
Q9NRN5	**OLFML3**	**Olfactomedin-like protein 3**	**0.389**	**0.066**	**0.002**
P53396	**ACLY**	**ATP-citrate synthase**	**0.389**	**0.066**	**0.001**

Q16363	LAMA4	Laminin subunit alpha-4	0.407	0.091	0.001
P14625	**HSP90B1**	**Endoplasmin**	**0.414**	**0.068**	**0.025**
Q9BU40	CHRDL1	Chordin-like protein 1	0.419	0.264	0.001
P02649	**APOE**	**Apolipoprotein E**	**0.421**	**0.053**	**0.001**
Q9NS98	**SEMA3G**	**Semaphorin-3G**	**0.425**	**0.161**	**0.001**
P02751	**FN1**	**Fibronectin**	**0.441**	**0.146**	**0.001**
P14543	**NID1**	**Nidogen-1**	**0.442**	**0.190**	**0.006**
Q08431	**MFGE8**	**Lactadherin**	**0.446**	**0.167**	**0.026**
Q15848	**ADIPOQ**	**Adiponectin**	**0.449**	**0.652**	**0.005**
O75390	CS	Citrate synthase, mitochondrial	0.454	0.183	0.012
Q92626	PXDN	Peroxidasin homolog	0.457	0.200	0.001
P07942	LAMB1	Laminin subunit beta-1	0.484	0.110	0.001
Q08629	SPOCK1	Testican-1	0.497	0.055	0.014
O00462	MANBA	Beta-mannosidase	2.180	2.560	0.034
Q13510	ASAH1	Acid ceramidase	2.222	3.135	0.048
P02794	**FTH1**	**Ferritin heavy chain**	**2.451**	**0.769**	**0.030**
Q02952	AKAP12	A-kinase anchor protein 12	2.665	0.572	0.047
A6NCN2	KRT87P	Putative keratin-87 protein	4.113	0.011	0.022
P23468	PTPRD	Receptor-type tyrosine-protein phosphatase delta	10.687	2.199	0.003
P10586	PTPRF	Receptor-type tyrosine-protein phosphatase F	11.935	3.955	0.001

Of these candidate proteins, we focused on ApoE for two main reasons. Firstly, the effects of iron on ApoE secretion from adipocytes has not to our knowledge previously been studied. Secondly, ApoE has been proposed as having a protective role in NAFLD pathogenesis.[163] We found a consistently reproducible effect of iron on ApoE by western blot in both 12 well plate (non-SILAC) and 100mm plate (SILAC) models. Densitometry of secretome ApoE was reduced by 76% ($p=0.007$), consistent with effect seen with SILAC signal intensity analysis of 58% reduction ($p=0.001$) (Figures 6.5(b) and 6.5(d)). Conversely, whole cell lysate samples demonstrated a greater than 11-fold increase in intracellular ApoE in response to iron ($p=0.0005$), without a significant change in ApoE mRNA levels (Figures 6.5(a), 6.5(c) and 6.5(e)).

Figure 6.5: SBGS ApoE expression following FAC treatment

(a) ApoE mRNA (NS, ratio paired t-test), (b) Secretome ApoE densitometry (* denotes p=0.001, ratio paired t-test), (c) Lysate ApoE densitometry normalized to β-actin (# denotes p=0.0005, ratio paired t-test), (d) Secretome ApoE immunoblot, (e) Whole cell lysate ApoE and β-actin immunoblots (n=3 per group)

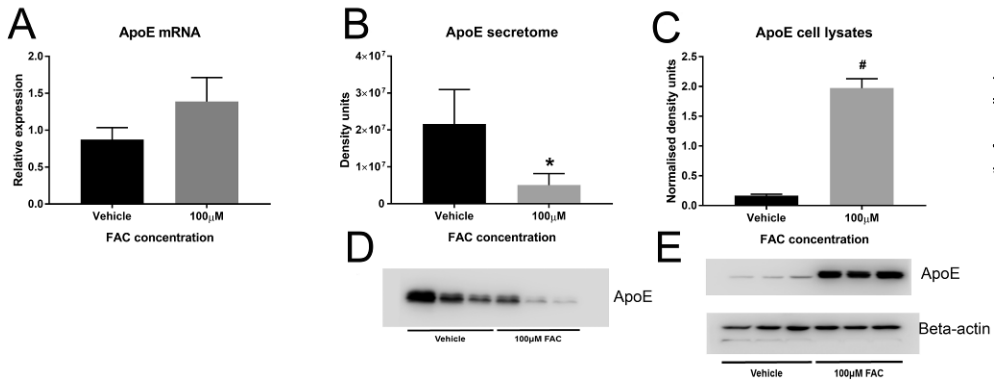

In order to evaluate whether, the effects of FAC were iron-specific or a more generalised toxic effect, we examined oxidative stress, inflammatory and endoplasmic reticulum (ER) stress responses. We found transcriptional upregulation of anti-oxidant responses with an increase in heme-oxygenase-1 (HO-1) (p=0.01) and glutathione peroxidase-1 (GPX-1) mRNA (p=0.049). Interleukin-6 (IL-6) mRNA as a marker of inflammation was not significantly altered by iron, although there was a trend towards a decrease in IL-6 mRNA with iron treatment (43% decrease, p=0.08). (Figures 6.6(a-c))

We also examined X-box binding protein (XBP-1) mRNA (spliced and unspliced) which in its spliced form is a master regulator of the unfolded protein response caused by endoplasmic reticulum (ER) stress.[164] Iron had no effect on quantities of both unspliced and spliced XBP-1 mRNA. (Figures 6.6(d) and 6.6(e)) In addition, there was no effect on downstream transcriptional targets of spliced XBP-1, such as immunoglobulin binding protein (BiP) and ER-degradation-enhancing-α-mannidose-like protein (EDEM). (Figures 6.6(f) and 6.6(g)) Furthermore, signalling in the ER stress induced apoptosis pathway was evaluated by quantifying activating transcription factor 4 (ATF4) and CCAAT/enhancer-binding protein homologous protein (CHOP) mRNA. (Figures 6.6(h) and 6.6(i)) Again these were unaffected by iron.

Given that a large number of proteins had lower secretome signal intensity in response to iron, we hypothesized that iron targets selected mechanisms of protein secretion. To investigate the potential secretion pathways regulated by iron, we evaluated two characterized protein secretion mechanisms, namely, the classical secretory pathway

mediated by signal peptide and vesicle-mediated secretion. The effect of iron on the classical secretion pathway was evaluated using signal peptide annotations from the Uniprot database.[161] To do this, we performed an enrichment analysis comparing the 61 significantly down-regulated proteins ($p<0.05$) with the remaining 277 proteins in the adipocyte secretome. Of the 61 significantly downregulated proteins, 62% (38/61) had signal peptide, whereas of the remaining proteins only 47% (129/277) had signal peptide (Figures 6.3, 6.6(j) and 6.6(k)). One-tailed Fisher's-exact test showed significant enrichment with signal peptide ($p=0.02$) amongst the significantly downregulated group. In contrast, there was no significant enrichment of the exosomal pathway ($p=0.51$, one-tailed Fisher's-exact test), as 15% (9/61) of significantly down-regulated proteins and 14% (39/277) of the remaining secretome proteins had been previously reported in the high confidence proteins from the EVpedia database, [165] (Figures 6.6(l) and 6.6(m)). These results suggest that iron selectively blocks the classical secretory pathway.

Figure 6.6: Mechanistic aspects of iron-related dysregulation of protein secretion

(a) Interleukin-6 (IL-6) mRNA (non-significant (NS), paired t-test, n=3 per group). (b-c) Oxidative stress * indicates $p<0.05$, both n=3 per group (b) Heme-oxygenase (HO-1) mRNA ($p=0.01$, paired t-test). (c) Glutathione peroxidase 1 (GPX-1) mRNA ($p=0.049$, paired t-test). (d-i) Endoplasmic reticulum (ER) stress, all n=3 per group. (d) Unspliced X-box binding protein (XBP-1) mRNA (NS, paired t-test). (e) Spliced X-box binding protein (XBP-1) mRNA (NS, paired t-test). (f) Immunoglobulin binding protein (BiP) mRNA (NS, paired t-test). (g) ER-degradation-enhancing-α-mannidose-like protein (EDEM) mRNA (NS, paired t-test). (h) Activating transcription factor 4 (ATF4) mRNA (NS, paired t-test). (i) CCAAT/enhancer-binding protein homologous protein (CHOP) mRNA (NS, paired t-test). (j-m) Enrichment with signal peptide and exosome proteins. (j) Proportion of proteins significantly down regulated by iron with signal peptide vs no signal peptide. (k) Proportion of proteins not significantly down regulated by iron with signal peptide vs no signal peptide. (l) Proportion of proteins significantly down regulated by iron with exosome secretion vs no exosome secretion. (m) Proportion of proteins not significantly down-regulated by iron with exosome secretion vs no exosome secretion. Of the 61 significantly down-regulated proteins, 62% (38/61) had signal peptide, whereas of the remaining proteins only 47% (129/277) had signal peptide. One-tailed Fisher's-exact test showed significant enrichment with signal peptide ($p=0.02$) amongst the significantly down-regulated group. In contrast, there was no significant enrichment of the exosomal pathway ($p=0.51$, one-tailed Fisher's-exact test), as 15% (9/61) of significantly down-regulated proteins and 14% (39/277) of the remaining secretome proteins had been previously reported in the high confidence proteins from the EVpedia database.

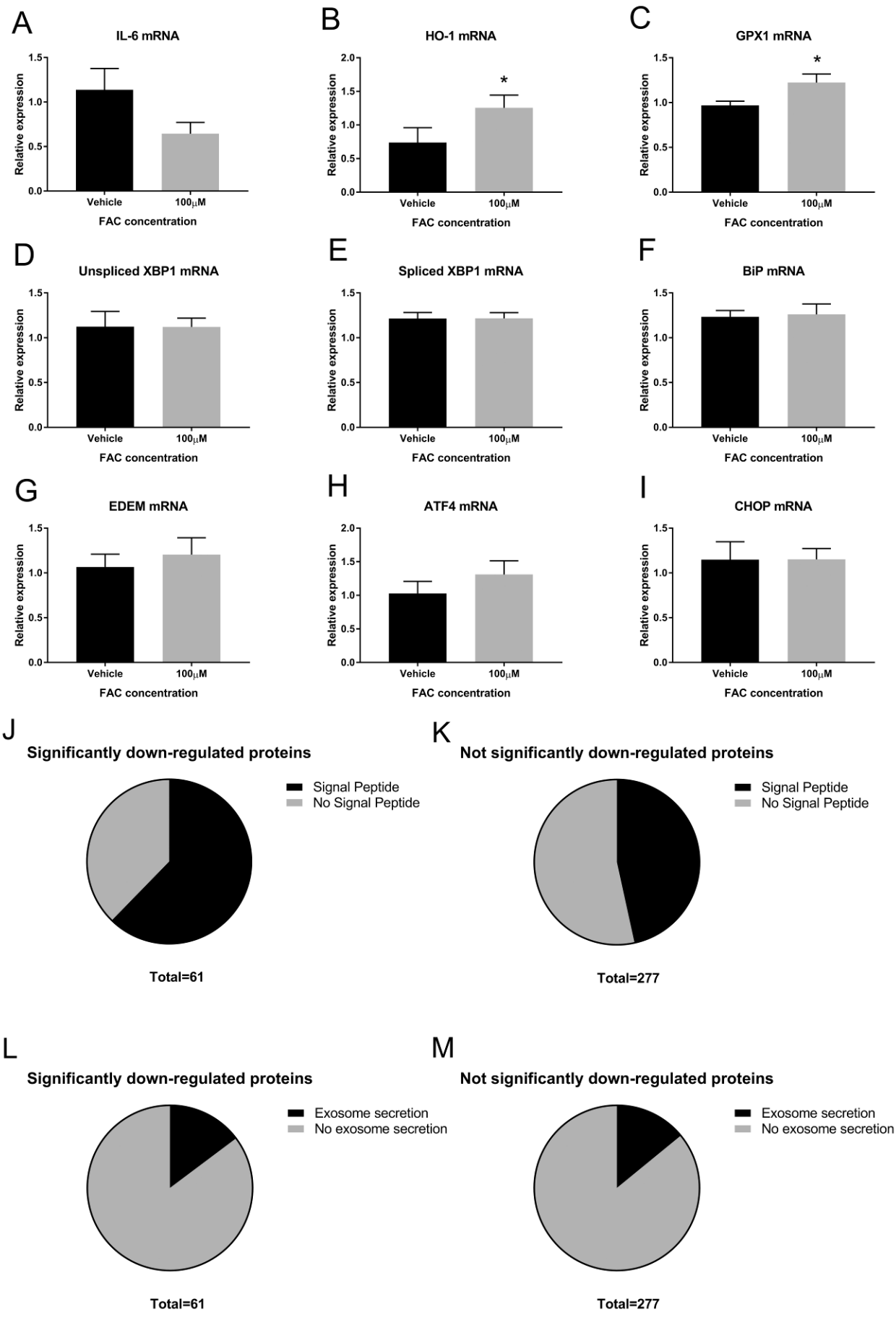
A
IL-6 mRNA
B
HO-1 mRNA
C
GPX1 mRNA
D
Unspliced XBP1 mRNA
E
Spliced XBP1 mRNA
F
BiP mRNA
G
EDEM mRNA
H
ATF4 mRNA
I
CHOP mRNA
Relative expression
Vehicle
100μM
FAC concentration
J
Significantly down-regulated proteins
Signal Peptide
No Signal Peptide
Total=61
K
Not significantly down-regulated proteins
Signal Peptide
No Signal Peptide
Total=277
L
Significantly down-regulated proteins
Exosome secretion
No exosome secretion
Total=61
M
Not significantly down-regulated proteins
Exosome secretion
No exosome secretion
Total=277

Discussion

In this study, we have identified 72 proteins secreted from human adipocytes which were significantly dysregulated in response to iron. Of these, we have identified a number of proteins with particular relevance to NAFLD, including ApoE, adiponectin and annexin A1.

Furthermore, we showed using immunoblotting that ApoE becomes sequestered within adipocytes in response to iron. This may be an important pathogenic phenomenon in humans with NAFLD, as ApoE appears to protect against steatohepatitis. In a mouse model of ApoE knockout, unlike wild type controls, mice fed seven weeks of Western diet developed impaired glucose tolerance, steatohepatitis and hepatic fibrosis.[163] ApoE is a component of lipoproteins, such as Very Low Density Lipoprotein (VLDL) and High Density Lipoprotein (HDL) and promotes VLDL induced adipogenesis.[166] ApoE knockout mice also readily develop atherosclerosis on an atherogenic diet and have been widely used as models for this condition.[167]

As ApoE is also synthesized by other tissues, notably the liver, it is important to consider the role of ApoE derived from other tissues in the phenotypes seen in global knockout models. In order to overcome this issue, Huang et al utilized an AP2 Cre-lox model of adipocyte-specific ApoE deletion which demonstrated increased insulin sensitivity compared to genetic controls.[168] This suggests that ApoE deficiency in other cells types, such as hepatocytes, may offset this benefit in global knockout models. Therefore, in future studies, it will be essential to determine whether iron impacts on ApoE secretion in other cells, particularly hepatocytes.

With regards to other cell types, iron has been shown to dysregulate ApoE in primary cultured astrocytes and in cortical neurons. This is important, as the ApoEε4 polymorphism of the ApoE gene is common and is the strongest genetic risk factor for Alzheimer's disease.[169] In addition, impaired iron homeostasis has been strongly linked to disease pathogenesis in this condition.[170] It has recently been shown that in primary cultured astrocytes and cortical neurons, iron treatment led to increased intracellular concentrations of ApoE and reduced ApoE secretion.[171] Taken together with our data, it seems possible that iron may indeed have similar effects on a range of cell types and represents a clear target for further investigation.

Our SILAC analysis showed that iron treatment resulted in an 81% reduction in Annexin A1 secretome signal intensity. This is interesting as AnnexinA1 knock-out mice exhibit

greater degrees of hepatic lobular inflammation and fibrosis than controls when fed a methionine-choline deficient diet.[172] Annexin A1 therefore is potentially an important mechanism of iron-related adipocyte dysfunction in NAFLD and a candidate for future research. Furthermore, adipocyte iron has previously been shown to down-regulate serum adiponectin in a mouse derived adipocytes, 3T3-L1 cells. [17] Our findings support this in a human adipocyte cell line with a 55% reduction in adiponectin signal intensity in iron-treated SGBS cells.

In order to understand better whether FAC was having an iron-specific effect or a more general effect, we examined pathways of oxidative stress, inflammation and ER stress. Treatment with iron in our study, demonstrated an upregulation of anti-oxidant responses (heme-oxygenase-1 (HO-1) and glutathione peroxidase-1 (GPX-1) mRNA) indicating the presence of oxidative stress. However, interleukin-6 (IL-6) mRNA as a marker in inflammation was not increased with iron treatment, nor was there any difference among multiple markers of endoplasmic reticulum stress. Taken together, our model demonstrates oxidative stress responses without any evidence of ER stress or unfolded protein responses and no evidence of an impairment of cellular viability.

We considered whether iron may have a generalized effect on pathways of protein secretion, utilized by a variety of proteins. We evaluated the role of iron in the secretion of proteins by the classical and exosomal pathways using the Uniprot and EVpedia databases respectively. We found enrichment of signal peptide-containing, but not exosome-secreted proteins amongst the iron-dysregulated proteins suggesting that iron may have a specific effect on proteins secreted via the classical pathway. Further investigation is still needed to clarify the mechanistic details of this effect.

STRING pathway analysis has identified central roles for a number of important proteins in relation to dysregulation by iron. No clear unifying pathway was identified however. It is worth noting though, that such network analysis is primarily designed for identifying intracellular pathway and as such, it may be considered unsurprising that a clear and clinically relevant pathway has not been identified.

Given the lack of quality human data regarding physiological adipocyte iron concentrations, a limitation of this study is that it is difficult to determine the physiological relevance of the concentrations of iron used. Nonetheless, it is reassuring that there was no observed iron-effect on cellular viability, total mRNA, or total protein.

This research has characterized the effect of iron on the adipocyte secretome. These data provide a platform for multiple avenues for future research. In addition, we have been able to show that increased iron results in sequestration of ApoE within adipocytes, which may be of key importance in the regulation of insulin resistance and liver injury in NAFLD. Further work is required to identify how iron and oxidative stress might regulate this effect and whether therapeutic manipulation of adipocyte iron in humans may be of benefit in NAFLD.

Chapter 7 : Conclusions

The burden of non-alcoholic liver disease (NAFLD) represents a global epidemic.[1] The condition can lead to cirrhosis, liver failure and hepatocellular carcinoma.[2] The pathogenesis of this condition is not well understood and treatments that are substantially and consistently beneficial have not been developed. Dealing with this issue effectively will require major societal changes in diet and lifestyle and will almost certainly depend heavily upon governmental and public health initiatives. Nevertheless, for the foreseeable future, we are faced with an extraordinary burden of disease that urgently requires the development of improved medical therapy.

Given the multifaceted nature of its pathophysiology and the heterogeneous nature of the disease, it seems unlikely that a single treatment approach will be effective for the majority of people with NAFLD. It may even be that fatty liver disease or steatohepatitis becomes regarded as a histologic result of a series of sub-classifications of fatty liver disease, including alcohol, insulin resistance and diabetes predominant, other genetic predispositions, iron-related, a number of other as yet unknown co-factors and various combinations of the above. Given the probable heterogeneity in pathogenesis, NAFLD treatment is likely to require a personalised-medicine approach.

Manipulation of iron homeostasis, by venesection has been used in medicine for thousands of years. [173] More recently, venesection has proven to be an effective treatment for conditions such as haemochromatosis. Indeed venesection has been proposed as a treatment for NAFLD, although no large scale randomised trial has convincingly demonstrated effectiveness.[104] It could be argued though, that a subpopulation of NAFLD patients with certain iron phenotype may yet benefit from this treatment. Alternatively, it may be considered that venesection is too blunt a tool with which to benefit patients with NAFLD who may have complex derangements in iron homeostasis. Our understanding of cellular and systemic iron homeostasis mechanisms including the hepcidin-ferroportin axis have raised the promise of a more sophisticated and targeted manipulation of iron homeostasis.[152] Before such treatments might be developed for conditions such as NAFLD and possibly type II diabetes, it is essential that we more clearly define whether iron really might have an important role and if so, what the mechanism and location of iron's effect might be.

This thesis has examined the role of iron homeostasis in NAFLD pathogenesis across a range of tissues. The effect of subtle changes in enterocyte, and therefore systemic, iron

homeostasis in the context of HFE and hepcidin deficiency has been evaluated in an *Hfe* heterozygous knockout mouse model of NAFLD. Focus then shifted to examining the links between hepatic iron concentration (HIC) and insulin sensitivity, before evaluating the role of adipose tissue iron using *in vivo* and *in vitro* models. The key findings from these studies are described below.

In the first of four original research chapters, Chapter 3, describes the use of an animal model of heterozygous *Hfe* deletion fed a high calorie diet as a model for humans with heterozygous *HFE* gene mutations who have co-existent NAFLD. This is a commonly encountered clinical scenario, given the high prevalence of both *HFE* gene polymorphisms and NAFLD.[14, 96] Given the observed co-toxic effect of HFE-haemochromatosis and NAFLD seen in humans and in mice with homozygous *Hfe* deletion, it has been important to explore the role of heterozygous gene mutations in NAFLD pathogenesis. Indeed it has been suggested that functional HFE deficiency itself may play an iron-independent role in NAFLD pathogenesis.[15] Human data and meta-analyses have led to conflicting results, yet this topic had not previously been studied in an animal model.[14, 96]

Although increased hepatic iron accumulation with heterozygous *Hfe* deletion was observed, there was no evidence of increased liver injury as a result. It is unclear however whether effects may have been seen with a more prolonged exposure high calorie diet. *Hamp1* (encoding Hepcidin) mRNA / HIC ratios demonstrated an approximate 50% decrease in $Hfe^{+/-}$ mice in both dietary groups compared with wild-type littermate controls. These findings are consistent with true haploinsufficiency regarding the translation of *HFE* and its interaction with *Hamp1*.

The most remarkable finding from the study was the observation of increased serum glucose concentrations and HOMA-IR scores in $Hfe^{+/-}$ mice compared with wild-type controls. Unfortunately, the experiment was primarily designed to investigate liver injury and hepatic lipid metabolism As such, a detailed understanding of the impairment in glucose metabolism in this model would only be possible with a repeat study involving the use of techniques such as glucose tolerance tests and hyperinsulinaemic-euglycaemic clamps. Such a study would be readily achievable and is required to confirm these findings and explore the mechanisms by which HFE deficiency and/or mild iron excess can disrupt glucose homeostasis.

In order to explore further the role of iron in glucose homeostasis and insulin resistance, Chapter 4 draws upon human data and stored serum samples from a prospective,

randomised, controlled trial of venesection in humans with NAFLD.[104] The original study, by Adams et al, showed a lack of effect of venesection on hepatic steatosis, serum ALT and measures of insulin sensitivity.[104] Nonetheless, given the quality of data available and unique access to paired serum samples before and after venesection, this was a useful opportunity with which to examine the relationships between iron, insulin resistance and adipokines further.

There is an increasing body of evidence, described in depth in Chapter 2 that links alterations in adipocyte iron content to the dysregulation of adipokines implicated in NAFLD pathogenesis.[17, 19, 92, 147] Although there is a conspicuous lack of human data describing adipocyte iron concentration in NAFLD, a four-fold increase in adipocyte iron content was observed in a mouse model of obesity using a high fat diet.[24] This was shown to be associated with a reduction in HIC. A repartitioning of iron from the liver to adipose tissue was therefore proposed, but a mechanistic explanation remains elusive.[24] Chapter 4 describes the effect of venesection on serum concentrations of six key adipokines over a six month period, compared to randomised controls in participants with NAFLD. In addition, the relationships between, measures of iron homeostasis and insulin resistance were explored in depth.

Venesection had no impact on serum concentrations of the six adipokines; adiponectin, leptin, resistin, RBP-4, TNFα and IL-6. There are a number of possible explanations for this. These include 1) these six adipokines are not regulated by iron, 2) venesection did not significantly mobilise adipose tissue iron, either due to treatment intensity or other unknown reasons, or 3) the study was insufficiently powered to detect changes in these adipokine concentrations. It should be noted however, that there was no real suggestion of a trend towards venesection effect for any of the adipokines studied.

Further analysis of baseline data did however uncover modest but highly consistent associations between multiple surrogates of insulin sensitivity demonstrating an HIC. In addition there was a significant positive correlation between HIC and serum adiponectin concentration. These results challenge the conventional assumption that increasing HIC in the non-haemochromatotic range is associated with insulin resistance and diabetes. Indeed, other recently published data indicate that in the non-haemochromatotic range, increasing iron may be metabolically advantageous with respect to insulin resistance.[61, 128] However, causal relationships based on our study cannot be established. This is in keeping with the observation of improved glucose tolerance in mice with homozygous *Hfe*

deletion [124]. However, this is seemingly at odds with the observation in Chapter 3 that heterozygous *Hfe* gene deletion is associated with a small increase in HIC, raised fasting serum glucose and HOMA-IR scores. The unknown factor though, in the human study and in both mouse models is the concentration of iron in adipose tissue and in particular adipocytes. This is particularly relevant when one considers the data that show increased adipocyte iron concentration in mice fed a high fat diet. [24]

In order to explore further the relationships between adipose tissue iron and insulin resistance in NAFLD pathogenesis, Chapters 5 and 6 utilise *in vivo* (Chapter 5) and *in vitro* (Chapter 6) models of adipocyte iron loading. In Chapter 5, a model of selective adipocyte ferroportin knockout using a Cre-lox system driven by Cre in the promotor region the adiponectin gene (*Adipoq*) was developed. This model convincingly demonstrates effective selective knockout of the ferroportin gene (*Fpn1*) in adipocytes. However, this did not lead to increased adipocyte iron levels as measured by multiple means, implying that ferroportin may not be a key determinant of mammalian adipocyte iron homeostasis. It was then as expected that adipocyte ferroportin deletion did not lead to increased liver injury or evidence of altered glucose homeostasis. It remains unclear whether a higher dietary iron content would help to expose the desired phenotype or whether ferroportin really does have an insignificant role in iron homeostasis in adipocytes.

In Chapter 6, a proteomic approach was employed in order to identify novel therapeutic targets in relation to dysregulation of adipokines by iron. Using stable isotope labelled amino acids in cell culture (SILAC), the iron-effect on the human Simpson-Golabi-Behmel syndrome (SGBS) adipocyte secretome was characterised. Sixty proteins with a greater than two-fold change in secretion and statistical significance of $p<0.05$ in response to iron were identified. Notable proteins that have been implicated in NAFLD pathogenesis were highlighted after a literature review relating to these proteins. Of these, adiponectin, annexin A1 and apolipoprotein E (ApoE) may be particularly relevant. The findings of a reduction in mass spectrometry signal intensity of adiponectin in response to iron replicate in human adipocytes, a similar observation, previously only seen in mouse 3T3-L1 adipocytes. [17] Similarly a knockout model of annexin A1 has previously indicated a protective role for this protein in NAFLD pathogenesis. [172]

The most striking finding from this study relates to ApoE. Immunoblotting of the secretome and intracellular protein indicated that iron profoundly inhibits secretion of ApoE causing it to become sequestered within adipocytes. There was evidence of transcriptional

responses to oxidative stress, without an upregulation of IL-6 or ER stress responses. This finding may be of importance in NAFLD given that ApoE appears to have a strongly protective effect against diet induced steatohepatitis in mice. [163]

The research reported in this thesis has described a recurring theme regarding the interplay between iron and insulin resistance. *Hfe* heterozygous knockout in mice was associated with modest increases in hepatic iron and serum glucose. In humans however, HIC in the non-haemochromatotic range positively correlated with multiple measures of insulin sensitivity, including fasting serum glucose. Increasing adipocyte iron has been shown in animal and tissue culture models to lead to dysregulation of adipokines that typically are associated with increased insulin resistance and hepatic injury, such as reduced adiponectin, leptin and increased resistin. [17-19] Some of the discordance between these findings may be explained by the proposed repartitioning of iron from the liver to adipocytes that is seen in mice fed a high fat diet. [24] If this were the case in humans, the association between lower HIC and insulin resistance could, in part, be explained by an increase in adipocyte iron with reduced adiponectin transcription and increased adipose tissue insulin resistance.

The missing data that would go some way to evaluating this hypothesis of iron-repartitioning are human adipocyte iron concentrations in NAFLD. Perhaps unsurprisingly, it has been learned during the course of this research that individuals with NAFLD are generally reluctant to undergo percutaneous adipose tissue biopsy for ethically approved clinical research purposes. One way around this issue would be a cross sectional study of patients with NAFLD undergoing elective laparoscopic surgery, such as cholecystectomy. Such a study would provide a relatively safe means with which to collect adipose and liver tissue samples and correlate with a range of fasting serum parameters including adipokines. This is a clear and immediate target for future study.

The model of adipocyte-specific ferroportin knockout did not lead to a phenotype of adipocyte iron overload. The development of a reliable *in vivo* model of adipocyte-specific iron loading would therefore undoubtedly be a hugely valuable tool for research in this field. However, the findings indicating that ferroportin may not be a key regulator of adipocyte iron homeostasis are in themselves instructive. If adipocyte iron is as important as we might imagine in NAFLD and diabetes pathogenesis, then identifying novel iron transport mechanisms that are unique to adipocytes may enable the development of relatively simple adipocyte-specific treatments targeting iron.

Finally, the use of a proteomic approach to analyse the effects of iron on the adipocyte secretome has provided a wealth of publicly available data as a platform for future studies. To date, there has only been a scratching of the surface of the potential of this data. Other than the effects on ApoE which need to be explored in more depth, the dysregulation of a number of other proteins may represent novel mechanisms pertaining to adipocyte iron's role in NAFLD pathogenesis.

In conclusion, multi-faceted links between iron, insulin sensitivity and the dysregulation of adipokines have been identified. These findings provide a strong rationale for further translational study in this field.

Appendix A: Research letter: Iron inhibits the secretion of apolipoprotein E in cultured human adipocytes

Below is the abridged version of Chapter 6 that is currently undergoing peer review after re-submission with revisions for Cellular and Molecular Gastroenterology and Hepatology.

Britton LJ, Bridle KR, Jaskowski L, He J, Ng C, Ruelcke J, Mohamed A, Reiling J, Santrampurwala N, Hill MM, Whitehead JP, Subramaniam VN, Crawford DHG
Iron inhibits the secretion of apolipoprotein E in cultured human adipocytes

Iron inhibits the secretion of apolipoprotein E in cultured human adipocytes

Laurence Britton[1,2,3,4], Kim Bridle[1,2], Lesley-Anne Jaskowski[1,2], Jingjing He[4], Choaping Ng[4,5], Jayde Ruelcke[6], Ahmed Mohamed[6,7], Janske Reiling[1,2,8], Nishreen Santrampurwala[1,2], Michelle Hill[6,7], Jonathan Whitehead[4,5], V. Nathan Subramaniam[9], Darrell Crawford[1,2]

1. Gallipoli Medical Research Institute, Greenslopes Private Hospital, Greenslopes, Queensland, Australia
2. The University of Queensland, Herston, Queensland, Australia
3. Department of Gastroenterology, Princess Alexandra Hospital, Queensland, Australia
4. Mater Research, Translational Research Institute, Woolloongabba, Queensland, Australia
5. School of Life Sciences, University of Lincoln, U.K
6. The University of Queensland Diamantina Institute, Faculty of Medicine, University of Queensland
7. QIMR Berghofer Medical Research Institute, Brisbane, Queensland, Australia
8. Department of Surgery, NUTRIM school of Nutrition and Translational Research in Metabolism, Maastricht University, Maastricht, the Netherlands
9. Institute of Health and Biomedical Innovation and School of Biomedical Sciences, Queensland University of Technology (QUT), Kelvin Grove, Queensland, Australia

Research Letter

Non-alcoholic steatohepatitis (NASH) is characterized by adipose tissue dysfunction with insulin resistance and the dysregulation of adipokines. [21] Recent data indicate repartitioning of iron from the liver to adipocytes in obesity and a role for iron in the development of adipose tissue dysfunction. [24, 34] However the molecular mechanisms have not been established. To test the hypothesis that iron modulates adipokine release, we performed a quantitative proteomics analysis of the human Simpson-Golabi-Behmel Syndrome (SGBS) adipocyte secretome following 48 hours of treatment with ferric ammonium citrate (FAC). We utilized stable isotope labelled amino acids in cell culture (SILAC) to characterize changes in the adipocyte secretome in response to iron. This technique has enabled direct comparison of quantities of individual proteins in the

adipocyte secretome in response to iron using a proteomics approach as a tool for the identification of novel treatment targets in NASH.

We first showed that 100μM FAC causes significant adipocyte iron loading without compromising cell viability. We found that compared to vehicle both 100 μM and 500 μM FAC caused significant increases in cellular iron concentration (p=0.007 and p=0.006 respectively, Figure 8.1(a)). There was no effect of iron loading on cellular viability (MTS) assay, total mRNA, total whole cell lysate protein or total secretome protein (Figure 8.1 (b-e)).

Figure 8.1: Optimization of iron loading in SGBS cells

(a) Iron assay, p=0.004 (one-way ANOVA), *indicates p<0.01 (Dunnett's multiple comparisons test compared to 0μM FAC, n=2 per group). (b) Total RNA (non-significant (NS) by one-way ANOVA, n=3 per group). (c) Total lysate protein (NS by one-way ANOVA, n=3 per group). (d) Total secretome protein (NS by one-way ANOVA, n=3 per group). (e) Viability assay (MTS) (NS by one-way ANOVA, n=3 per group). Data are presented as mean and standard error of the mean.

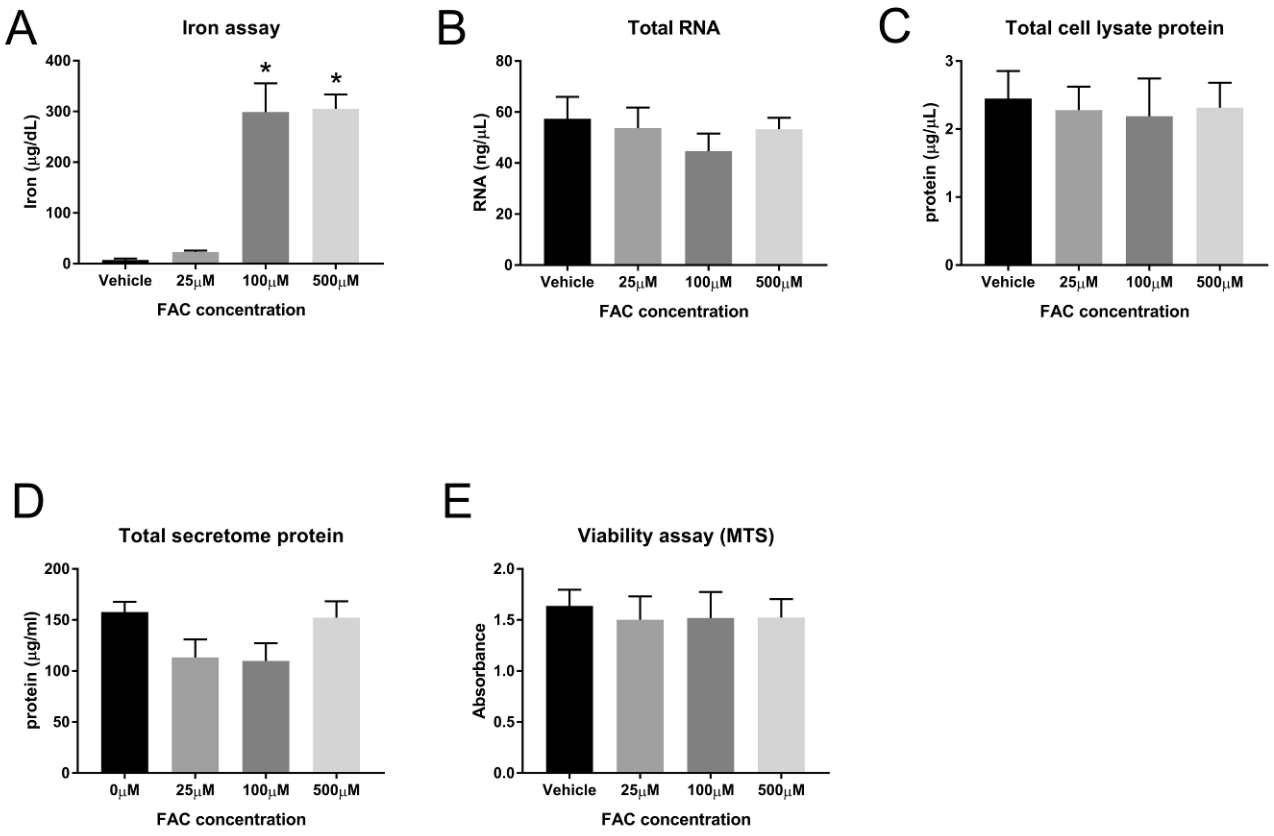

Given these findings, we selected 100 μM FAC as the concentration to compare with vehicle in the secretome SILAC proteomic analysis. A total of 338 proteins were quantified in the adipocyte secretome by SILAC proteomics. These are represented graphically as a volcano plot in Figure 8.2 and the proteomics data have been deposited to the ProteomeXchange Consortium via the PRIDE partner repository

(www.proteomexchange.org) with the dataset identifier PXD006341. Iron treatment led to significant differential secretion of 60 of these proteins (>2-fold change and p-value <0.05). We then manually reviewed Uniprot database descriptions of these 60 proteins. This generated a list of 20 proteins of interest (highlighted in bold in Table 8.1). These proteins of interest and their synonyms were then entered into a Pubmed title/abstract search in association with NASH and its synonyms. This identified three proteins as candidate intermediates for iron-induced adipose tissue dysfunction in NASH. These proteins were adiponectin, annexin A1 and apolipoprotein E (ApoE).

Figure 8.2: Volcano plot of relative signal intensity of proteins identified in the adipocyte secretome

The x-axis denotes log 2 of the ratio of iron/vehicle treated cells, with proteins to the left of zero representing those downregulated by iron and those to the right representing up-regulation by iron. The y-axis denotes statistical significance with a line representing a p-value of 0.05. Proteins above this line have p<0.05. SILAC labelled adipocytes generated 338 proteins that were identified in the secretome by mass spectrometry. Of these 213, had reduced signal intensity in response to iron, whereas 125 had increased signal intensity. Of the 213 proteins with reduced signal intensity, 61 had a statistically significant ($p < 0.05$) downregulation in response to iron. Of these, 53 had a greater than 2-fold decrease in response to iron. Of the 125 proteins with increased signal intensity, 11 had a statistically significant ($p < 0.05$) upregulation in response to iron. Of these, 7 proteins had a greater than 2-fold increase response to iron. Those proteins containing signal peptide (as determined by signal peptide annotations on the Uniprot database) are shown in red. Those without signal peptide are shown in blue.

Table 8.1: List of SGBS secretome proteins with significantly altered signal intensity in response to iron

Proteins shown had a greater than 2-fold change in signal intensity in response to iron, with a p-value <0.05. Proteins highlighted in bold represent the 20 proteins of interest after review of Uniprot protein descriptions. Data were analyzed using the online Quantitative Proteomics P-value Calculator (QPPC) using no normalization and non-adjusted p-values. n=3 per group

Accession number	Gene name	Protein name	Mean signal intensity ratio (iron/vehicle)	Standard deviation	P value
Q8IX30	**SCUBE3**	**Signal peptide, CUB and EGF-like domain-containing protein 3**	**0.026**	**0.016**	**0.001**
P61353	RPL27	60S ribosomal protein L27	0.060	0.005	0.001
Q9NQH7	XPNPEP3	Probable Xaa-Pro aminopeptidase 3	0.076	0.004	0.001
P07996	**THBS1**	**Thrombospondin-1**	**0.083**	**0.047**	**0.001**
Q76M96	CCDC80	Coiled-coil domain-containing protein 80	0.090	0.031	0.001
P78539	SRPX	Sushi repeat-containing protein SRPX	0.096	0.620	0.001
Q9UHI8	ADAMTS1	A disintegrin and metalloproteinase with thrombospondin motifs 1	0.114	0.090	0.002
Q92538	GBF1	Golgi-specific brefeldin A-resistance guanine nucleotide exchange factor 1	0.118	0.024	0.004
Q15063	**POSTN**	**Periostin**	**0.121**	**0.149**	**0.001**
P08238	HSP90AB1	Heat shock protein HSP 90-beta	0.125	0.038	0.004
P24593	**IGFBP5**	**Insulin-like growth factor-binding protein 5**	**0.154**	**0.069**	**0.001**
Q15113	PCOLCE	Procollagen C-endopeptidase enhancer 1	0.155	0.088	0.001
Q9NTX5	ECHDC1	Ethylmalonyl-CoA decarboxylase	0.158	0.068	0.001
P25788	PSMA3	Proteasome subunit alpha type-3	0.176	0.442	0.001
Q12931	TRAP1	Heat shock protein 75 kDa, mitochondrial	0.186	0.028	0.018
P04083	**ANXA1**	**Annexin A1**	**0.192**	**0.049**	**0.001**
P30101	PDIA3	Protein disulfide-isomerase A3	0.198	0.059	0.001
Q99985	**SEMA3C**	**Semaphorin-3C**	**0.199**	**0.225**	**0.001**

Q6NZI2	PTRF	Polymerase I and transcript release factor	0.210	0.134	0.001
Q8TAV4	STOML3	Stomatin-like protein 3	0.220	0.084	0.006
Q9UKZ9	PCOLCE2	Procollagen C-endopeptidase enhancer 2	0.226	0.030	0.001
Q05469	LIPE	Hormone-sensitive lipase	0.231	0.196	0.023
Q13642	FHL1	Four and a half LIM domains protein 1	0.263	0.006	0.029
P02749	APOH	Beta-2-glycoprotein 1	0.286	0.310	0.048
P02462	COL4A1	Collagen alpha-1(IV) chain	0.286	0.351	0.001
P15311	EZR	Ezrin	0.296	0.077	0.003
P42765	ACAA2	3-ketoacyl-CoA thiolase, mitochondrial	0.308	0.136	0.001
P68104	**EEF1A1**	**Elongation factor 1-alpha 1**	**0.309**	**0.215**	**0.001**
Q9NQC3	**RTN4**	**Reticulon-4**	**0.312**	**0.119**	**0.007**
Q8IY17	PNPLA6	Neuropathy target esterase	0.316	0.028	0.026
Q92743	HTRA1	Serine protease HTRA1	0.324	0.075	0.001
P08294	**SOD3**	**Extracellular superoxide dismutase [Cu-Zn]**	**0.339**	**0.027**	**0.005**
Q16836	HADH	Hydroxyacyl-coenzyme A dehydrogenase, mitochondrial	0.348	0.207	0.011
Q99715	COL12A1	Collagen alpha-1(XII) chain	0.348	0.183	0.001
P07355	**ANXA2**	**Annexin A2**	**0.354**	**0.111**	**0.001**
P26038	MSN	Moesin	0.362	0.110	0.034
P23284	PPIB	Peptidyl-prolyl cis-trans isomerase B	0.374	0.122	0.001
O94769	ECM2	Extracellular matrix protein 2	0.375	0.060	0.005
Q9NRN5	**OLFML3**	**Olfactomedin-like protein 3**	**0.389**	**0.066**	**0.002**
P53396	**ACLY**	**ATP-citrate synthase**	**0.389**	**0.066**	**0.001**
Q16363	LAMA4	Laminin subunit alpha-4	0.407	0.091	0.001
P14625	**HSP90B1**	**Endoplasmin**	**0.414**	**0.068**	**0.025**
Q9BU40	CHRDL1	Chordin-like protein 1	0.419	0.264	0.001
P02649	**APOE**	**Apolipoprotein E**	**0.421**	**0.053**	**0.001**
Q9NS98	**SEMA3G**	**Semaphorin-3G**	**0.425**	**0.161**	**0.001**
P02751	**FN1**	**Fibronectin**	**0.441**	**0.146**	**0.001**
P14543	**NID1**	**Nidogen-1**	**0.442**	**0.190**	**0.006**
Q08431	**MFGE8**	**Lactadherin**	**0.446**	**0.167**	**0.026**
Q15848	**ADIPOQ**	**Adiponectin**	**0.449**	**0.652**	**0.005**
O75390	CS	Citrate synthase,	0.454	0.183	0.012

		mitochondrial			
Q92626	PXDN	Peroxidasin homolog	0.457	0.200	0.001
P07942	LAMB1	Laminin subunit beta-1	0.484	0.110	0.001
Q08629	SPOCK1	Testican-1	0.497	0.055	0.014
O00462	MANBA	Beta-mannosidase	2.180	2.560	0.034
Q13510	ASAH1	Acid ceramidase	2.222	3.135	0.048
P02794	**FTH1**	**Ferritin heavy chain**	**2.451**	**0.769**	**0.030**
Q02952	AKAP12	A-kinase anchor protein 12	2.665	0.572	0.047
A6NCN2	KRT87P	Putative keratin-87 protein	4.113	0.011	0.022
P23468	PTPRD	Receptor-type tyrosine-protein phosphatase delta	10.687	2.199	0.003
P10586	PTPRF	Receptor-type tyrosine-protein phosphatase F	11.935	3.955	0.001

Our SILAC analysis showed that iron treatment resulted in an 81% reduction in Annexin A1 secretome signal intensity (p=0.001). This may be important as AnnexinA1 knock-out mice exhibit greater degrees of hepatic lobular inflammation and fibrosis than controls when fed a methionine-choline deficient diet.[172] Adipocyte iron has also previously been shown to transcriptionally down-regulate serum adiponectin in a mouse derived adipocytes, 3T3-L1 cells. [17] Our findings now support this in a human adipocyte cell line with a 55% reduction in adiponectin signal intensity in iron-treated SGBS cells (p=0.005).

We next focused on the iron-regulation of ApoE secretion. ApoE appears to protect against steatohepatitis in mice. In an ApoE knockout model, unlike wild type controls, ApoE KO mice fed seven weeks of a Western diet developed impaired glucose tolerance, steatohepatitis and hepatic fibrosis.[163] ApoE is a component of lipoproteins and promotes VLDL induced adipogenesis.[166] ApoE knockout mice also readily develop atherosclerosis on an atherogenic diet.[167]

Iron reduced secreted ApoE by 58% (p=0.001) and 76% (p=0.007), as measured by SILAC and western blot respectively. Conversely, iron treatment increased intracellular ApoE levels by more than 11-fold (p=0.0005), without causing a significant change in mRNA levels (Figure 8.3). It therefore appears that iron inhibits the secretion of ApoE from adipocytes, causing ApoE to become sequestered intracellularly.

Figure 8.3: SBGS ApoE expression following FAC treatment

(a) ApoE mRNA (NS, ratio paired t-test), (b) Secretome ApoE densitometry (* denotes p=0.001, ratio paired t-test), (c) Lysate ApoE densitometry normalized to β-actin (# denotes p=0.0005, ratio paired t-test), (d) Secretome ApoE immunoblot, (e) Whole cell lysate ApoE and β-actin immunoblots (n=3 per group). Data are presented as mean and standard error of the mean.

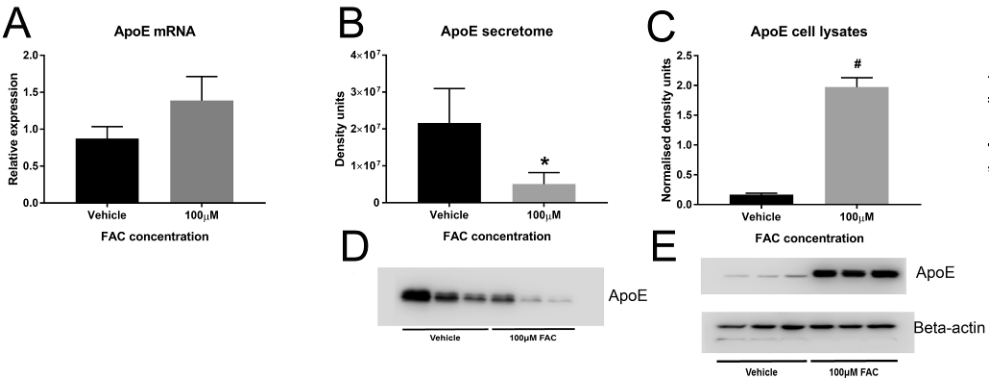

Similar effects on ApoE secretion have been shown with iron treatment in primary cultured astrocytes and cortical neurons. [171] Taken together with our data, it seems possible that iron may have similar effects on a range of cell types and represents a clear target for further investigation. Treatment with iron in our study, demonstrated an upregulation of anti-oxidant responses (heme-oxygenase-1 (HO-1) and glutathione peroxidase-1 (GPX-1) mRNA) indicating the presence of oxidative stress. Interleukin-6 (IL-6) mRNA however was not increased with iron treatment, nor was there any difference among multiple markers of endoplasmic reticulum stress (Figure 8.4 (a-i))

We considered whether iron may have a generalized effect on pathways of protein secretion, utilized by a variety of proteins. We evaluated the role of iron in the secretion of proteins by the classical and exosomal pathways using the Uniprot and EVpedia databases respectively [161, 165]. We found enrichment of signal peptide-containing (p=0.02), but not exosome-secreted proteins (p=0.51) among the iron-dysregulated proteins suggesting that iron may have a specific effect on proteins secreted via the classical pathway (Figure 8.4(j-m)).

Figure 8.4: Mechanistic aspects of iron-related dysregulation of protein secretion

(a) Interleukin-6 (IL-6) mRNA (non-significant (NS), paired t-test, n=3 per group). (b-c) Oxidative stress * indicates $p<0.05$, both n=3 per group (b) Heme-oxygenase (HO-1) mRNA ($p=0.01$, paired t-test). (c) Glutathione peroxidase 1 (GPX-1) mRNA ($p=0.049$, paired t-test). (d-i) Endoplasmic reticulum (ER) stress, all n=3 per group. (d) Unspliced X-box binding protein (XBP-1) mRNA (NS, paired t-test). (e) Spliced X-box binding protein (XBP-1) mRNA (NS, paired t-test). (f) Immunoglobulin binding protein (BiP) mRNA (NS, paired t-test). (g) ER-degradation-enhancing-α-mannidose-like protein (EDEM) mRNA (NS, paired t-test). (h) Activating transcription factor 4 (ATF4) mRNA (NS, paired t-test). (i) CCAAT/enhancer-binding protein homologous protein (CHOP) mRNA (NS, paired t-test). (j-m) Enrichment with signal peptide and exosome proteins. (j) Proportion of proteins significantly down regulated by iron with signal peptide vs no signal peptide. (k) Proportion of proteins not significantly down regulated by iron with signal peptide vs no signal peptide. (l) Proportion of proteins significantly down regulated by iron with exosome secretion vs no exosome secretion. (m) Proportion of proteins not significantly down-regulated by iron with exosome secretion vs no exosome secretion. Of the 61 significantly down-regulated proteins, 62% (38/61) had signal peptide, whereas of the remaining proteins only 47% (129/277) had signal peptide. One-tailed Fisher's-exact test showed significant enrichment with signal peptide ($p=0.02$) amongst the significantly down-regulated group. In contrast, there was no significant enrichment of the exosomal pathway ($p=0.51$, one-tailed Fisher's-exact test), as 15% (9/61) of significantly down-regulated proteins and 14% (39/277) of the remaining secretome proteins had been previously reported in the high confidence proteins from the EVpedia database.

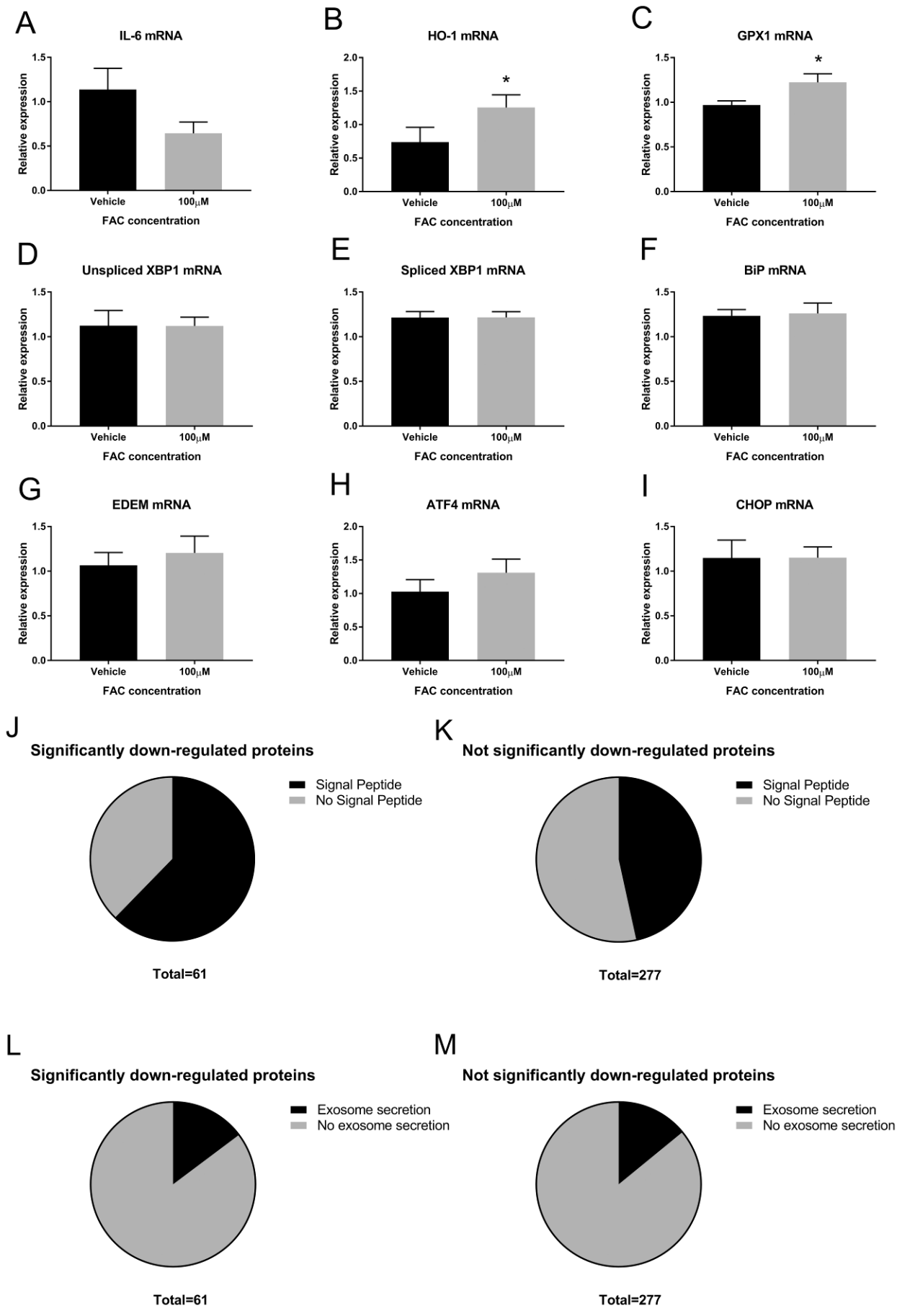
A
IL-6 mRNA
B
HO-1 mRNA
C
GPX1 mRNA
D
Unspliced XBP1 mRNA
E
Spliced XBP1 mRNA
F
BiP mRNA
G
EDEM mRNA
H
ATF4 mRNA
I
CHOP mRNA
Relative expression
Vehicle
100μM
FAC concentration
*
J
Significantly down-regulated proteins
Signal Peptide
No Signal Peptide
Total=61
K
Not significantly down-regulated proteins
Signal Peptide
No Signal Peptide
Total=277
L
Significantly down-regulated proteins
Exosome secretion
No exosome secretion
Total=61
M
Not significantly down-regulated proteins
Exosome secretion
No exosome secretion
Total=277

This research has characterized the effect of iron on the adipocyte secretome. These data provide a platform for multiple avenues of future research. In addition, we have been able to show that increased iron results in sequestration of ApoE within adipocytes, which may be of key importance in the regulation of insulin resistance and liver injury in NASH. Identifying the molecular mechanisms of iron-induced inhibition of ApoE secretion from adipocytes, particularly relating to the role of oxidative stress, may reveal novel therapeutic strategies for improving adipocyte function in NASH.

Supplementary methods

SGBS differentiation and iron treatment

SGBS pre-adipocytes were a gift from Martin Wabitsch (University of Ulm, Germany). [158, 174] SGBS cells were passaged, proliferated and differentiated at less than 50 generations in 12 well plates and 100 mm dishes as previously described.[157] Cells were treated with 90 µg/ml heparin and 1 ng/ml fibroblast growth factor-1 (FGF-1) (both Sigma-Aldrich, St Louis, Missouri) throughout proliferation and differentiation. After 14 days of differentiation, cells were incubated with 0, 25, 100 or 500 µM ferric ammonium citrate (FAC) (Sigma- Aldrich) for 24 hrs. After this media was replaced with the same for a further 24 hrs to the end of experiment.

RNA extraction and real-time quantitative PCR (RT-qPCR)

RNA was extracted from treated SGBS adipocytes using a PureLink RNA mini kit (Invitrogen, Carlsbad, California). Complementary DNA was synthesized from 1 µg RNA using a Sensifast cDNA synthesis kit (Bioline, London, UK) after treatment with DNase 1 (Invitrogen). Samples underwent thermal cycling using a ViiA7 real-time PCR machine (Invitrogen) with a Sensifast SYBR Lo-ROX Kit (Bioline). The following protocol was used: 2 min at 95^{o}C, then 40 cycles of 5 sec at 95^{o}C alternating with 20 sec at 63^{o}C, followed by a melt curve analysis. Relative mRNA quantities were determined by calibration of Ct values to standard curve of pooled cDNA samples. Results were normalized to Ct values of Cyclophillin.

Iron, cellular viability (MTS) and protein assays.

Iron levels were quantified using a chromagen reagent method. [159] Cellular viability was assessed using a CellTiter 96 AQueous One Solution Cell Proliferation Assay (Promega, Madison, Wisconsin) according to the manufacturer's instructions. Whole cell lysate and

secretome samples underwent protein estimation using a Pierce BCA protein assay kit (Thermofisher Scientific, Waltham, Massachusetts).

SILAC proteomics

SILAC incorporates stbale amino acids isotopes, without altering cellular biology, allowing direct comparison of the secretome by mass spectrometry between treatment groups. [175] SGBS pre-adipocytes were grown in SILAC DMEM: F12 media (Thermofisher Scientific) supplemented with dialyzed fetal bovine serum (Thermofisher Scientific,) and 22.81mg/L $^{2}H_{4}$-Lysine and 36.88mg/L $^{13}C_{6}$-Arginine (K4R6) or 22.81mg/L $^{13}C_{6}{}^{15}N_{2}$-Lysine and 36.88mg/L $^{13}C_{6}{}^{15}N_{4}$-Arginine (K8R10). Incorporation of labelled amino acids was confirmed by liquid chromatography tandem mass spectrometry (LC-MS/MS) on tryptic peptides prepared from whole cell lysates. Cell pellets were lysed in 8M urea in 100mM TEAB (Triethylamonium bicarbonate), and protein concentration estimated using Bradford assay (BioRad, Hercules, California). Thirty µg of cell lysate was reduced and alkylated by incubating samples for 30 min at 37^{o}C with 2.5mM TCEP (tris(2-carboxyethyl)phosphine) and then 5mM 2CAA (2-Chloroacetamide). Urea concentration was diluted to 1M with 100mM TEAB before adding 0.6 µg of trypsin. Samples were incubated overnight then acidified to 1% trifluoroacetic acid (TFA) and cleaned with OMIX C18 tips according to the manufacturers' protocol (Agilent, Santa Clara, California). LC-MS/MS was performed as described below.

Labelled (>97%) cells underwent differentiation to adipocytes as described above. At day 14 post differentiation, cells were treated with vehicle (media) (K4R6, medium weight cells) or 100 µM FAC (in media) (K8R10, heavy weight cells) for a further 48 hours using exactly equal volumes of media, replacing the media after 24 hrs. Media for secretome analysis was collected from K4R6 and K8R10 cells and mixed 1:1 (v/v) before centrifugation at 600 x G at 4^{o}C for 10 min to remove cell debris. Supernatant was then concentrated using Amicon Ultra 15ml 10 kDa centrifugal filter units (Merck Millipore, Burlington, Massachusetts) in a fixed angle centrifuge at 5000 x G to provide approximately 1 ml samples of concentrated mixed secretome. Thirty µg of protein was separated on 10% SDS-PAGE gels to 10 mm. Protein visualization, excision of bands and in-gel trypsin digest were performed using a semi-automated method as described.[160] A band corresponding to the same molecular weight as transferrin (media additive) was removed prior to digestion, in order to provide a protein sample exclusively secreted from cultured adipocytes.

Mass spectrometry

A Q Exactive Plus Orbitrap Mass Spectrometer (Thermofisher Scientific), coupled with Easy-nLC 1000 and EASY-spray ion source (both Thermofisher Scientific), was used to analyze the digested peptides. Samples were loaded onto an EASY-Spray PepMap RSLC C18 2 µm column (50 cm x 75 µm ID), with a Nanoviper Acclaim C18 guard (75 µm x 2 cm) (both Thermofisher Scientific). A 90 min method was run using a combination of Buffer A (0.1% Formic acid) and Buffer B (0.1% Formic acid: Acetonitrile). A two-step gradient was run comprising a 60 min gradient from 3% to 25% Buffer B and a 12 min gradient from 25% to 40% Buffer B. Flow rate was at 250 nL/min. The mass spectrometer was programmed to acquire a full mass spectrometry (MS) resolution of 70,000 with an ACG target of $3x10^6$ with a maximum injection time of 100 ms. The MS scan range was from 350 to 1400 m/z. MS/MS was set to acquire a resolution of 17,500 with an ACG target of $5x10^5$ and maximum injection time of 55 ms. The loop count was set to 20 with a dynamic exclusion after 30 sec.

Raw data were processed with Spectrum mill (Rev B.05.00.181 SP1, Agilent). Selected modifications included fixed carbamidomethylation of cysteine and SILAC labels (Arg 0-6-10 Da Lys 0-4-8 Da) and variable oxidized methionine. Results were searched against the Human Uniprot database (downloaded 06/01/2015).[161] Trypsin was selected as digest enzyme, with two maximum missed cleavages allowed. The precursor mass tolerance was set at +/- 20 ppm and product mass tolerance was +/- 20 ppm. Data were analyzed using the online Quantitative Proteomics P-value Calculator (QPPC) using no normalization and non-adjusted p-values.[162]

Immunoblotting

Western blotting using whole cell lysate samples (10 µg) and 5 µL concentrated secretome samples was performed as previously described.[147] A 1:500 dilution of primary antibody against Apolipoprotein E (ApoE) (sc-53570, Santa Cruz, Dallas, Texas) was applied to the membranes. A 1:100,000 dilution of goat anti-mouse horseradish peroxidase antibody (Invitrogen) was applied as secondary antibody. ApoE whole cell lysate densitometry was normalized against densitometry using beta-actin as a reference protein (1:2000 primary antibody) (Cat No. 4967, Cell Signaling, Danvers, Massachusetts) and 1:20,000 goat anti-rabbit horseradish peroxidase antibody (Invitrogen).

Appendix B: Ethics committee approvals

GREENSLOPES
PRIVATE HOSPITAL

9th September 2014

Professor Darrell Crawford
Gallipoli Medical Research Foundation
Greenslopes Private Hospital
Newdegate Street
GREENSLOPES Q 4120

Dear Prof Crawford

Protocol 11/56 – IRON. Impact of Iron and Insulin Resistance on Liver Histology in Non-Alcohol Steatohepatitis (IRON)

The following correspondence was considered by the Greenslopes Research and Ethics Committee at its meeting held on Monday, 8th September, 2014.

- Cover letter dated 20th August 2014
- Amendment 4 dated 20th August 2014
- Study protocol, version dated 20th August 2014, incorporating Amendment 4 (final version)
- Study protocol, version dated 20th August 2014, incorporating Amendment 4 (tracked changes version)

The Committee reviewed these documents and agreed to grant approval for use in this study.

The Greenslopes Research and Ethics Committee is constituted and functions in accordance with the National Statement on Ethical Conduct in Research involving humans (2007) – updated march 2014

Yours sincerely

Dr Jim Houston
Chair
Greenslopes Research and Ethics Committee

Certified Copy

Initial	Date
	22 Sept 2014

QIMR Berghofer
Medical Research Institute

5 March 2018

Phone: 07 3362 0259
Fax: 07 3362 0109
Pearl.Swe-Kay@qimrberghofer.edu.au

To whom it may concern,

I wish to confirm that Mr. Laurence Britton has been authorised by the QIMR Berghofer Medical Research Institute Animal Ethics Committee (QIMR-Berghofer AEC) to conduct animal research under projects P1446, P1462 and P1489 with corresponding animal ethics approval numbers A1203-602, A1210-611M and A1210-610M respectively. QIMR-Berghofer AEC approved projects are subject to the provision of a satisfactory annual report to the QIMR-Berghofer AEC, as a minimum requirement per the *Australian code of practice for the care and use of animals for scientific purposes, 8th edition, 2013*.

Should you wish to discuss this matter, please contact Dr Pearl Swe-Kay, AEC Secretariat, on 3362 0259 or Pearl.Swe-Kay@qimrberghofer.edu.au.

Yours sincerely,

Dr Pearl Swe-Kay on behalf of **Mr Bob Beattie**
QIMR Berghofer-AEC Chair

References

[1] Loomba R, Sanyal AJ. The global NAFLD epidemic. Nat Rev Gastroenterol Hepatol 2013;10(11):686-90.

[2] Anstee QM, Targher G, Day CP. Progression of NAFLD to diabetes mellitus, cardiovascular disease or cirrhosis. Nat Rev Gastroenterol Hepatol 2013;10(6):330-44.

[3] Smith BW, Adams LA. Nonalcoholic fatty liver disease and diabetes mellitus: pathogenesis and treatment. Nat Rev Endocrinol 2011;7(8):456-65.

[4] Cheung O, Sanyal AJ. Recent advances in nonalcoholic fatty liver disease. Curr Opin Gastroenterol 2010;26(3):202-8.

[5] Babitt JL, Lin HY. The molecular pathogenesis of hereditary hemochromatosis. Seminars in liver disease 2011;31(3):280-92.

[6] Powell EE, Ali A, Clouston AD, Dixon JL, Lincoln DJ, Purdie DM, et al. Steatosis is a cofactor in liver injury in hemochromatosis. Gastroenterology 2005;129(6):1937-43.

[7] Dongiovanni P, Fracanzani AL, Fargion S, Valenti L. Iron in fatty liver and in the metabolic syndrome: a promising therapeutic target. Journal of hepatology 2011;55(4):920-32.

[8] Nelson JE, Klintworth H, Kowdley KV. Iron metabolism in Nonalcoholic Fatty Liver Disease. Current gastroenterology reports 2012;14(1):8-16.

[9] Barnette AR, Horbar JD, Soll RF, Pfister RH, Nelson KB, Kenny MJ, et al. Neuroimaging in the evaluation of neonatal encephalopathy. Pediatrics 2014;133(6):e1508-17.

[10] Day CP, James OF. Steatohepatitis: a tale of two "hits"? Gastroenterology 1998;114(4):842-5.

[11] Buzzetti E, Pinzani M, Tsochatzis EA. The multiple-hit pathogenesis of non-alcoholic fatty liver disease (NAFLD). Metabolism 2016;65(8):1038-48.

[12] Utzschneider KM, Kahn SE. Review: The role of insulin resistance in nonalcoholic fatty liver disease. J Clin Endocrinol Metab 2006;91(12):4753-61.

[13] Allen KJ, Gurrin LC, Constantine CC, Osborne NJ, Delatycki MB, Nicoll AJ, et al. Iron-overload-related disease in HFE hereditary hemochromatosis. The New England journal of medicine 2008;358(3):221-30.

[14] Ellervik C, Birgens H, Tybjaerg-Hansen A, Nordestgaard BG. Hemochromatosis genotypes and risk of 31 disease endpoints: meta-analyses including 66,000 cases and 226,000 controls. Hepatology 2007;46(4):1071-80.

[15] Tan TC, Crawford DH, Jaskowski LA, Murphy TM, Heritage ML, Subramaniam VN, et al. Altered lipid metabolism in Hfe-knockout mice promotes severe NAFLD and early fibrosis. Am J Physiol Gastrointest Liver Physiol 2011;301(5):G865-76.

[16] Marra F, Bertolani C. Adipokines in liver diseases. Hepatology 2009;50(3):957-69.

[17] Gabrielsen JS, Gao Y, Simcox JA, Huang J, Thorup D, Jones D, et al. Adipocyte iron regulates adiponectin and insulin sensitivity. J Clin Invest 2012;122(10):3529-40.

[18] Gao Y, Li Z, Gabrielsen JS, Simcox JA, Lee SH, Jones D, et al. Adipocyte iron regulates leptin and food intake. J Clin Invest 2015;125(9):3681-91.

[19] Dongiovanni P, Ruscica M, Rametta R, Recalcati S, Steffani L, Gatti S, et al. Dietary Iron Overload Induces Visceral Adipose Tissue Insulin Resistance. Am J Pathol 2013.

[20] Fernandez-Real JM, Moreno JM, Ricart W. Circulating retinol-binding protein-4 concentration might reflect insulin resistance-associated iron overload. Diabetes 2008;57(7):1918-25.

[21] Hebbard L, George J. Animal models of nonalcoholic fatty liver disease. Nat Rev Gastroenterol Hepatol 2011;8(1):35-44.

[22] Pihan-Le Bars F, Bonnet F, Loreal O, Le Loupp AG, Ropert M, Letessier E, et al. Indicators of iron status are correlated with adiponectin expression in adipose tissue of patients with morbid obesity. Diabetes Metab 2016;42(2):105-11.

[23] Bekri S, Gual P, Anty R, Luciani N, Dahman M, Ramesh B, et al. Increased adipose tissue expression of hepcidin in severe obesity is independent from diabetes and NASH. Gastroenterology 2006;131(3):788-96.

[24] Orr JS, Kennedy A, Anderson-Baucum EK, Webb CD, Fordahl SC, Erikson KM, et al. Obesity alters adipose tissue macrophage iron content and tissue iron distribution. Diabetes 2014;63(2):421-32.

[25] Charlton M, Krishnan A, Viker K, Sanderson S, Cazanave S, McConico A, et al. Fast food diet mouse: novel small animal model of NASH with ballooning, progressive fibrosis, and high physiological fidelity to the human condition. Am J Physiol Gastrointest Liver Physiol 2011;301(5):G825-34.

[26] Lee KY, Russell SJ, Ussar S, Boucher J, Vernochet C, Mori MA, et al. Lessons on conditional gene targeting in mouse adipose tissue. Diabetes 2013;62(3):864-74.

[27] Eguchi J, Wang X, Yu S, Kershaw EE, Chiu PC, Dushay J, et al. Transcriptional control of adipose lipid handling by IRF4. Cell Metab 2011;13(3):249-59.

[28] Chitturi S, Farrell GC, Hashimoto E, Saibara T, Lau GK, Sollano JD. Non-alcoholic fatty liver disease in the Asia-Pacific region: definitions and overview of proposed guidelines. J Gastroenterol Hepatol 2007;22(6):778-87.

[29] Charlton MR, Burns JM, Pedersen RA, Watt KD, Heimbach JK, Dierkhising RA. Frequency and outcomes of liver transplantation for nonalcoholic steatohepatitis in the United States. Gastroenterology 2011;141(4):1249-53.

[30] Vernon G, Baranova A, Younossi ZM. Systematic review: The epidemiology and natural history of non-alcoholic fatty liver disease and non-alcoholic steatohepatitis in adults. Alimentary Pharmacology and Therapeutics 2011;34(3):274-85.

[31] Khan FZ, Perumpail RB, Wong RJ, Ahmed A. Advances in hepatocellular carcinoma: Nonalcoholic steatohepatitis-related hepatocellular carcinoma. World journal of hepatology 2015;7(18):2155-61.

[32] Lade A, Noon LA, Friedman SL. Contributions of metabolic dysregulation and inflammation to nonalcoholic steatohepatitis, hepatic fibrosis, and cancer. Curr Opin Oncol 2014;26(1):100-7.

[33] Moirand R, Mortaji AM, Loreal O, Paillard F, Brissot P, Deugnier Y. A new syndrome of liver iron overload with normal transferrin saturation. Lancet 1997;349(9045):95-7.

[34] Simcox JA, McClain DA. Iron and diabetes risk. Cell Metab 2013;17(3):329-41.

[35] Watt RK. The many faces of the octahedral ferritin protein. Biometals : an international journal on the role of metal ions in biology, biochemistry, and medicine 2011;24(3):489-500.

[36] Anderson GJ, Vulpe CD. Mammalian iron transport. Cell Mol Life Sci 2009;66(20):3241-61.

[37] Fleming DJ, Jacques PF, Tucker KL, Massaro JM, D'Agostino RB, Sr., Wilson PW, et al. Iron status of the free-living, elderly Framingham Heart Study cohort: an iron-replete population with a high prevalence of elevated iron stores. Am J Clin Nutr 2001;73(3):638-46.

[38] Fleming RE, Ponka P. Iron overload in human disease. The New England journal of medicine 2012;366(4):348-59.

[39] Takamura T, Misu H, Ota T, Kaneko S. Fatty liver as a consequence and cause of insulin resistance: lessons from type 2 diabetic liver. Endocr J 2012;59(9):745-63.

[40] Weisberg SP, McCann D, Desai M, Rosenbaum M, Leibel RL, Ferrante AW, Jr. Obesity is associated with macrophage accumulation in adipose tissue. J Clin Invest 2003;112(12):1796-808.

[41] Larter CZ, Chitturi S, Heydet D, Farrell GC. A fresh look at NASH pathogenesis. Part 1: the metabolic movers. J Gastroenterol Hepatol 2010;25(4):672-90.

[42] Carmen GY, Victor SM. Signalling mechanisms regulating lipolysis. Cell Signal 2006;18(4):401-8.

[43] Donnelly KL, Smith CI, Schwarzenberg SJ, Jessurun J, Boldt MD, Parks EJ. Sources of fatty acids stored in liver and secreted via lipoproteins in patients with nonalcoholic fatty liver disease. J Clin Invest 2005;115(5):1343-51.

[44] Samuel VT, Shulman GI. Mechanisms for insulin resistance: common threads and missing links. Cell 2012;148(5):852-71.

[45] Malhi H, Bronk SF, Werneburg NW, Gores GJ. Free fatty acids induce JNK-dependent hepatocyte lipoapoptosis. J Biol Chem 2006;281(17):12093-101.

[46] Wei Y, Wang D, Topczewski F, Pagliassotti MJ. Saturated fatty acids induce endoplasmic reticulum stress and apoptosis independently of ceramide in liver cells. Am J Physiol Endocrinol Metab 2006;291(2):E275-81.

[47] Li Y, Jadhav K, Zhang Y. Bile acid receptors in non-alcoholic fatty liver disease. Biochem Pharmacol 2013;86(11):1517-24.

[48] Rolo AP, Teodoro JS, Palmeira CM. Role of oxidative stress in the pathogenesis of nonalcoholic steatohepatitis. Free Radic Biol Med 2012;52(1):59-69.

[49] Frazier TH, DiBaise JK, McClain CJ. Gut microbiota, intestinal permeability, obesity-induced inflammation, and liver injury. JPEN J Parenter Enteral Nutr 2011;35(5 Suppl):14S-20S.

[50] Puri P, Mirshahi F, Cheung O, Natarajan R, Maher JW, Kellum JM, et al. Activation and dysregulation of the unfolded protein response in nonalcoholic fatty liver disease. Gastroenterology 2008;134(2):568-76.

[51] Zhang XQ, Xu CF, Yu CH, Chen WX, Li YM. Role of endoplasmic reticulum stress in the pathogenesis of nonalcoholic fatty liver disease. World J Gastroenterol 2014;20(7):1768-76.

[52] Paradies G, Paradies V, Ruggiero FM, Petrosillo G. Oxidative stress, cardiolipin and mitochondrial dysfunction in nonalcoholic fatty liver disease. World J Gastroenterol 2014;20(39):14205-18.

[53] Bohinc BN, Diehl AM. Mechanisms of disease progression in NASH: new paradigms. Clin Liver Dis 2012;16(3):549-65.

[54] Huang J, Gabrielsen JS, Cooksey RC, Luo B, Boros LG, Jones DL, et al. Increased glucose disposal and AMP-dependent kinase signaling in a mouse model of hemochromatosis. J Biol Chem 2007;282(52):37501-7.

[55] Ford ES, Cogswell ME. Diabetes and serum ferritin concentration among U.S. adults. Diabetes Care 1999;22(12):1978-83.

[56] Jiang R, Manson JE, Meigs JB, Ma J, Rifai N, Hu FB. Body iron stores in relation to risk of type 2 diabetes in apparently healthy women. Jama 2004;291(6):711-7.

[57] Montonen J, Boeing H, Steffen A, Lehmann R, Fritsche A, Joost HG, et al. Body iron stores and risk of type 2 diabetes: results from the European Prospective Investigation into Cancer and Nutrition (EPIC)-Potsdam study. Diabetologia 2012;55(10):2613-21.

[58] Orban E, Schwab S, Thorand B, Huth C. Association of iron indices and type 2 diabetes: a meta-analysis of observational studies. Diabetes/metabolism research and reviews 2014;30(5):372-94.

[59] Huth C, Beuerle S, Zierer A, Heier M, Herder C, Kaiser T, et al. Biomarkers of iron metabolism are independently associated with impaired glucose metabolism and type 2 diabetes: the KORA F4 study. Eur J Endocrinol 2015;173(5):643-53.

[60] Podmore C, Meidtner K, Schulze MB, Scott RA, Ramond A, Butterworth AS, et al. The Association of Multiple Biomarkers of Iron Metabolism and Type 2 Diabetes: The EPIC-InterAct Study. Diabetes Care 2016.

[61] Bugianesi E, Manzini P, D'Antico S, Vanni E, Longo F, Leone N, et al. Relative contribution of iron burden, HFE mutations, and insulin resistance to fibrosis in nonalcoholic fatty liver. Hepatology 2004;39(1):179-87.

[62] Kowdley KV, Belt P, Wilson LA, Yeh MM, Neuschwander-Tetri BA, Chalasani N, et al. Serum ferritin is an independent predictor of histologic severity and advanced fibrosis in patients with nonalcoholic fatty liver disease. Hepatology 2012;55(1):77-85.

[63] Sumida Y, Yoneda M, Hyogo H, Yamaguchi K, Ono M, Fujii H, et al. A simple clinical scoring system using ferritin, fasting insulin, and type IV collagen 7S for predicting

steatohepatitis in nonalcoholic fatty liver disease. Journal of gastroenterology 2011;46(2):257-68.

[64] Valenti L, Fracanzani AL, Bugianesi E, Dongiovanni P, Galmozzi E, Vanni E, et al. HFE genotype, parenchymal iron accumulation, and liver fibrosis in patients with nonalcoholic fatty liver disease. Gastroenterology 2010;138(3):905-12.

[65] Chandok N, Minuk G, Wengiel M, Uhanova J. Serum ferritin levels do not predict the stage of underlying non-alcoholic fatty liver disease. Journal of gastrointestinal and liver diseases : JGLD 2012;21(1):53-8.

[66] Chitturi S, Weltman M, Farrell GC, McDonald D, Kench J, Liddle C, et al. HFE mutations, hepatic iron, and fibrosis: ethnic-specific association of NASH with C282Y but not with fibrotic severity. Hepatology 2002;36(1):142-9.

[67] Kim CW, Chang Y, Sung E, Shin H, Ryu S. Serum ferritin levels predict incident non-alcoholic fatty liver disease in healthy Korean men. Metabolism 2012;61(8):1182-8.

[68] Pan M, Cederbaum AI, Zhang YL, Ginsberg HN, Williams KJ, Fisher EA. Lipid peroxidation and oxidant stress regulate hepatic apolipoprotein B degradation and VLDL production. J Clin Invest 2004;113(9):1277-87.

[69] Minamiyama Y, Takemura S, Kodai S, Shinkawa H, Tsukioka T, Ichikawa H, et al. Iron restriction improves type 2 diabetes mellitus in Otsuka Long-Evans Tokushima fatty rats. Am J Physiol Endocrinol Metab 2010;298(6):E1140-9.

[70] MacDonald GA, Bridle KR, Ward PJ, Walker NI, Houglum K, George DK, et al. Lipid peroxidation in hepatic steatosis in humans is associated with hepatic fibrosis and occurs predominately in acinar zone 3. J Gastroenterol Hepatol 2001;16(6):599-606.

[71] Fujita N, Miyachi H, Tanaka H, Takeo M, Nakagawa N, Kobayashi Y, et al. Iron overload is associated with hepatic oxidative damage to DNA in nonalcoholic steatohepatitis. Cancer Epidemiol Biomarkers Prev 2009;18(2):424-32.

[72] Nakashima T, Sumida Y, Furutani M, Hirohama A, Okita M, Mitsuyoshi H, et al. Elevation of serum thioredoxin levels in patients with nonalcoholic steatohepatitis. Hepatol Res 2005;33(2):135-7.

[73] Messner DJ, Rhieu BH, Kowdley KV. Iron overload causes oxidative stress and impaired insulin signaling in AML-12 hepatocytes. Digestive diseases and sciences 2013;58(7):1899-908.

[74] Maliken BD, Nelson JE, Klintworth HM, Beauchamp M, Yeh MM, Kowdley KV. Hepatic reticuloendothelial system cell iron deposition is associated with increased apoptosis in nonalcoholic fatty liver disease. Hepatology 2013.

[75] Chen L, Xiong S, She H, Lin SW, Wang J, Tsukamoto H. Iron causes interactions of TAK1, p21ras, and phosphatidylinositol 3-kinase in caveolae to activate IkappaB kinase in hepatic macrophages. J Biol Chem 2007;282(8):5582-8.

[76] Handa P, Morgan-Stevenson V, Maliken BD, Nelson JE, Washington S, Westerman M, et al. Iron overload results in hepatic oxidative stress, immune cell activation, and hepatocellular ballooning injury, leading to nonalcoholic steatohepatitis in genetically obese mice. Am J Physiol Gastrointest Liver Physiol 2016;310(2):G117-27.

[77] Ruddell RG, Hoang-Le D, Barwood JM, Rutherford PS, Piva TJ, Watters DJ, et al. Ferritin functions as a proinflammatory cytokine via iron-independent protein kinase C zeta/nuclear factor kappaB-regulated signaling in rat hepatic stellate cells. Hepatology 2009;49(3):887-900.

[78] Tan TC, Crawford DH, Jaskowski LA, Subramaniam VN, Clouston AD, Crane DI, et al. Excess iron modulates endoplasmic reticulum stress-associated pathways in a mouse model of alcohol and high-fat diet-induced liver injury. Lab Invest 2013;93(12):1295-312.

[79] Graham RM, Chua AC, Carter KW, Delima RD, Johnstone D, Herbison CE, et al. Hepatic iron loading in mice increases cholesterol biosynthesis. Hepatology 2010;52(2):462-71.

[80] George DK, Goldwurm S, MacDonald GA, Cowley LL, Walker NI, Ward PJ, et al. Increased hepatic iron concentration in nonalcoholic steatohepatitis is associated with increased fibrosis. Gastroenterology 1998;114(2):311-8.

[81] Fargion S, Mattioli M, Fracanzani AL, Sampietro M, Tavazzi D, Fociani P, et al. Hyperferritinemia, iron overload, and multiple metabolic alterations identify patients at risk for nonalcoholic steatohepatitis. Am J Gastroenterol 2001;96(8):2448-55.

[82] Bonkovsky HL, Jawaid Q, Tortorelli K, LeClair P, Cobb J, Lambrecht RW, et al. Non-alcoholic steatohepatitis and iron: increased prevalence of mutations of the HFE gene in non-alcoholic steatohepatitis. Journal of hepatology 1999;31(3):421-9.

[83] Nelson JE, Wilson L, Brunt EM, Yeh MM, Kleiner DE, Unalp-Arida A, et al. Relationship between the pattern of hepatic iron deposition and histological severity in nonalcoholic fatty liver disease. Hepatology 2011;53(2):448-57.

[84] Kleiner DE, Brunt EM, Van NM, Behling C, Contos MJ, Cummings OW, et al. Design and validation of a histological scoring system for nonalcoholic fatty liver disease. Hepatology 2005;41(6):1313-21.

[85] Cildir G, Akincilar SC, Tergaonkar V. Chronic adipose tissue inflammation: all immune cells on the stage. Trends Mol Med 2013;19(8):487-500.

[86] Wynn TA, Chawla A, Pollard JW. Macrophage biology in development, homeostasis and disease. Nature 2013;496(7446):445-55.

[87] Feuerer M, Herrero L, Cipolletta D, Naaz A, Wong J, Nayer A, et al. Lean, but not obese, fat is enriched for a unique population of regulatory T cells that affect metabolic parameters. Nat Med 2009;15(8):930-9.

[88] Nishimura S, Manabe I, Nagasaki M, Eto K, Yamashita H, Ohsugi M, et al. CD8+ effector T cells contribute to macrophage recruitment and adipose tissue inflammation in obesity. Nat Med 2009;15(8):914-20.

[89] Despres JP, Lemieux I. Abdominal obesity and metabolic syndrome. Nature 2006;444(7121):881-7.

[90] Wlazlo N, van Greevenbroek MM, Ferreira I, Jansen EH, Feskens EJ, van der Kallen CJ, et al. Iron metabolism is associated with adipocyte insulin resistance and plasma adiponectin: the Cohort on Diabetes and Atherosclerosis Maastricht (CODAM) study. Diabetes Care 2013;36(2):309-15.

[91] Pihan-Le Bars F, Bonnet F, Loreal O, Le Loupp AG, Ropert M, Letessier E, et al. Indicators of iron status are correlated with adiponectin expression in adipose tissue of patients with morbid obesity. Diabetes Metab 2015.

[92] Rumberger JM, Peters T, Jr., Burrington C, Green A. Transferrin and iron contribute to the lipolytic effect of serum in isolated adipocytes. Diabetes 2004;53(10):2535-41.

[93] Chirumbolo S, Rossi AP, Rizzatti V, Zoico E, Franceschetti G, Girelli D, et al. Iron primes 3T3-L1 adipocytes to a TLR4-mediated inflammatory response. Nutrition 2015;31(10):1266-74.

[94] Deugnier Y, Turlin B. Pathology of hepatic iron overload. Seminars in liver disease 2011;31(3):260-71.

[95] McLaren GD, Gordeuk VR. Hereditary hemochromatosis: insights from the Hemochromatosis and Iron Overload Screening (HEIRS) Study. Hematology Am Soc Hematol Educ Program 2009:195-206.

[96] Hernaez R, Yeung E, Clark JM, Kowdley KV, Brancati FL, Kao WH. Hemochromatosis gene and nonalcoholic fatty liver disease: a systematic review and meta-analysis. Journal of hepatology 2011;55(5):1079-85.

[97] Nelson JE, Brunt EM, Kowdley KV, Nonalcoholic Steatohepatitis Clinical Research N. Lower serum hepcidin and greater parenchymal iron in nonalcoholic fatty liver disease patients with C282Y HFE mutations. Hepatology 2012;56(5):1730-40.

[98] Valenti L, Rametta R, Dongiovanni P, Motta BM, Canavesi E, Pelusi S, et al. The A736V TMPRSS6 polymorphism influences hepatic iron overload in nonalcoholic fatty liver disease. PLoS One 2012;7(11):e48804.

[99] Fernandez-Real JM, Penarroja G, Castro A, Garcia-Bragado F, Hernandez-Aguado I, Ricart W. Blood letting in high-ferritin type 2 diabetes: effects on insulin sensitivity and beta-cell function. Diabetes 2002;51(4):1000-4.

[100] Facchini FS. Effect of phlebotomy on plasma glucose and insulin concentrations. Diabetes Care 1998;21(12):2190.

[101] Houschyar KS, Ludtke R, Dobos GJ, Kalus U, Broecker-Preuss M, Rampp T, et al. Effects of phlebotomy-induced reduction of body iron stores on metabolic syndrome: results from a randomized clinical trial. BMC Med 2012;10:54.

[102] Facchini FS, Hua NW, Stoohs RA. Effect of iron depletion in carbohydrate-intolerant patients with clinical evidence of nonalcoholic fatty liver disease. Gastroenterology 2002;122(4):931-9.

[103] Valenti L, Fracanzani AL, Dongiovanni P, Rovida S, Rametta R, Fatta E, et al. A randomized trial of iron depletion in patients with nonalcoholic fatty liver disease and hyperferritinemia. World J Gastroenterol 2014;20(11):3002-10.

[104] Adams LA, Crawford DH, Stuart K, House MJ, St Pierre TG, Webb M, et al. The impact of phlebotomy in nonalcoholic fatty liver disease: A prospective, randomized, controlled trial. Hepatology 2015;61(5):1555-64.

[105] Adams PC. The (II)logic of iron reduction therapy for steatohepatitis. Hepatology 2015;62(3):668-70.

[106] Senates E, Yilmaz Y, Colak Y, Ozturk O, Altunoz ME, Kurt R, et al. Serum levels of hepcidin in patients with biopsy-proven nonalcoholic fatty liver disease. Metabolic syndrome and related disorders 2011;9(4):287-90.

[107] Dongiovanni P, Lanti C, Gatti S, Rametta R, Recalcati S, Maggioni M, et al. High fat diet subverts hepatocellular iron uptake determining dysmetabolic iron overload. PLoS One 2015;10(2):e0116855.

[108] Hoki T, Miyanishi K, Tanaka S, Takada K, Kawano Y, Sakurada A, et al. Increased duodenal iron absorption through up-regulation of divalent metal transporter 1 from enhancement of iron regulatory protein 1 activity in patients with nonalcoholic steatohepatitis. Hepatology 2015;62(3):751-61.

[109] Otogawa K, Kinoshita K, Fujii H, Sakabe M, Shiga R, Nakatani K, et al. Erythrophagocytosis by liver macrophages (Kupffer cells) promotes oxidative stress, inflammation, and fibrosis in a rabbit model of steatohepatitis: implications for the pathogenesis of human nonalcoholic steatohepatitis. Am J Pathol 2007;170(3):967-80.

[110] Wang H, Li H, Jiang X, Shi W, Shen Z, Li M. Hepcidin is directly regulated by insulin and plays an important role in iron overload in streptozotocin-induced diabetic rats. Diabetes 2014;63(5):1506-18.

[111] Coimbra S, Catarino C, Santos-Silva A. The role of adipocytes in the modulation of iron metabolism in obesity. Obes Rev 2013.

[112] Siddique A, Nelson JE, Aouizerat B, Yeh MM, Kowdley KV, Network NCR. Iron deficiency in patients with nonalcoholic Fatty liver disease is associated with obesity, female gender, and low serum hepcidin. Clin Gastroenterol Hepatol 2014;12(7):1170-8.

[113] Fleming DJ, Tucker KL, Jacques PF, Dallal GE, Wilson PW, Wood RJ. Dietary factors associated with the risk of high iron stores in the elderly Framingham Heart Study cohort. Am J Clin Nutr 2002;76(6):1375-84.

[114] Bowers K, Yeung E, Williams MA, Qi L, Tobias DK, Hu FB, et al. A prospective study of prepregnancy dietary iron intake and risk for gestational diabetes mellitus. Diabetes Care 2011;34(7):1557-63.

[115] Qiu C, Zhang C, Gelaye B, Enquobahrie DA, Frederick IO, Williams MA. Gestational diabetes mellitus in relation to maternal dietary heme iron and nonheme iron intake. Diabetes Care 2011;34(7):1564-9.

[116] Amarapurkar DN, Hashimoto E, Lesmana LA, Sollano JD, Chen PJ, Goh KL, et al. How common is non-alcoholic fatty liver disease in the Asia-Pacific region and are there local differences? J Gastroenterol Hepatol 2007;22(6):788-93.

[117] Vernon G, Baranova A, Younossi ZM. Systematic review: the epidemiology and natural history of non-alcoholic fatty liver disease and non-alcoholic steatohepatitis in adults. Alimentary pharmacology & therapeutics 2011;34(3):274-85.

[118] Bacon BR, Adams PC, Kowdley KV, Powell LW, Tavill AS. Diagnosis and management of hemochromatosis: 2011 practice guideline by the American Association for the Study of Liver Diseases. Hepatology 2011;54(1):328-43.

[119] Chen H, Su T, Attieh ZK, Fox TC, McKie AT, Anderson GJ, et al. Systemic regulation of Hephaestin and Ireg1 revealed in studies of genetic and nutritional iron deficiency. Blood 2003;102(5):1893-9.

[120] Fuqua BK, Lu Y, Darshan D, Frazer DM, Wilkins SJ, Wolkow N, et al. The multicopper ferroxidase hephaestin enhances intestinal iron absorption in mice. PLoS One 2014;9(6):e98792.

[121] Leavens KF, Birnbaum MJ. Insulin signaling to hepatic lipid metabolism in health and disease. Crit Rev Biochem Mol Biol 2011;46(3):200-15.

[122] Matthews DR, Hosker JP, Rudenski AS, Naylor BA, Treacher DF, Turner RC. Homeostasis model assessment: insulin resistance and beta-cell function from fasting plasma glucose and insulin concentrations in man. Diabetologia 1985;28(7):412-9.

[123] Rong Y, Bao W, Rong S, Fang M, Wang D, Yao P, et al. Hemochromatosis gene (HFE) polymorphisms and risk of type 2 diabetes mellitus: a meta-analysis. Am J Epidemiol 2012;176(6):461-72.

[124] Huang J, Jones D, Luo B, Sanderson M, Soto J, Abel ED, et al. Iron overload and diabetes risk: a shift from glucose to Fatty Acid oxidation and increased hepatic glucose production in a mouse model of hereditary hemochromatosis. Diabetes 2011;60(1):80-7.

[125] Sonnweber T, Ress C, Nairz M, Theurl I, Schroll A, Murphy AT, et al. High-fat diet causes iron deficiency via hepcidin-independent reduction of duodenal iron absorption. J Nutr Biochem 2012;23(12):1600-8.

[126] Hotamisligil GS. Mechanisms of TNF-alpha-induced insulin resistance. Exp Clin Endocrinol Diabetes 1999;107(2):119-25.

[127] Kristiansen OP, Mandrup-Poulsen T. Interleukin-6 and diabetes: the good, the bad, or the indifferent? Diabetes 2005;54 Suppl 2:S114-24.

[128] Laine F, Ruivard M, Loustaud-Ratti V, Bonnet F, Cales P, Bardou-Jacquet E, et al. Metabolic and hepatic effects of bloodletting in dysmetabolic iron overload syndrome: A randomized controlled study in 274 patients. Hepatology 2017;65(2):465-74.

[129] Adams LA, George J, Bugianesi E, Rossi E, De Boer WB, van der Poorten D, et al. Complex non-invasive fibrosis models are more accurate than simple models in non-alcoholic fatty liver disease. J Gastroenterol Hepatol 2011;26(10):1536-43.

[130] van Rijnsoever M, Galhenage S, Mollison L, Gummer J, Trengove R, Olynyk JK. Dysregulated Erythropoietin, Hepcidin, and Bone Marrow Iron Metabolism Contribute to Interferon-Induced Anemia in Hepatitis C. J Interferon Cytokine Res 2016;36(11):630-4.

[131] Gummer J, Trengove R, Pascoe EM, Badve SV, Cass A, Clarke P, et al. Association between Serum Hepcidin-25 and Primary Resistance to Erythropoiesis Stimulating Agents in Chronic Kidney Disease: A Secondary Analysis of the HERO Trial. LID - 10.1111/nep.12815 [doi]. 2016(1440-1797 (Electronic)).

[132] Litton E, Baker S, Erber WN, Farmer S, Ferrier J, French C, et al. Intravenous iron or placebo for anaemia in intensive care: the IRONMAN multicentre randomized blinded trial : A randomized trial of IV iron in critical illness. 2016(1432-1238 (Electronic)).

[133] House MJ, Gan EK, Adams LA, Ayonrinde OT, Bangma SJ, Bhathal PS, et al. Diagnostic performance of a rapid magnetic resonance imaging method of measuring hepatic steatosis. PLoS One 2013;8(3):e59287.

[134] St Pierre TG, Clark PR, Chua-anusorn W, Fleming AJ, Jeffrey GP, Olynyk JK, et al. Noninvasive measurement and imaging of liver iron concentrations using proton magnetic resonance. Blood 2005;105(2):855-61.

[135] Adamia N, Virsaladze D, Charkviani N, Skhirtladze M, Khutsishvili M. Effect of metformin therapy on plasma adiponectin and leptin levels in obese and insulin resistant postmenopausal females with type 2 diabetes. Georgian Med News 2007(145):52-5.

[136] Lomonaco R, Ortiz-Lopez C, Orsak B, Webb A, Hardies J, Darland C, et al. Effect of adipose tissue insulin resistance on metabolic parameters and liver histology in obese patients with nonalcoholic fatty liver disease. Hepatology 2012;55(5):1389-97.

[137] Matsuda M, DeFronzo RA. Insulin sensitivity indices obtained from oral glucose tolerance testing: comparison with the euglycemic insulin clamp. Diabetes Care 1999;22(9):1462-70.

[138] Bassett ML, Halliday JW, Powell LW. Value of hepatic iron measurements in early hemochromatosis and determination of the critical iron level associated with fibrosis. Hepatology 1986;6(1):24-9.

[139] Pippard MJ. Measurement of iron status. Prog Clin Biol Res 1989;309:85-92.

[140] Ryan JD, Armitage AE, Cobbold JF, Banerjee R, Borsani O, Dongiovanni P, et al. Hepatic iron is the major determinant of serum ferritin in NAFLD patients. Liver Int 2018;38(1):164-73.

[141] Bekri S, Gual P, Anty R, Luciani N, Dahman M, Ramesh B, et al. Increased adipose tissue expression of hepcidin in severe obesity is independent from diabetes and NASH. Gastroenterology 2006;131(3):788-96.

[142] Green A, Basile R, Rumberger JM. Transferrin and iron induce insulin resistance of glucose transport in adipocytes. Metabolism 2006;55(8):1042-5.

[143] Casey JL, Hentze MW, Koeller DM, Caughman SW, Rouault TA, Klausner RD, et al. Iron-responsive elements: regulatory RNA sequences that control mRNA levels and translation. Science 1988;240(4854):924-8.

[144] Wang ZV, Deng Y, Wang QA, Sun K, Scherer PE. Identification and characterization of a promoter cassette conferring adipocyte-specific gene expression. Endocrinology 2010;151(6):2933-9.

[145] Donovan A, Lima CA, Pinkus JL, Pinkus GS, Zon LI, Robine S, et al. The iron exporter ferroportin/Slc40a1 is essential for iron homeostasis. Cell metabolism 2005;1(3):191-200.

[146] Brunt EM. Nonalcoholic fatty liver disease: What the pathologist can tell the clinician. Digestive Diseases 2012;30(SUPPL. 1):61-8.

[147] Britton L, Jaskowski L, Bridle K, Santrampurwala N, Reiling J, Musgrave N, et al. Heterozygous Hfe gene deletion leads to impaired glucose homeostasis, but not liver injury in mice fed a high-calorie diet. Physiol Rep 2016;4(12).

[148] Xirouchaki CE, Mangiafico SP, Bate K, Ruan Z, Huang AM, Tedjosiswoyo BW, et al. Impaired glucose metabolism and exercise capacity with muscle-specific glycogen synthase 1 (gys1) deletion in adult mice. Mol Metab 2016;5(3):221-32.

[149] Bridle KR, Sobbe AL, de Guzman CE, Santrampurwala N, Jaskowski LA, Clouston AD, et al. Lack of efficacy of mTOR inhibitors and ACE pathway inhibitors as antifibrotic agents in evolving and established fibrosis in Mdr2(-)/(-) mice. Liver Int 2015;35(4):1451-63.

[150] Cinti S, Mitchell G, Barbatelli G, Murano I, Ceresi E, Faloia E, et al. Adipocyte death defines macrophage localization and function in adipose tissue of obese mice and humans. J Lipid Res 2005;46(11):2347-55.

[151] Lickteig AJ, Fisher CD, Augustine LM, Cherrington NJ. Genes of the antioxidant response undergo upregulation in a rodent model of nonalcoholic steatohepatitis. J Biochem Mol Toxicol 2007;21(4):216-20.

[152] Rishi G, Wallace DF, Subramaniam VN. Hepcidin: regulation of the master iron regulator. Biosci Rep 2015;35(3).

[153] Kroot JJ, Tjalsma H, Fleming RE, Swinkels DW. Hepcidin in human iron disorders: diagnostic implications. Clin Chem 2011;57(12):1650-69.

[154] Chung J, Kim MS, Han SN. Diet-induced obesity leads to decreased hepatic iron storage in mice. Nutrition research (New York, NY) 2011;31(12):915-21.

[155] Wolfs MG, Gruben N, Rensen SS, Verdam FJ, Greve JW, Driessen A, et al. Determining the association between adipokine expression in multiple tissues and phenotypic features of non-alcoholic fatty liver disease in obesity. Nutr Diabetes 2015;5:e146.

[156] Alkhouri N, Lopez R, Berk M, Feldstein AE. Serum retinol-binding protein 4 levels in patients with nonalcoholic fatty liver disease. J Clin Gastroenterol 2009;43(10):985-9.

[157] Luo X, Hutley LJ, Webster JA, Kim YH, Liu DF, Newell FS, et al. Identification of BMP and activin membrane-bound inhibitor (BAMBI) as a potent negative regulator of adipogenesis and modulator of autocrine/paracrine adipogenic factors. Diabetes 2012;61(1):124-36.

[158] Wabitsch M, Brenner RE, Melzner I, Braun M, Moller P, Heinze E, et al. Characterization of a human preadipocyte cell strain with high capacity for adipose differentiation. Int J Obes Relat Metab Disord 2001;25(1):8-15.

[159] Kohyama M, Ise W, Edelson BT, Wilker PR, Hildner K, Mejia C, et al. Role for Spi-C in the development of red pulp macrophages and splenic iron homeostasis. Nature 2009;457(7227):318-21.

[160] Ruelcke JE, Loo D, Hill MM. Reducing the cost of semi-automated in-gel tryptic digestion and GeLC sample preparation for high-throughput proteomics. J Proteomics 2016;149:3-6.

[161] The UniProt C. UniProt: the universal protein knowledgebase. Nucleic Acids Res 2017;45(D1):D158-D69.

[162] Chen D, Shah A, Nguyen H, Loo D, Inder KL, Hill MM. Online quantitative proteomics p-value calculator for permutation-based statistical testing of peptide ratios. J Proteome Res 2014;13(9):4184-91.

[163] Schierwagen R, Maybuchen L, Zimmer S, Hittatiya K, Back C, Klein S, et al. Seven weeks of Western diet in apolipoprotein-E-deficient mice induce metabolic syndrome and non-alcoholic steatohepatitis with liver fibrosis. Sci Rep 2015;5:12931.

[164] Oslowski CM, Urano F. Measuring ER stress and the unfolded protein response using mammalian tissue culture system. Methods Enzymol 2011;490:71-92.

[165] Kim DK, Lee J, Kim SR, Choi DS, Yoon YJ, Kim JH, et al. EVpedia: a community web portal for extracellular vesicles research. Bioinformatics 2015;31(6):933-9.

[166] Chiba T, Nakazawa T, Yui K, Kaneko E, Shimokado K. VLDL induces adipocyte differentiation in ApoE-dependent manner. Arterioscler Thromb Vasc Biol 2003;23(8):1423-9.

[167] Pendse AA, Arbones-Mainar JM, Johnson LA, Altenburg MK, Maeda N. Apolipoprotein E knock-out and knock-in mice: atherosclerosis, metabolic syndrome, and beyond. J Lipid Res 2009;50 Suppl:S178-82.

[168] Huang ZH, Reardon CA, Getz GS, Maeda N, Mazzone T. Selective suppression of adipose tissue apoE expression impacts systemic metabolic phenotype and adipose tissue inflammation. J Lipid Res 2015;56(2):215-26.

[169] Caselli RJ, Beach TG, Knopman DS, Graff-Radford NR. Alzheimer Disease: Scientific Breakthroughs and Translational Challenges. Mayo Clin Proc 2017;92(6):978-94.

[170] Castellani RJ, Moreira PI, Perry G, Zhu X. The role of iron as a mediator of oxidative stress in Alzheimer disease. Biofactors 2012;38(2):133-8.

[171] Xu H, Perreau VM, Dent KA, Bush AI, Finkelstein DI, Adlard PA. Iron Regulates Apolipoprotein E Expression and Secretion in Neurons and Astrocytes. J Alzheimers Dis 2016;51(2):471-87.

[172] Locatelli I, Sutti S, Jindal A, Vacchiano M, Bozzola C, Reutelingsperger C, et al. Endogenous annexin A1 is a novel protective determinant in nonalcoholic steatohepatitis in mice. Hepatology 2014;60(2):531-44.

[173] Parapia LA. History of bloodletting by phlebotomy. Br J Haematol 2008;143(4):490-5.

[174] Fischer-Posovszky P, Newell FS, Wabitsch M, Tornqvist HE. Human SGBS cells - a unique tool for studies of human fat cell biology. Obes Facts 2008;1(4):184-9.

[175] Ong SE, Mann M. A practical recipe for stable isotope labeling by amino acids in cell culture (SILAC). Nat Protoc 2006;1(6):2650-60.